

Modulation of Histone Deacetylases Attenuates the Pathogenesis of Alzheimer's disease

Dissertation submitted to

Faculty of Biology incl. Psychology
Georg-August-Universität Göttingen, Germany

for the award of the degree of

Doctor of Philosophy

Nambirajan Govindarajan

Born in Kolkata, India

Göttingen 2010



PhD Thesis Committee

1. **Dr. André Fischer:** Laboratory of Aging and Cognitive Diseases, European Neuroscience Institute, Göttingen, Germany
2. **Prof. Ralf Heinrich:** Dept. of Invertebrate Pharmacology, Johann-Friedrich-Blumenbach-Institute for Zoology and Anthropology, Georg-August-University, Göttingen, Germany
3. **Prof. Michael Hörner:** Dept. of Cell Biology, Johann-Friedrich-Blumenbach-Institute for Zoology and Anthropology, Georg-August-University, Göttingen, Germany

Declaration

I herewith declare that I have prepared the dissertation “Modulation of histone deacetylases attenuates the pathogenesis of Alzheimer’s disease” entirely by myself with no other aids or sources than quoted.

Göttingen, 20.09.2010

Nambirajan Govindarajan

Table of Contents

Table of Contents	4
Summary.....	9
1. Introduction.....	11
1.1. Learning and memory	11
1.1.1. Memory Storage in the Brain	12
1.1.2. Forms of Memory	13
1.1.2.1. Short-term and Long-term Memories	13
1.1.2.2. Declarative and Procedural Memories.....	13
1.1.2.3. Associative Memory	14
1.1.2.4. Spatial Memory	15
1.1.3. Molecular Mechanisms of Memory	15
1.1.4. Learning and Memory Disorders.....	16
1.2. Alzheimer’s disease.....	17
1.2.1. Pathology of Alzheimer’s disease	18
1.2.1.1. Amyloid Pathology.....	18
1.2.1.2. Tau Pathology.....	19
1.2.2. Treatment of Alzheimer’s disease	20
1.3. Epigenetics.....	21
1.3.1. Chromatin Plasticity	21
1.3.2. Histone Acetylation	22
1.3.3. Histone Acetylation in Memory	22
1.3.4. Histone Acetyltransferases	23
1.3.5. Histone Deacetylases.....	24
1.3.5.1. Class I HDACs	24
1.3.5.2. Class IIa HDACs	25
1.3.5.3. Class IIb HDACs.....	25
1.3.5.4. Class IV HDAC	26
1.3.6. HDAC Inhibition in Neurodegeneration	26
1.3.6.1. Non-specific HDAC Inhibition.....	26
1.3.6.2. HDAC6 Inhibition	27
1.4. Objectives of the study	27
1.4.1. Treatment of advanced AD Pathology with SB	27

1.4.2. Role of HDAC6 in Cognition and AD	28
2. Materials and Methods.....	29
2.1. Animals	29
2.1.1. <i>Hdac6</i> Knockout Mice	29
2.1.2. Double Transgenic APPPS1-21 Mice	29
2.1.3. Implantation of Microcannulae	30
2.1.4. Intra-Hippocampal Drug Administration	31
2.1.5. Brain Extraction for Molecular Analysis	31
2.1.6. Brain Extraction for Histology	32
2.2. Behavioural Analysis of Mice	32
2.2.1. Open Field	33
2.2.2. Elevated Plus-Maze	33
2.2.3. Contextual Fear Conditioning	33
2.2.4. Tone Fear Conditioning.....	34
2.2.5. Morris Water Maze	34
2.2.6. Rotarod Performance Test.....	35
2.3. Molecular Biology.....	36
2.3.1. Nucleic Acid Extraction	36
2.3.1.1. DNA Isolation for Genotyping	36
2.3.1.2. RNA Isolation.....	37
2.3.2. Reverse Transcription.....	37
2.3.3. Polymerase Chain Reaction.....	38
2.3.3.1. <i>Hdac6</i> Genotyping PCR	38
2.3.3.2. APPPS1-21 Genotyping PCR.....	39
2.3.3.3. Semi-Quantitative PCR for Gene Expression Analysis	40
2.3.3.4. Quantitative Real-Time PCR for Gene Expression Analysis	41
2.3.3.5. PCR Amplification of <i>Hdac6</i> for Cloning	42
2.3.3.6. Primers for PCR	43
2.3.3.7. Chromatin Immunoprecipitation	46
2.3.4. DNA Electrophoresis	47
2.3.5. Restriction Digestion	47
2.3.6. DNA Ligation.....	48
2.3.7. Transformation of <i>Escherichia coli</i>	49
2.3.8. Plasmid Purification	49
2.3.9. Protein Extraction.....	50
2.3.9.1. Crude Extraction of Proteins from Brain Tissue.....	50

2.3.9.2. Extraction of Proteins Using TRI-Reagent	51
2.3.9.3. Isolation of Synaptosomal and PSD Protein Fractions	51
2.3.9.4. Determination of Protein Concentration	53
2.3.10. Protein Electrophoresis	54
2.3.10.1. Preparation of Protein Lysates for SDS-PAGE	54
2.3.10.2. SDS-PAGE	54
2.3.11. Coomassie Staining	55
2.3.12. Western Blot	56
2.3.12.1. Protein Transfer	56
2.3.12.2. Immunoblot	56
2.4. Immunohistochemistry	57
2.4.1. Immunohistochemistry on Paraffin Sections	57
2.4.2. Immunohistochemistry on Frozen Sections	58
2.4.3. Confocal Microscopy	59
2.4. Cell Culture	59
2.4.1. Primary Hippocampal Neurons	59
2.4.2. Generation of Lentivirus and Infection of Neurons	59
2.4.3. β -Amyloid Oligomerisation and Neuronal Treatment	60
2.4.4. Live Imaging of Mitochondrial Trafficking	61
2.4.5. Immunocytochemistry	61
2.5. Data Analysis	62
3. Results	63
3.1. HDAC Inhibition in APPPS1-21 mice	63
3.1.1. Cognition in APPPS1-21 mice upon SB treatment	63
3.1.2. Histone acetylation in APPPS1-21 mice upon SB treatment	66
3.1.3. Gene expression changes upon SB treatment	67
3.1.4. SNAP-25 protein levels upon SB treatment	68
3.1.5. Amyloid plaque levels upon SB treatment	69
3.2. HDAC6 in the mouse brain	70
3.2.1. <i>Hdac6</i> expression in brain regions	70
3.2.2. HDAC6 protein levels in the brain	71
3.2.3. Subcellular localisation of HDAC6 by Western Blot	71
3.2.4. Overexpression of <i>Hdac6</i> in neuronal culture	72
3.3. Basic Characterisation of <i>Hdac6</i> knockout mice	73
3.3.6. <i>Hdac6</i> mRNA and protein levels in <i>Hdac6</i> KO mice	73
3.3.1. Phenotype of <i>Hdac6</i> KO mice	74

3.3.2. Brain morphology in <i>Hdac6</i> KO mice	74
3.3.3. Analysis of proteins in <i>Hdac6</i> KO mice.....	76
3.3.4. Histone acetylation in <i>Hdac6</i> KO mice.....	77
3.3.5. Expression of histone deacetylases in <i>Hdac6</i> KO mice	78
3.3.6. Expression of cognition-induced genes in <i>Hdac6</i> KO mice.....	79
3.4. Behavioural Characterisation of <i>Hdac6</i> KO mice	79
3.4.1. Basal anxiety and exploratory behaviour in <i>Hdac6</i> KO mice.....	79
3.4.2. Associative memory in <i>Hdac6</i> KO mice.....	81
3.4.3. Spatial memory in <i>Hdac6</i> KO mice	81
3.4.4. Motor function in <i>Hdac6</i> KO mice	82
3.5. Acute inhibition of HDAC6 in mice	83
3.6. Loss of <i>Hdac6</i> in APPPS1-21 mice	84
3.6.1. Basal anxiety and exploration in APPPS1-21-HD6 ^{-/-} mice.....	84
3.6.2. Associative memory in APPPS1-21-HD6 ^{-/-} mice	85
3.6.3. Spatial memory in APPPS1-21-HD6 ^{-/-} mice.....	85
3.6.4. Molecular analysis of loss of <i>Hdac6</i> in APPPS1-21 mice	86
3.6.4.1. Tubulin acetylation in APPPS1-21-HD6 ^{-/-} mice	86
3.6.4.2. Levels of synaptic markers in APPPS1-21-HD6 ^{-/-} mice.....	88
3.6.4.3. Analysis of hippocampal synaptosomal and post-synaptic density fractions from APPPS1-21-HD6 ^{-/-} mice	89
3.6.4.4. Levels of β -amyloid plaques upon loss of <i>Hdac6</i> in APPPS1-21 mice.....	89
3.7. Mitochondrial trafficking in neurons	90
4. Discussion	91
4.1. HDAC inhibition in APPPS1-21 mice	91
4.1.1. SB treatment improves cognition in APPPS1-21 mice	91
4.1.2. SB treatment upregulates histone acetylation.....	93
4.1.3. Enhanced gene expression upon SB treatment.....	94
4.1.4. SB treatment does not affect β -amyloid plaques.....	94
4.1.5. Summary	95
4.2. HDAC6 in the brain.....	95
4.2.1. HDAC6 in the mouse brain	95
4.2.2. Subcellular localisation of HDAC6.....	96
4.2.3. Basic characterisation of <i>Hdac6</i> knockout mice	97
4.2.3.1. Basic morphology and brain structure in <i>Hdac6</i> KO mice	97
4.2.3.2. Histone acetylation in <i>Hdac6</i> KO mice	98
4.2.3.3. Tubulin acetylation in <i>Hdac6</i> KO mice.....	98

4.2.3.4. Expression of <i>Hdac</i> genes in <i>Hdac6</i> KO mice	99
4.2.3.5. Role of HDAC6 in gene expression	99
4.2.4. Behavioural analysis of <i>Hdac6</i> KO mice	100
4.2.5. Pharmacological inhibition of HDAC6 in mice	100
4.2.6. Summary	101
4.3. Loss of <i>Hdac6</i> attenuates AD pathology	101
4.3.1. Loss of <i>Hdac6</i> improves cognition in APPPS1-21 mice.....	102
4.3.2. Molecular analysis of <i>Hdac6</i> loss in AD pathology.....	102
4.3.3. Summary	104
4.4. Future Outlook.....	104
Acknowledgement.....	106
References.....	108
Curriculum Vitae.....	120

Summary

We are yet to learn precisely how we learn. The molecular and physiological mechanisms that govern the process of cognition remain a mystery to scientific minds around the globe. This also greatly limits our capability to encounter cognitive diseases efficaciously. With an ageing world population, it is crucial to understand and develop effective therapeutic strategies against age-associated neurodegenerative disorders such as dementia and Alzheimer's disease (AD).

Previous research has shown that the process of memory formation involves the regulation of gene expression in the brain. Apart from genes, key proteins are also known to be differentially regulated by post-translational modifications during the acquisition and consolidation of new memories. One such mechanism is the acetylation and deacetylation of histones. Histone modifications serve as crucial players in the process of epigenetic regulation of gene expression. The acetylation of histones is specific in nature and can also be modulated by environmental stimuli. This concept is called the "histone code". Histone acetylation is balanced by the action of histone acetyltransferases (HATs) and histone deacetylases (HDACs) and has been shown to be beneficial for memory consolidation. This study shows that elevation of histone acetylation by HDAC inhibition is beneficial for cognition in a mouse model for AD. This involves the upregulation of genes associated with the process of memory formation. However, HDAC inhibition did not exert any effect on β -amyloid pathology exhibited by this mouse model. This shows that cognitive improvement in AD could be independent of ongoing pathology and HDAC inhibition could serve to significantly facilitate cognitive recovery in AD.

Apart from histone acetylation, some HDACs also catalyse the deacetylation of lysine residues on cytoplasmic proteins. A classic example of a non-histone deacetylase is HDAC6. It is known that HDAC6 acts on cytoplasmic substrates such as α -tubulin, a component of microtubules, and Hsp90, a molecular chaperone. Through its action on α -tubulin, HDAC6 has been shown to negatively regulate microtubular transport of

essential cellular cargo such as mitochondria. Interestingly, microtubular transport of mitochondria is affected in AD and that of other cargo proteins in neurodegenerative disorders like Huntington's disease. Therefore, HDAC6 inhibition could prove to be beneficial against neurodegeneration.

The findings presented here show that HDAC6, a cytoplasmic protein, does not affect gene expression in the brain. Loss of *Hdac6* was found to be beneficial for spatial memory in mice. Furthermore, loss of *Hdac6* in a transgenic AD mouse model was found to significantly facilitate cognition without affecting amyloid pathology. Subsequent analysis revealed that loss of HDAC6 activity could significantly prevent the impairment of mitochondrial trafficking in AD possibly by the elevation of tubulin acetylation. This shows that HDAC6 is a promising drug target to attenuate cognitive impairment in AD.

Taken together, the data presented in this dissertation demonstrate that the inhibition of HDACs, in particular HDAC6, might be highly beneficial against neurodegeneration.

1. Introduction

*“If the brain were so simple we could understand it,
we would be so simple we couldn’t”*

- *Lyall Watson*

The famous quote by Lyall Watson divulges the ironic complexity of the human brain. Being the only known species to possess a brain with the potential to understand itself, we humans have always been intrigued by the fascinating capabilities of this organ. Our mental abilities like thought, memory, speech and emotion are regulated by intricate molecular and physiological processes occurring in our brains. Together, these brain functions give us a distinct sense of identity as individuals and collectively as a species. The process of cognition is extremely vital to our daily lives. Our adaptability to different environments depends on our learning capability. This complex brain function has remained a mystery to scientific minds for many centuries. Cognition is severely affected in several neurological disorders such as dementia and Alzheimer’s disease. Therefore, unravelling the precise mechanisms that govern learning and memory is crucial to our understanding of neurophysiology and neurological disease.

1.1. Learning and memory

Learning and memory form the basis of our mental growth and development. Learning is the process of acquiring new knowledge, behaviours, skills, preferences or understanding. Memory is defined as an organism’s ability to store, retain and recall information and experiences. Modern science is only beginning to unravel the mechanisms behind mammalian memory processes.

1.1.1. Memory Storage in the Brain

One of the most intriguing questions in cognition is the place of memory storage in the brain. In the 1920s, Karl Lashley carefully damaged various cortical regions in rats that had acquired the memory of a route through a simple maze. He did not obtain any correlation between the memory performance and the amount or location of brain damage. Therefore, Lashley concluded that memory is delocalised in the brain. Subsequently, Wilder Penfield discovered that the stimulation of certain brain regions such as the temporal lobe in awake patients led them to experience specific memories. Penfield concluded that specific memories might be stored in individual brain regions. The disparity in the above two findings was resolved by Donald Hebb who proposed that thoughts and memories were supported by “cell assemblies” or networks of neurons (Hebb, 1949). Hebb also suggested that learning experiences could change the connections between cells (Hebb, 1949). This Hebbian hypothesis laid the foundation for our understanding of synaptic plasticity in cognition. The evidence for the involvement of one brain region, the hippocampus, in memory came from the most famous patient in neuroscience, late Henry Gustav Molaison, popularly known as H.M., who underwent brain surgery for the treatment of severe epilepsy. H.M.’s left and right medial temporal lobes (MTLs) were removed to treat his epilepsy. However, after this surgery, H.M. exhibited profound anterograde amnesia characterised by the inability to form lasting memories and loss of cognitive ability (Scoville, 1957). However, H.M.’s perception, abstract thinking and reasoning ability were all intact. Also, his ability to learn new motor skills was not affected (Corkin, 2002). This showed that memory and perception followed different cerebral pathways. It was found that nearly two-thirds of H.M.’s hippocampus, parahippocampal gyrus and amygdala were also removed along with his MTLs (Scoville, 1957). H.M.’s case showed us that specific brain regions such as the hippocampus were involved in memory formation. Several recent studies have reported that specific forms of memory can be stored in distinct brain structures.

1.1.2. Forms of Memory

Memory can be classified in different ways based on its different features such as acquisition, processing and recall. Certain forms of memory have been described below.

1.1.2.1. Short-term and Long-term Memories

Short-term memory (STM) is the capacity for holding a small amount of information for a short period of time. The capacity of STM in humans has been shown to be in the order of 4-5 items of information (Cowan, 2001). It has been proposed that STM causes depletion of the Readily Releasable Pool (RRP) of neurotransmitter vesicles at the presynaptic terminals (Tarnow, 2009).

Long-term memory (LTM) can store much larger quantities of information for potentially an unlimited duration of time. Unlike STM, the process of LTM storage is dependent on protein synthesis (Costa-Mattioli, 2008). Another study has shown that the persistence of long-term memories involves the brain-derived neurotrophic factor or BDNF (Bekinschtein, 2008).

1.1.2.2. Declarative and Procedural Memories

Declarative memory refers to memories like facts and events that can be consciously recalled (Ullman, 2004). Declarative memory can be divided into episodic memory that stores specific personal experiences and semantic memory that stores factual information (Tulving, 1972). It has been shown that the hippocampus mediates the encoding of declarative memories (Eichenbaum, 2001). Another study has shown that the pre-frontal cortex (PFC) is involved with episodic memory more than semantic memory (Levine, 2004). Interestingly, sleep has been shown to facilitate the consolidation of declarative memories (Ellenbogen, 2006).

Procedural memory is the memory of a specific procedure involving cognitive and motor skills. Procedural memory formation involves the plasticity of striatal neurons (Kreitzer, 2009). Additionally, the cerebellum is also known to be involved in procedural memory processing involving motor skills (Saywell, 2008). One of the key modulators of procedural memory is dopamine. A recent report indicates that the mesocorticolimbic dopamine pathway might be closely involved in procedural memory processing (Zellner, 2009).

1.1.2.3. Associative Memory

Associative memory, as the name suggests, involves the association between a stimulus and a response. It was first described by Ivan Pavlov in his classical conditioning experiments (Rescorla, 1972). In Pavlovian conditioning, a dog was presented with food, which serves as the unconditioned stimulus (US), causing the dog to salivate. A second stimulus such as the sound of a bell that did not elicit the salivation response alone was chosen to be the conditioned stimulus (CS). The US was coupled with the CS and presented to the dog. It was observed that the dog could associate the two stimuli and after repeated training exhibit salivation upon presentation of the CS alone. This was termed a conditional response (CR). To achieve classical conditioning, the US and CS should be presented simultaneously or the CS should be presented shortly before the US (Bear, 2006).

Associative memory can be tested in rodents using the fear conditioning paradigm (Blanchard, 1969). The rodent is exposed to the CS (novel context, tone or light) and then given a mild electric foot shock that serves as the US. Upon a second exposure to the CS, instead of its normal exploratory behaviour, the animal crouches at one location and exhibits no body movements except respiration and shivering (Section 2.2.3). This behaviour is termed “freezing”. The freezing behaviour can be quantified and the level of freezing represents the strength of the associative memory. Contextual fear conditioning, where the CS is a novel context, is dependent on an intact hippocampus (Kim, 1992). Tone-dependent fear conditioning is mediated through the amygdala and does not require an intact hippocampus (LeDoux, 1994).

1.1.2.4. Spatial Memory

Spatial memory is the part of memory responsible for recording information about our environment and spatial orientation. Spatial memories are formed based on the information conveyed through vision and proprioception. In mice, the hippocampus is known to be involved in acquisition and consolidation of spatial memory (Crusio, 2005; Rossi-Arnaud, 1991; Schwegler, 1995). A previous study has shown that the consolidation of spatial memory involves *N*-methyl-D-aspartate (NMDA) receptors and its retrieval requires α -amino-3-hydroxy-5-methyl-4-isoxazolepropionic acid (AMPA) receptors (Liang, 1994).

Spatial memory can be tested in rodents using the Morris Water Maze task developed by Richard Morris (Morris, 1981). The animal is required to locate a hidden platform in a pool of opaque water with the help of visual cues provided. The “escape latency” or the time required by the animal to find the platform negatively correlates with duration of training. After training, the spatial memory acquired can be tested by exposing the animal to the pool without the platform. Spatial memory consolidation is indicated by significantly longer time spent at the location of the platform during training (Section 2.2.5).

1.1.3. Molecular Mechanisms of Memory

The most significant hypothesis to address memory encoding so far was put forth by Donald Hebb in 1949. Hebb proposed that the connection between cells, later known as synapses, get modified during memory formation (Hebb, 1949). This idea was supported by the subsequent discovery of long-term potentiation of synaptic transmission or LTP (Lømo, 1966). Lømo proposed that if two neurons are synchronously stimulated, the synaptic transmission between them is enhanced. This principle forms the foundation of the phenomenon of synaptic plasticity (Cooke, 2006). Interestingly, the maintenance of LTP for a prolonged period of time required *de novo* protein synthesis (Lisman, 2002). Initial studies on the involvement of protein synthesis in long-term memory were conducted by Eric Kandel on the marine snail *Aplysia*

(Kandel, 2001). It was discovered that *de novo* protein synthesis was critical to the formation of long-term but not short-term memories (Castellucci, 1989; Kandel, 2001). Additionally, protein degradation in the 26 S proteasome was also found to be important in memory formation (Chain, 1999). It has also been shown that long-term memory involves the expression of *c-fos* in the dorsal hippocampus (Katche, 2009). Synaptic plasticity that occurs during memory formation involves the upregulation of immediate early genes (IEGs) such as *c-fos* and *Zif268* (Guzowski, 2002). Extensive research using both genetic and pharmacological manipulations has shown the importance of NMDA receptors in synaptic plasticity and memory (Lee, 2009). The cyclic-AMP response element-binding protein (CREB) has also been found to be upregulated during memory formation (Lee, 2009).

More recently, it has been discovered that epigenetic mechanisms play a role in memory formation and consolidation. Chromatin modifications have been implicated in synaptic plasticity occurring during the integration of long-term memories (Guan, 2002). Another interesting study has shown that behavioural memory involves the histone acetyltransferase activity of the CREB-binding protein or CBP (Korzus, 2004). The regulation of histone acetylation in the hippocampus has been shown to be important for memory formation (Levenson, 2004). Further research performed in David Sweatt's laboratory has revealed that DNA methylation is critical for memory formation in the adult mammalian nervous system (Miller, 2007). These studies tell us that epigenetic regulation of gene expression plays a critical role in memory formation in the adult mammalian brain. Further details on the role of epigenetics in cognition are discussed below (Section 1.3).

1.1.4. Learning and Memory Disorders

Learning and memory can be affected in several neurological disorders such as ageing, Mild Cognitive Impairment, Alzheimer's disease, Huntington's disease, Parkinson's disease, Wernicke-Korsakoff syndrome or traumatic brain injury. Cognitive decline and loss of memory are associated with the process of ageing (Bishop, 2010). The prevalence of age-related cognitive decline has increased with the rise in life expectancy

in the last few decades. The impairment of basic biological processes such as synaptic plasticity, gene expression and mitochondrial function contribute to the loss of cognitive ability observed upon ageing (Bishop, 2010). Mild Cognitive Impairment (MCI), also known as incipient dementia, is a disorder that features cognitive impairments that do not interfere significantly with a person's daily activities (Petersen, 1999). It is considered to be a transitional stage between normal ageing and dementia. MCI is also seen as a risk factor for the development of Alzheimer's disease (Grundman, 2004). Alzheimer's disease is a neurodegenerative disorder that causes severe dementia, loss of cognition and greatly restricts quality of life in the patients. Huntington's disease (HD) is a progressive neurodegenerative disorder characterised by cognitive decline, uncontrollable physical movements called chorea and changes in personality (Walker, 2007). Parkinson's disease (PD) is a degenerative disorder of the central nervous system that leads to impaired motor skills, speech and cognition (Jankovic, 2008). Wernicke-Korsakoff syndrome (WKS) is a clinical manifestation of alcohol abuse and thiamine deficiency that causes changes in vision, ataxia and memory impairment (Kopelman, 2009). Cognitive deficits have also been observed in people suffering from moderate to severe brain injury (Milders, 2003).

1.2. Alzheimer's disease

Alzheimer's disease (AD) is a debilitating age-related disorder that causes severe dementia and cognitive impairment resulting in a drastic decline in the quality of life. It was discovered by Alois Alzheimer (Alzheimer, 1995) in 1906 and named after him. AD is an age-associated disorder and people above the age of 65 years are at considerable risk of developing it (Brookmeyer, 1998). Senile dementia and loss of memory have been known to occur in the course of normal ageing (Berchtold, 1998). However, the development of AD greatly accelerates this process leading to presenile dementia. In modern times, the prevalence of AD has increased rapidly with the rise in life expectancy. According to the World Alzheimer Report 2009 (<http://www.alz.co.uk/>), approximately 115.38 million people could be suffering from dementia worldwide by 2050, which is roughly 1.67% of the entire human population today (6.87 billion approx.). Therefore, dementia and AD constitute a huge socio-

economic burden on our society. Therefore, it is imperative to develop effective therapeutic strategies to combat this neurological disorder in the coming decades.

1.2.1. Pathology of Alzheimer's disease

The classical pathological features of AD are β -amyloid plaques and neurofibrillary tangles in the brain (Tiraboschi, 2004). AD is also characterised by loss of neurons and synapses in the brain (Wenk, 2003). Magnetic resonance imaging (MRI) and positron emission tomography (PET) studies have reported a progressive reduction in the size of specific brain regions in patients as they proceed from MCI to AD (Karow, 2010). Lewy bodies that are aggregates of α -synuclein (Engelender, 2008) are also observed in the brains of AD patients (Kotzbauer, 2001). Genes involved in synaptic plasticity have also been found to be dysregulated in AD (Nelson, 2005).

1.2.1.1. Amyloid Pathology

The biochemical features of AD pathology involve the aggregation of $A\beta$ peptides in the brain (Hashimoto, 2003). $A\beta$ peptides are products of proteolytic cleavage of the β -amyloid precursor protein (APP) (Selkoe, 2001). Mutations in the *App* gene have been associated with the development of AD (Goate, 1998). APP is a type 1 membrane glycoprotein that undergoes ectodomain shedding by a proteolytic activity called α -secretase (Selkoe, 2002). Two disintegrin metalloproteinases, ADAM 10 and ADAM 17, have been shown to act as α -secretases for APP (Buxbaum, 1998; Kojro, 2001). The remaining C-terminal fragment (80 aa) is retained in the membrane and can then undergo constitutive cleavage by γ -secretase to release the p3 peptide that comprises of residues 17-40/42 of $A\beta$ (Selkoe, 2002) and the APP intracellular domain (AICD). Recent studies have shown that the AICD localises to both cytoplasm and nucleus (Cupers, 2001; Kimberly, 2001; Sastre, 2001). Alternatively, other APP holoproteins can be cleaved 16 residues N-terminal to the α -secretase site by a novel membrane-anchored aspartyl protease called β -secretase or BACE (Vassar, 2000). This scission creates C99 that is similarly processed by γ -secretase to yield $A\beta$ and AICD (Selkoe,

2002). A β peptides, particularly A β 42, when produced in excess or insufficiently cleared, can aggregate to form oligomers and large polymers and eventually amyloid fibrils (Selkoe, 2002). The aggregates are deposited extracellularly in the form of β -amyloid plaques (Selkoe, 2002). It is still not clear which of these aggregation states might be responsible for toxicity in AD. High levels of A β protein have been detected in the brains of AD patients (Gravina, 1995). Recently, it was shown that oligomers of A β impaired synaptic plasticity and memory (Shankar, 2008). Stable oligomers of A β have also been shown to block the maintenance of long-term potentiation (LTP) in rats (Walsh, 2002). Additionally, synthetic A β oligomers also impaired mitochondrial trafficking in neurons (Rui, 2006; Wang, 2010). Interestingly, intraneuronal mitochondrial distribution has been shown to be disrupted in AD (Wang, 2009a).

1.2.1.2. Tau Pathology

Along with the β -amyloid plaques, another characteristic feature of AD and the neurofibrillary tangles (NFTs) that comprise a hyperphosphorylated form of the microtubule-associated protein tau (Alonso, 2001; Goedert, 1993). The presence of NFTs is known to correlate with the severity of dementia in AD (Arriagada, 1992; Braak, 1991). The NFTs have been morphologically classified into three stages: pre-NFT, intraneuronal NFT and extraneuronal NFT. Specific sites on the tau protein have been shown to be hyperphosphorylated in AD. These sites include serine (S) 199, S202 and S409 in pre-NFTs, S396 and threonine (T) 231 in intraneuronal NFTs and S396 in extraneuronal NFTs (Kimura, 1996). Additionally, specific tau phosphorylation sites have been shown to correlate with cytopathology in AD (Augustinack, 2002). Recent studies have shown that tau mediates A β toxicity in AD (Ittner, 2010; Roberson, 2007). It was discovered that the deficiency of tau prevented memory deficits and improved survival in an AD transgenic mouse model (Ittner, 2010; Roberson, 2007). Another interesting study has revealed that the loss of Tau prevented A β -induced impairment of mitochondrial trafficking (Vossel, 2010).

1.2.2. Treatment of Alzheimer's disease

AD is still an incurable disease. The treatments currently available are palliative in nature and offer only mild symptomatic benefits. The activity of cholinergic neurons is reduced in AD (Geula, 1995). Therefore, inhibitors of cholinesterase have been used to maintain an elevated level of acetylcholine (ACh) and prevent the death of cholinergic neurons (Stahl, 2000). Currently, three cholinesterase inhibitors are being used to treat AD symptoms: Donepezil, Galantamine and Rivastigmine. These drugs have been shown to be effective in mild to moderate AD (Birks, 2006a; Birks, 2009) but only donepezil has been approved for the treatment of advanced AD (Birks, 2006b). Additionally, a non-competitive NMDA receptor antagonist, memantine, has been shown to be moderately efficacious in the treatment of moderate to severe AD (Areosa Sastre, 2004). All these drugs are only moderately effective against advanced AD and also produce significant adverse effects like muscle cramps, bradycardia, anorexia, hallucinations, confusion and fatigue.

Another compound shown to be effective against AD pathology is 3,5,4'-trihydroxy-trans-stilbene or resveratrol, a phytoalexin produced by plants under pathogenic attack. Recently, it was discovered that dietary supplementation with resveratrol reduced plaque pathology in a transgenic AD mouse model (Karuppagounder, 2009). Subsequent studies have revealed a protective effect of resveratrol treatment against pharmacologically induced cognitive impairment (Kumar, 2007; Kumar, 2006; Sharma, 2002). Resveratrol has also been shown to promote clearance of β -amyloid peptides (Marambaud, 2005). However, in spite of its beneficial effects in animal models, resveratrol has not been successfully tested in humans so far. Vitamin E has been shown to be protective against β -amyloid-induced oxidative stress in neurons (Butterfield, 1999). Another report has shown that users of antioxidant vitamin supplements exhibit a reduced risk of developing AD (Zandi, 2004).

Psychosocial interventions have also been used in combination with pharmaceutical treatments. Approaches such as cognitive rehabilitation, reminiscence therapy, validation therapy and sensory integration, also called snoezelen, have been effective in the treatment of cognitive symptoms (Bottino, 2005; Neal, 2003; Woods, 2005).

1.3. Epigenetics

The human DNA is organised into 23 pairs of chromosomes containing 3×10^9 base pairs. This adds up to two metres of DNA, which needs to be packed into the nucleus. To accomplish this, DNA is organised into chromatin, a complex of condensed DNA bound to proteins. Interestingly, the three-dimensional structure of chromatin is an important mechanism to regulate gene expression. The condensed form of chromatin is termed heterochromatin. This form of chromatin is generally inaccessible to the RNA transcription machinery. In contrast, the euchromatin represents a more open conformation and facilitates gene expression. The chromatin structure is extremely plastic and represents an important mechanism to translate environmental stimuli into alterations in gene expression. Conrad H. Waddington coined the term “epigenetics” to signify that it is not simply the DNA sequence that defines a cellular phenotype (Waddington, 1953). Epigenetics is now defined as heritable changes in gene expression that cannot be explained by the DNA sequence alone (Holliday, 1994). Epigenetic regulation of gene expression occurs chiefly through the covalent modification of DNA and histone proteins that together comprise the nucleosome (Sananbenesi, 2009).

1.3.1. Chromatin Plasticity

The basic structural unit of chromatin is the nucleosome, which consists of 147 bp of DNA wrapped around a protein octamer core made of two molecules each of histones H2A, H2B, H3 and H4 (Sananbenesi, 2009). Both the DNA and the histones are prone to covalent modifications that together form the basis of chromatin plasticity. The histones contain N-terminal tails that are susceptible to covalent post-translational modifications such as acetylation, phosphorylation, methylation, ubiquitination, sumoylation and ADP-ribosylation (Strahl, 2000; Vaquero, 2003). Histone acetylation is maintained at a steady state under physiological conditions in the cell (Shahbazian, 2007). Histone hyperacetylation is associated with elevated gene expression and the hypoacetylation of histones represses gene expression (Kurdistani, 2004; Li, 2007). Histone methylation is regarded to be a marker for gene repression (Li, 2007). DNA

methylation involves the addition of a methyl group to a cytosine base at CpG dinucleotides called CpG islands that occur in gene promoters and regulate gene expression (Klose, 2006). These covalent modifications collectively render the chromatin highly dynamic and regulate gene transcription.

1.3.2. Histone Acetylation

The lysine residues on the N-terminal tails of histones are prone to acetylation (Roth, 2001). A balanced state of histone acetylation is maintained by two families of enzymes: Histone Acetyltransferases (HATs) that add an acetyl group to lysine residues on histones and Histone Deacetylases (HDACs) that remove acetyl groups from the histones (Reid, 2000; Vogelauer, 2000). Increased acetylation at the promoter regions of genes has been shown to correlate with the recruitment of HATs and increased gene expression (Kuo, 2000). Conversely, the hypoacetylation of histones correlates with the recruitment of HDACs to repressed genes (Khochbin, 2001; Li, 2007). It has been shown that histone acetylation enhances the accessibility of DNA to transcription factors possibly by lowering the positive charge on the N-terminal tails of histones and thereby reducing DNA-histone interaction. It has been proposed that distinct histone modifications, such as acetylation, act sequentially or collectively to form a “histone code” that leads to further downstream events by binding transcription factors (Strahl, 2000).

1.3.3. Histone Acetylation in Memory

The process of memory formation is associated with altered gene expression (Peleg, 2010). It has been found that associative memory formation in rats displays a transient increase in histone H3 acetylation in the hippocampus (Levenson, 2004). Similar results have been obtained in the crab showing that total histone H3 levels are elevated after strong training (Federman, 2009). The process of fear conditioning leads to altered histone acetylation and methylation in the regions of memory-related genes such as *Bdnf*, *Zif268*, *PP1* and *reelin* (Gupta, 2010; Lubin, 2008). Previous work from our

laboratory has revealed that acetylation of histone H4 lysine 12 (H4K12) is crucial for memory consolidation and also specifically deregulated in age-associated memory impairment (AAMI) (Peleg, 2010). The same study also revealed that H4K12 acetylation is associated with the upregulation of certain genes during memory consolidation. These include *Fmn2*, *Myst4*, *Prkca*, *Shank3*, *Gsk3a*, *Marcks11*, *Acly* and *Ncdn* (Peleg, 2010). Interestingly, one of these upregulated genes, *Myst4*, codes for a histone acetyltransferase (Avvakumov, 2007). Further unpublished research from our laboratory has shown dysregulated histone acetylation in the brain in APPPS1-21 mice, a double transgenic AD mouse model (Radde, 2006). By immunohistochemical analysis, it was shown that histone acetylation was significantly decreased at H3K9, H3K14, H4K8, H4K12 and H4K16 in the hippocampi and cortices of APPPS1-21 mice compared to age-matched wild type controls. As described in section 2.1.2, the APPPS1-21 mice exhibit robust β -amyloid pathology accompanied by cognitive impairment.

1.3.4. Histone Acetyltransferases

Histone acetyltransferases (HATs) are enzymes that add an acetyl group to lysine residues on histone tails (Narlikar, 2002). The two main classes of HATs are the type A nuclear HATs and type B cytoplasmic HATs (Narlikar, 2002). Type A HATs can be further subdivided into three families: the GNAT family, the MYST family and the P300/CBP family (Narlikar, 2002). The MYST family of HATs are highly conserved in eukaryotes and are known to play critical roles in gene-specific transcription regulation, DNA damage response and repair and DNA replication (Avvakumov, 2007). A member of the GNAT family, *Gcn5* has been shown to acetylate lysines 9, 13, 18 and 27 on histone H3 (Grant, 1999). The type B HATs have not been very well characterised so far. The only known member is HAT1 that is involved in the acetylation of newly formed histones during chromatin assembly (Parthun, 2007), catalyses the acetylation of lysines 5 and 12 on histone H4 and is also involved in DNA repair (Benson, 2007). It has been shown that increased HAT activity in the insular cortex is associated with novel taste learning (Swank, 2001).

1.3.5. Histone Deacetylases

Histone deacetylases (HDACs) are enzymes that catalyse the removal of acetyl groups from histones and lead to repression of gene expression (Haberland, 2009). There are 11 proteins with a conserved deacetylase domain encoded by mammalian genomes. These are classified into 4 classes (class I, IIa, IIb and IV). This classification was primarily based on protein sequence. Therefore, the HDACs vary greatly in terms of expression, localisation and functions. Additionally, another group of enzymes called Sirtuins also function as HDACs in mammals (Schwer, 2008). There are 7 Sirt proteins known and they require NAD⁺ for their action. Recent findings have suggested that both HATs and HDACs might have substrates other than histones (Glozak, 2005). Therefore, HDACs are referred to as lysine deacetylases (KDACs) emphasising their action on non-histone proteins apart from histones (Choudhary, 2009).

1.3.5.1. Class I HDACs

Class I consists of HDAC1, HDAC2, HDAC3 and HDAC8. These HDACs share homology with the yeast protein Rpd3 (Taunton, 1996; Yang, 2008). HDAC1 and HDAC2 associate with repressor complexes such as the Sin3, NuRD, CoREST and PRC2 (Yang, 2003). HDAC1 has been shown to a major deacetylase in embryonic stem (ES) cells (Haberland, 2009). The null mutant of *Hdac1* is lethal before embryonic day 10.5 (E10.5) (Lagger, 2002). HDAC2-null mice die within 24 h of birth due to excessive proliferation of cardiomyocytes (Montgomery, 2007). An interesting study has shown that neuron-specific overexpression of *Hdac2* caused impairment of memory and reduction in spine density and synapse number in mice (Guan, 2009). Conversely, the deficiency of HDAC2 was found to be beneficial for memory (Guan, 2009). The same study shows that the overexpression of *Hdac1* is not detrimental to memory formation. This shows that HDAC2 negatively regulates cognition in mice. Additionally, Loss of *Hdac3* has been shown cause defective DNA double-stranded break repair (Bhaskara, 2008).

1.3.5.2. Class IIa HDACs

HDAC4, HDAC5, HDAC7 and HDAC9 belong to the class IIa HDAC family. HDAC5 and HDAC9 are enriched in the muscle, HDAC7 in the endothelial cells and thymocytes and HDAC4 is abundant in the brain and growth plates of the skeleton (Haberland, 2009). HDAC 5 and 9 have been shown to be essential for cardiovascular growth and development (Chang, 2004). HDAC9 modulates motor innervation of skeletal muscle (Mejat, 2005). An interesting study has shown that HDAC4 is exported out of the nucleus upon spontaneous electrical stimulation in neurons (Chawla, 2003). However, in the same study, HDAC5 translocation required the stimulation of calcium flux (Chawla, 2003). This shows that, in neurons, HDAC4 and HDAC5 could be associated with neuronal activity.

1.3.5.3. Class IIb HDACs

The class IIb HDAC family comprises a unique member of the HDAC superfamily, HDAC6, and HDAC10 (Haberland, 2009). HDAC6 is an atypical member that contains two catalytic domains and acts on cytoplasmic substrates such as α -tubulin, Hsp90 and cortactin (Haggarty, 2003; Verdel, 2000; Zhang, 2006). HDAC6 is mainly localised in the cytoplasm but can shuttle to the nucleus by virtue of its N-terminal nuclear export signal (Verdel, 2000). HDAC6 is known to regulate cytoskeletal stability, intracellular transport and cell motility through the deacetylation of lysine 40 of α -tubulin (Hubbert, 2002). HDAC6 is also involved in the regulation of protein ubiquitination via its zinc finger domain (Seigneurin-Berny, 2001). HDAC6 has been shown to rescue neurodegeneration in *Drosophila* by activating an autophagy-dependent pathway upon impairment of the ubiquitin-proteasome system (Pandey, 2007). Collectively, these studies implicate HDAC6 in the regulation of neuronal functions (Valenzuela-Fernandez, 2008).

1.3.5.4. Class IV HDAC

Only one member of the HDAC family has been classified to class IV, HDAC11. It has been shown that HDAC11 regulates oligodendrocyte-specific gene expression and oligodendrocyte development (Liu, 2009).

1.3.6. HDAC Inhibition in Neurodegeneration

As described above, HDACs are known to act as negative regulators of gene expression. Therefore, inhibition of HDAC activity promotes gene expression under physiological and pathological conditions. This makes HDAC inhibitors promising therapeutic agents in treating neurodegenerative disorders that involve the deregulation of gene expression like AD, HD and MCI.

1.3.6.1. Non-specific HDAC Inhibition

Broad-spectrum HDAC inhibitors like sodium butyrate (SB) have proven to be beneficial against cognitive impairment in animal models of neurodegeneration (Fischer, 2007). The administration of valproate, another non-specific HDAC inhibitor, immediately after traumatic brain injury has been found to be neuroprotective (Dash, 2010). In a study conducted on the Tg2576 AD mouse model, treatment with sodium 4-phenylbutyrate (4-PBA) could reverse spatial memory impairment and reduce tau phosphorylation (Ricobaraza, 2009). Another study has reported that SB, valproate and suberoylanilide hydroxamic acid (SAHA) ameliorated contextual fear memory deficit in APP^{swe}/PS1^{dE9} mice (Kilgore, 2010). HDAC inhibitors have also shown therapeutic potential in against polyglutamine disorders such as HD (Butler, 2006).

1.3.6.2. HDAC6 Inhibition

Due to its atypical nature, HDAC6 is an interesting molecule in the context of cognition and neurodegeneration. HDAC6 is known to be a deacetylase of α -tubulin. It has been shown that acetylation of α -tubulin at lysine 40 could enhance the recruitment of kinesin-1 to microtubules and facilitate the anterograde transport of kinesin-1 cargo protein JIP1 in differentiated neuronal cells from *Tetrahymena thermophila* (Reed, 2006). In another study, elevation of α -tubulin acetylation by HDAC6 inhibition was shown to enhance BDNF transport and rescue the transport deficient in HD (Dompierre, 2007). Neuronal migration has also been shown to be dependent on α -tubulin acetylation (Creppe, 2009). Knockdown of *Hdac6* using siRNA was found to enhance the delivery of EGF and EGF-bound EGFR to late endosomes (Deribe, 2009). Additionally, knockdown of *Hdac6* using siRNAs was also shown to protect cultured cortical neurons against neurodegeneration induced by oxidative stress and promote neurite outgrowth (Rivieccio, 2009). Additionally, pharmacological inhibition of HDAC6 by tubacin resulted in enhanced mitochondrial trafficking in cultured hippocampal neurons (Chen, 2010). Taken together, the loss of HDAC6 activity could be significantly beneficial in neurodegenerative disorders via the facilitation of intraneuronal transport. This makes HDAC6 a promising drug target against neurological disorders such as AD and HD and merits deeper investigation.

1.4. Objectives of the study

Based on the data available so far, this study was designed to investigate the role of HDAC inhibition in a double transgenic AD mouse model. The project consisted of two basic objectives.

1.4.1. Treatment of advanced AD Pathology with SB

HDAC inhibitors like SB have been shown to improve cognition in other animal models of AD. However, the previous studies have focused on early pathological stages in their

respective AD mouse models. Since patients of AD are often diagnosed late and found to be suffering from advanced stages of pathology, it is crucial to investigate therapeutic approaches in corresponding stages in mice. Therefore, this project was aimed at studying the role of HDAC inhibition by orally administered SB on cognition in APPPS1-21 (described in Section 2.1.2) mice. Furthermore, analysis of the molecular mechanisms underlying the effects of SB treatment was also planned. This objective aims to understand the mechanism underlying the beneficial effect of HDAC inhibition in neurodegeneration.

1.4.2. Role of HDAC6 in Cognition and AD

Given its unique function on cytoplasmic non-histone proteins like α -tubulin, HDAC6 was an obvious choice to study the role of lysine deacetylation outside the nucleus. For this purpose, this research study was aimed at analysing mice globally deficient in HDAC6 (Section 2.1.1) using behavioural and molecular techniques. Additionally, to study the specific loss of *Hdac6* in AD, the APPPS1-21 and *Hdac6* knockout mice were to be interbred and analysed using behavioural and molecular techniques. This objective aims at understanding the role of a HDAC6 in cognition and AD.

2. Materials and Methods

2.1. Animals

The model organism used for this study was *Mus musculus* (house mouse). The mouse strain used was C57BL/6, unless otherwise mentioned. All mice were housed in individually ventilated cages (IVC, 32 cm × 16 cm × 14 cm, TECNIPLAST, Buguggiate, Italy) at the Animal Facility of the European Neuroscience Institute, Göttingen, Germany. Mice were fed nutritionally balanced food pellets and drinking water ad libitum. They were maintained under standard light/dark conditions (12 h light, 12 h dark). Behavioural experiments were performed during the light period of the cycle. The knockout and transgenic mouse models used in this study are explained below (Sections 2.1.1 and 2.1.2).

2.1.1. *Hdac6* Knockout Mice

The 129/Sv mouse strain was used to generate global *Hdac6* knockout (KO) mice (Dr. Jianrong Lu, Current Affiliation: Asst. Prof., Dept. of Biochemistry and Molecular Biology, University of Florida, USA). The initial breeding pairs were transported from Harvard University, Boston, USA to our animal facility and inbred to form our own colony. The newborn pups were weaned at three weeks of age, males and females were separated and group housed. The male mice used for behavioural characterisation were individually housed. For all experiments, age- and sex-matched wild type (WT) littermates were taken as controls.

2.1.2. Double Transgenic APPPS1-21 Mice

As a mouse model for Alzheimer's disease (AD), the APPPS1-21 double transgenic mice were employed (Radde, 2006). This is a novel transgenic mouse model that

coexpresses KM670/671NL ‘Swedish’ mutated amyloid precursor protein (APP) and L166P mutated presenilin 1 (PS1) genes on a C57BL/6J background (Radde, 2006). The L166P mutation in PS1 is known to cause severe pathology in AD patients with early disease onset and high A β 42 to A β 40 ratio in the brain (Bentahir, 2006; Moehlmann, 2002). The APP ‘Swedish’ mutation LM670/671NL is also commonly found in familial cases of AD and has been used to generate transgenic mouse models (Hsiao, 1996; Sturchler-Pierrat, 1997). The APPPS1-21 double transgenic mice generated by Radde and colleagues exhibit an aggressive β -amyloid pathology similar to that observed in familial AD brain and cognitive deficits at an early age. Therefore, this mouse model was selected to study the effect of loss of HDAC activity in AD.

2.1.3. Implantation of Microcannulae

For the purpose of intra-cerebral drug administration, microcannulae were implanted on the mouse skull using stereotaxic surgery. The mouse was anaesthetised with a single intra-peritoneal injection of 500 μ l of Avertin. The mouse was then placed on the stereotaxic stage. The mouthpiece was hooked on the incisors and the head was held firm using the ear bars. The head was maintained in a horizontal position and the mouthpiece and ear bars were firmly screwed in place. The skin on the head was incised between one eye and the contralateral ear. The hypodermal connective tissue was removed using a scalpel and the bregma was located. A micro-drill with a 0.2 mm drill bit was used to drill holes in the skull. The coordinates for drilling holes were determined based on the position of the target region according to the Mouse Brain Atlas (Paxinos and Franklin). For intra-hippocampal injections, the drill was initially placed above the bregma and moved 1.2 μ posterior to the bregma. One hole was drilled on each side, right and left, 1.0 μ away from the midline. Any bleeding was cleaned with a cotton swab soaked in 70% ethanol. A microcannula was then affixed on the skull holes using dental cement paste. The skin was also sealed with the dental cement paste. Upon solidification of the dental cement, the mouse was wrapped up in a soft paper towel and warmed on a warm plate (37 °C) for 10 min and finally returned to its home cage. The mice implanted with microcannulae were individually housed and observed for a week before commencement of experiments.

2.1.4. Intra-Hippocampal Drug Administration

Pharmacological treatment of the hippocampus was achieved by injecting a drug directly into the hippocampus through microcannulae implanted on the mouse skull (Section 2.4) using a SP2201Z Syringe Pump (WPI, Berlin, Germany).

The effect of acute HDAC6 inhibition was studied by injecting a specific HDAC6 inhibitor, ST27 (Prof. Manfred Jung, University of Freiburg, Germany). ST27 was dissolved in DMSO to give a 5 mM stock, which was further diluted to a 2.5 mM solution in 2x ACSF. From this solution, 1 μ l was injected into the hippocampus (0.5 μ l bilaterally) using a 2 mm micro-injector at a rate of 1 μ l/min. The control received the same volume of vehicle solution (50% DMSO + 50% 2x ACSF) at the same rate. Mice were anaesthetised using isoflurane prior to and during injection.

2.1.5. Brain Extraction for Molecular Analysis

For molecular and biochemical analysis, a mouse was sacrificed by cervical dislocation. The blunt edge of a butter knife was used to hold the back of the mouse's neck and its tail was pulled immediately to break its cervical vertebrae. The mouse cadaver was decapitated, the skin on the head was cut along the midline and the skull bones were severed with one cut along the median fissure and one lateral cut along the temporal bones using surgical scissors. The bones were removed using surgical forceps and the brain was scooped out as a whole with a surgical spatula on a cold surface. The optic nerves were severed to separate the brain from the head. The brain was cut along the midline using a scalpel. The cortical hemispheres were opened using the blunt edge of a scalpel blade to reveal the hippocampus beneath, which was isolated along with the cortex and cerebellum. The isolated tissues were enclosed in 1.5 ml microcentrifuge tubes with pierced lids and frozen immediately in liquid N₂ and subsequently stored till further use at -80 °C.

2.1.6. Brain Extraction for Histology

For histological analysis, a mouse was anaesthetised with a single intra-peritoneal injection of 1 ml of Avertin. A peristaltic pump (Heidolph, Schwabach, Germany) was setup with 0.01 M PBS and 4% paraformaldehyde (PFA) on ice. A sterile needle was fixed to one end of the duct for perfusion. The duct was washed with sterile PBS solution before perfusion and any air present in the duct was pumped out. The anaesthetized mouse was placed on a Styrofoam stage and its limbs were fixed using sterile needles. The abdominal skin and body wall were severed using surgical scissors and the diaphragm was cut to expose the beating heart. The perfusion needle was inserted into the left ventricle of the heart and the mouse was perfused with 0.01 M PBS for 2 min to wash away the blood from the circulatory system. Thereafter, the pump was stopped, the perfusion duct was immersed in 4% PFA and the pump was turned on again for about to perfuse the mouse with PFA for 5 min. Optimal perfusion was indicated by the twitching of the tail. After perfusion, the mouse cadaver was decapitated and the brain was extracted as described above (Section 2.1.5). The brain was post-fixed in 4% PFA for 24 h at 4 °C in 50 ml conical tubes (Sarstedt, Nümbrecht, Germany). The brain was then cryoprotected by immersing in 30% sucrose solution in 0.01 M PBS at 4 °C in 50 ml conical tubes till the brain sank completely and finally frozen over liquid N₂ and subsequently stored at -80 °C.

2.2. Behavioural Analysis of Mice

Cognition in mice was assessed using a battery of behavioural tests. Exploratory behaviour was assessed in an open field. Basal anxiety was measured with an elevated plus-maze task. The fear conditioning paradigm was employed to analyse associative memory and spatial memory was tested in the Morris Water Maze task. Motor functions were analysed on the rotarod. All behavioural tests were carried out during the light phase (Section 2.1).

2.2.1. Open Field

The open field was used to assess exploratory behaviour in mice. Mice were exposed to a square open arena (80 cm) with an opaque base and transparent walls (20 cm high). Each mouse was subjected to the open field for 5 min and its activity was recorded using the VIDEOMot2 (version 5.72) video tracking system (TSE, Berlin, Germany). The field was evenly lit using dim incandescent light bulbs and cleaned with 70% ethanol after every mouse. The time spent by the mouse in the central part of the field versus the periphery was taken as a measure of exploratory behaviour.

2.2.2. Elevated Plus-Maze

The elevated plus-maze was used to assess basal anxiety in rodents. Our setup consisted of a plus shaped arena situated at an elevation of 53 cm from the ground. Each rectangular arm measured 45 cm × 10 cm and the central field was a square measuring 10 cm. Two opposite arms were closed on three sides by opaque walls 30 cm high. The mouse was placed in the centre and allowed to explore the maze for 5 min while its activity was recorded using the VIDEOMot2 (version 5.72) video tracking system (TSE, Berlin, Germany). The plus-maze was evenly lit using dim incandescent lights and cleaned with 70% ethanol after each mouse. The times spent by the mouse in the closed and open arms were taken as a measure of basal anxiety level. Longer time spent in the closed arms indicates a higher level of anxiety.

2.2.3. Contextual Fear Conditioning

To assess associative memory in mice, the contextual fear conditioning paradigm was used. In this test, a conditioned stimulus (CS, context) was paired with an unconditioned stimulus (US, electric foot shock) to yield a conditioned response (CR, freezing). In our paradigm, the training session consisted of exposure to a novel context for 3 min followed by a single electric foot shock (0.7 mA). This hippocampus-dependent task leads to robust memory formation with a single associative event. Upon re-exposure to

the same context at a later time, unlike the first exposure, the mouse sits still without showing any movement apart from respiration and shivering, a behaviour known as “freezing”. This freezing behaviour was quantified by observing the mouse even tenth second during a 3 min re-exposure to the context and recording if the mouse was freezing. The number of freezes exhibited by the mouse over 3 min (18 recordings) indicates the strength of the fear memory. Repeated exposures to the context (CS) without the electric shock (US) leads to a progressive decline in freezing behaviour exhibited by the mouse, a process called “extinction of learned fear” or “fear extinction”.

2.2.4. Tone Fear Conditioning

Tone fear conditioning involves the coupling of a tone (CS) along with an electric foot shock (US) that causes a mouse to freeze (CR). Unlike contextual fear conditioning, this is an amygdala-dependent task. In our paradigm, the training was performed in conjunction with contextual fear conditioning. After the 3 min exposure to the context (Section 2.2.3), the mouse was subjected to a tone for 30 sec followed by the electric foot shock (0.7 mA). To test tone-dependent associative memory, the mouse was then exposed to the same tone in a different context at a later time. The mouse exhibited freezing behaviour similar to contextual fear conditioning. Freezing was scored as described in section 2.2.3.

2.2.5. Morris Water Maze

Spatial memory was tested in mice using the Morris Water Maze task. This test was first described by Richard G. M. Morris in rats (Morris, 1981) and has been subsequently modified for mice. Mice were exposed to a circular pool of water (maintained at 18 °C) with a submerged platform. The water was made opaque by adding a non-toxic white dye. Visual orientation cues were provided around the pool. The room was even lit with dim incandescent lights.

Each trial consisted of exposing the mouse to the pool from the periphery for 1 min or till it located the platform and allowed to sit on the platform for 15 sec. This was intended to let the mouse orient itself according to the visual cues. Each mouse was given four trials, one each from four starting points in the periphery of the pool. The swim pattern of the mouse was recorded using the VIDEOMot2 (version 5.72) video tracking system (TSE, Berlin, Germany). The training session comprising four trials was performed everyday and the time taken by the mouse to locate the platform, the escape latency, was plotted to monitor its progress. When the mice could locate the platform within 10 sec (criterion), training was considered accomplished.

The day after the accomplishment of training, the platform was removed from the pool and each mouse was allowed to swim in the pool for 1 min. This test, called the probe test, gives an indication of the spatial memory acquired by the mouse based on its swim pattern. A mouse that has acquired a specific strategy to locate the platform tends to swim directly to the location and continues swimming around it. However, a mouse that could locate the platform during training by chance or thigmotaxis swims around the entire pool without any definite preference to the region of the platform. The water pool can be virtually divided into four quadrants, one of which contains the platform, and the time spent by the mouse in each quadrant can be plotted. A significant preference to the quadrant that contained the platform, the target quadrant, indicates a strong spatial memory acquisition.

2.2.6. Rotarod Performance Test

Motor function was assessed using the Rotarod test (TSE, Berlin, Germany). The task involves placing a mouse on a rotating rod to test its endurance in staying on the rod. Each mouse was initially habituated on the rotarod at 10 rpm for 3 min. Four habituation sessions of 3 min each were given to each mouse over 2 days. During habituation, a mouse that fell off the rotating rod was placed back on the rod again till the end of 3 min. The testing phase consisted of four testing sessions over four days, each comprising 3 min on the rotarod with constant acceleration (5-40 rpm) followed by

1 min with constant speed (40 rpm). The time required by the mouse to fall off the rotating rod in each testing session was plotted to assess performance.

2.3. Molecular Biology

2.3.1. Nucleic Acid Extraction

The nucleic acids, DNA and RNA, were extracted from animal tissue for molecular biological applications. The extraction protocols followed are described below.

2.3.1.1. DNA Isolation for Genotyping

Genomic DNA isolated from tail tissue was used to genotype all knockout and transgenic mice. Genotyping was performed using polymerase chain reaction (PCR) as explained below (Section). Mice pups were weaned at three weeks of age and tail biopsies were taken in 1.5 ml tubes (Eppendorf, Hamburg, Germany) for genomic DNA isolation and stored at -20 °C. Tail tissue was digested by incubation in 500 µl of tail lysis buffer (100 mM Tris-HCl, 5 mM EDTA, 200 mM NaCl, 0.2% SDS, pH 8.0) with 12.5 µl of Proteinase K solution (20 mg/ml, Carl Roth, Karlsruhe, Germany) per tail biopsy in a Thermomixer comfort (Eppendorf, Hamburg, Germany) at 55 °C and 800 rpm for 14-16 h. After digestion, the lysate was spun at 10,000 rpm in an Eppendorf Centrifuge 5425 (Eppendorf, Hamburg, Germany) for 10 min at room temperature (RT). The supernatant was transferred to a new 1.5 ml tube and 500 µl of isopropanol (Carl Roth, Karlsruhe, Germany) were added and mixed by inversion. The solution was centrifuged at 10,000 rpm for 10 min at RT. The supernatant was discarded and the pellet containing genomic DNA was washed once by adding 500 µl of 70% ethanol and centrifuging at 10,000 rpm for 10 min at room temperature (RT). The supernatant was discarded and the pellet was dried at RT for about 10 min. After drying, the pellet was dissolved in 100 µl ddH₂O and stored at 4 °C.

2.3.1.2. RNA Isolation

Total RNA was isolated from frozen brain tissue (Section 2.1.5) using the TRI-Reagent (Sigma-Aldrich, Steinheim, Germany). Frozen brain tissue was manually homogenised in 500 μ l of TRI-Reagent using a micropestle. After complete homogenisation, 500 μ l of TRI-Reagent were added and the lysate was transferred to a new 1.5 ml microcentrifuge tube and incubated at RT for 5 min. Thereafter, 0.2 ml of chloroform were added to the lysate and mixed by inverting the tube vigorously. The mixture was spun at $12,000 \times g$ for 15 min at 4 °C. Following centrifugation, the mixture separated into a lower red, phenol-chloroform phase, an interphase and a colourless upper aqueous phase, which was transferred to a new 1.5 ml microcentrifuge tube. The other two phases were stored at -20 °C for protein isolation (Section 2.3.9.2). RNA precipitation was achieved by adding 0.5 ml isopropanol to the aqueous phase and incubating at RT for 10 min. The solution was spun at $12,000 \times g$ for 10 min at 4 °C. The RNA precipitate formed a gel-like pellet on the side and bottom of the tube. The supernatant was carefully removed with a micropipette and discarded. The RNA pellet was washed by adding 1 ml of 75% ethanol and centrifuging at $7,500 \times g$ for 5 min at 4 °C. The supernatant was discarded and the pellet was dried at RT briefly and dissolved in 30 μ l ddH₂O. The RNA solution was stored on ice and its concentration was measured using a NanoDrop Spectrophotometer (Peqlab, Erlangen, Germany). The RNA solution was either used immediately for cDNA synthesis or stored at -80 °C till further use.

2.3.2. Reverse Transcription

Total RNA isolated from brain tissue (Section 2.3.1.2) was used to synthesise cDNA by *in vitro* reverse transcription using the Transcriptor First Strand cDNA Synthesis Kit (Roche Applied Science, Mannheim, Germany). Initially, 1.0 μ g of RNA were mixed with 2.0 μ l of random hexamers (600 pmol/ μ l) and PCR-grade H₂O upto a volume of 13.0 μ l in a 0.2 ml micro test tube (Nerbe Plus, Winsen/Luhe, Germany). The mixture was incubated at 65 °C for 10 min in a Mastercycler ep *gradient* S (Eppendorf, Hamburg, Germany) to allow denaturation of RNA secondary structures. Following

denaturation, 0.5 μ l of the Transcriptor Reverse Transcriptase enzyme (20 U/ μ l), 2.0 μ l of the Deoxynucleotide Mix (10 mM each), 4.0 μ l of the 5x Transcriptor Reverse Transcriptase Reaction Buffer and 0.5 μ l of the Protector RNase Inhibitor (40 U/ μ l) were mixed in the tube and incubated at 25 °C for 10 min followed by incubation at 55 °C for 30 min in the Mastercycler ep *gradient* S. The Transcriptor Reverse Transcriptase enzyme was inactivated by incubating at 85 °C for 5 min in the Mastercycler ep *gradient* S. The cDNA was then stored at 4 °C.

2.3.3. Polymerase Chain Reaction

DNA was amplified by the process of polymerase chain reaction (PCR). DNA oligonucleotides targeting a specific region on the template DNA strand were used as primers (Section 2.3.3.6).

2.3.3.1. Hdac6 Genotyping PCR

The *Hdac6* genotyping PCR was performed using the RedTaq™ Readymix™ PCR Reaction Mix (Sigma-Aldrich, Germany) in a Mastercycler ep *gradient* S (Eppendorf, Hamburg, Germany). The PCR reaction mix protocol and the PCR program are explained below (Tables 2.1 & 2.2). Thin walled 0.2 ml micro test tubes were used (Nerbe Plus, Winsen/Luhe, Germany).

Table 2.1: Reaction mix for *Hdac6* genotype PCR.

Reagent	Amount
Genomic DNA (100 ng/ μ l)	5.00 μ l
RedTaq PCR Mix	10.00 μ l
<i>Hdac6</i> Genotype F (10 μ M)	1.00 μ l
<i>Hdac6</i> Genotype R (10 μ M)	1.00 μ l
NEO Genotype F (10 μ M)	1.00 μ l
NEO Genotype R (10 μ M)	1.00 μ l
ddH ₂ O	1.00 μ l
Total Volume	20.00 μl

Table 2.2: Cyclor program for *Hdac6* genotype PCR.

Temperature	Duration	
95 °C	3 min	
95 °C	1 min	35 X
62 °C	1 min	
72 °C	1 min	
72 °C	10 min	
4 °C	∞	

2.3.3.2. APPPS1-21 Genotyping PCR

In the APPPS1-21 double transgenic mice, the mutant APP and PS1 genes are linked. Therefore, these mice were genotyped by PCR using primers targeting the mutant APP gene (Tables 2.3 & 2.4). The PCR was performed as explained in Tables 2.3 and 2.4, in a Mastercycler ep *gradient* S (Eppendorf, Hamburg, Germany) using DreamTaq™ DNA Polymerase (5 U/μl), 10x DreamTaq Buffer (including 20 mM MgCl₂) and dNTP mix (25 mM each) from Fermentas, St. Leon-Rot, Germany.

Table 2.3: Reaction mix for APPPS1-21 genotype PCR reaction mix.

Reagent	Amount
Genomic DNA (100 ng/μl)	5.00 μl
10x DreamTaq Buffer	2.50 μl
dNTP Mix (25 mM each)	1.00 μl
APPforward (10 mM)	0.50 μl
APPreverse (10 mM)	0.50 μl
DreamTaq Polymerase (5 U/μl)	0.05 μl
ddH ₂ O	15.45 μl
Total Volume	25.00 μl

Table 2.4: Cycler program for APPPS1-21 genotype PCR.

Temperature	Duration	
95 °C	3 min	
95 °C	1 min	35 X
62 °C	1 min	
72 °C	1 min	
72 °C	10 min	
4 °C	∞	

2.3.3.3. Semi-Quantitative PCR for Gene Expression Analysis

The expression of *Hdac6* in the brains of wild type and *Hdac6* knockout mice was analysed by semi-quantitative PCR. As described in sections 2.3.1.2 and 2.3.2, total mRNA was isolated from hippocampus and cortex of wild type and *Hdac6* knockout mice and 1.0 µg was used to synthesise cDNA by reverse transcription. Expression of *Hdac6* was analysed using semi-quantitative PCR using the reagents mentioned in section 2.3.3.2 as outlined in Tables 2.5 & 2.6. The primers used are mentioned in Table 2.13. DMSO was added to enhance specific primer binding. The PCR products were resolved by electrophoresis on a 1% agarose gel (Section 2.3.4). The housekeeping gene *Gapdh* was taken as an internal reference.

Table 2.5: Reaction mix for *Hdac6* semi-quantitative PCR mix.

Reagent	Amount
cDNA (100 ng/µl)	2.00 µl
10x DreamTaq Buffer	2.50 µl
MgCl ₂ (25 mM)	1.50 µl
DMSO	1.25 µl
dNTP Mix (25 mM each)	1.00 µl
Forward Primer (10 mM)	1.00 µl
Reverse Primer (10 mM)	1.00 µl
DreamTaq Polymerase (5 U/µl)	0.05 µl
ddH ₂ O	14.70 µl
Total Volume	25.00 µl

Table 2.6: Cycler program for *Hdac6* semi-quantitative PCR.

Temperature	Duration	
95 °C	5 min	
95 °C	30 sec	30 X
61 °C	30 sec	
72 °C	30 sec	
72 °C	5 min	
4 °C	∞	

2.3.3.4. Quantitative Real-Time PCR for Gene Expression Analysis

Gene expression analysis was performed using quantitative real-time PCR (qPCR) using primers specified by the Roche Universal Probe Library (UPL) and the specific fluorescence probe recommended in an LC480 LightCycler (Roche Applied Science, Mannheim, Germany). The primers and the respective UPL probes are listed in Table 2.12. As described in section 2.3.2, cDNA was synthesised from 1.0 µg of RNA and diluted 10-fold. The control cDNA samples were pooled to yield the undiluted standard sample that was serially diluted (1:5; 1:10; 1:50; 1:100 and 1:500) using PCR-grade water to yield standard dilutions that were used to generate a standard curve of fluorescence intensity versus DNA concentration. A 10-fold dilution of the undiluted standard sample was used as a positive calibrator. The qPCR was performed using the LightCycler PCR Mix (Roche Applied Science, Mannheim, Germany). The protocol for the PCR mix and the PCR program are described in Tables 2.7 & 2.8. All steps were carried out on ice under a sterile laminar hood. Initially, cDNA template was pipetted into the wells on a 96-well plate and a master mix was prepared with the primers, LightCycler PCR Mix and water and pipetted into the wells. The plate was sealed using the cellophane foil provided and spun at 1,250 rpm for 1 min in an Eppendorf Centrifuge 5810 R before starting the PCR. The housekeeping gene hypoxanthine guanine phosphoribosyltransferase 1 (*Hprt1*) was taken as an internal reference for normalisation of gene expression.

Table 2.7: Reaction mix for qPCR using the Roche UPL Probe.

Reagent	Amount
cDNA (100 ng/μl)	2.00 μl
Forward Primer (20 μM)	0.15 μl
Reverse Primer (20 μM)	0.15 μl
LC480 Probe Master Mix (2x)	7.50 μl
UPL Probe	0.15 μl
PCR-grade Water	5.05 μl
Total Volume	15.00 μl

Table 2.8: Cyclor program for qPCR in the Roche LightCycler 480.

Temperature	Duration	
95 °C	5 min	
95 °C	10 sec	30 X
60 °C	30 sec	
72 °C	10 sec	
40 °C	30 sec	

2.3.3.5. PCR Amplification of Hdac6 for Cloning

A human *Hdac6* cDNA clone was available in the pcDNA3.1+ vector with a poly-histidine tag. The *Hdac6* cDNA sequence was amplified using the pcDNA3.1+ construct as a template by PCR (Tables 2.9 & 2.10) using the forward primer: 5'-TCTAGACCACCATGACCTCAACCGGCCAGG-3' and the reverse primer: 5'-ACCGGTGGATCCGCGTGTGGGTGGGGCATATCCT-3' that contain the *XbaI* and *AgeI* restriction sites respectively. The PCR mix (Table 2.9) was prepared using *Pfu* II Ultra DNA polymerase and other reagents mentioned in section 2.3.3.2.

Table 2.9: Reaction mix for PCR amplification of *Hdac6* cDNA from pcDNA3.1+ construct.

Reagent	Amount
DNA Template (200 ng/ μ l)	1.00 μ l
10x DreamTaq Buffer	5.00 μ l
Forward Primer (10 μ M)	1.00 μ l
Reverse Primer (10 μ M)	1.00 μ l
dNTP Mix (25 mM each)	5.00 μ l
Pfu II Ultra DNA Polymerase	1.00 μ l
DreamTaq DNA Polymerase (5 U/ μ l)	0.10 μ l
PCR-grade Water	35.90 μ l
Total Volume	50.00 μl

Table 2.10: PCR program for amplification of *Hdac6* cDNA from pcDNA3.1+ construct.

Temperature	Duration	
95 °C	2 min	
95 °C	20 sec	30 X
61 °C	20 sec	
72 °C	1 min	
72 °C	3 min	
4 °C	∞	

2.3.3.6. Primers for PCR

Specific primers (Table 2.11, T_M : Melting Temperature) were used to perform genotyping PCR for the *Hdac6* knockout and APPPS1-21 double transgenic mice. The *Hdac6* genotyping primer sequences were obtained from Dr. Jianrong Lu, Harvard University, Boston, USA. To genotype the APPPS1-21 mice, primer sequences published by Radde and colleagues were used (Radde, 2006). The primer oligomers were ordered from Sigma-Aldrich, Taufkirchen, Germany in a lyophilised form and reconstituted with ddH₂O to a concentration of 100 μ M and further diluted with ddH₂O to a concentration of 10 μ M to be used for PCR.

Table 2.11: Primer sequences used for genotyping *Hdac6* knockout and APPPS1-21 transgenic mice.

S. No.	Primer	Sequence (5' – 3')	T _M
1.	<i>Hdac6</i> Genotype F	GCCAGGGATTGGGTAAACACAAGCTAG	60 °C
2.	<i>Hdac6</i> Genotype R	CACACGCACGCACACCAGATAAACAC	60 °C
3.	NEO Genotype F	AGGATCTCCTGTCATCTCACCTTGCTCCTG	64 °C
4.	NEO Genotype R	AAGAACTCGTCAAGAAGGCGATAGAAGGCG	64 °C
5.	APPforward	GAATTCGACATGACTCAGG	58 °C
6.	APPreverse	GTTCTGCTGCATCTTGGACA	58 °C

The following primers were used to perform qPCR using the Roche Universal Probe Library (UPL, Table 2.12). The primer oligomers were ordered from Sigma-Aldrich, Taufkirchen, Germany in a lyophilised form and reconstituted with ddH₂O to a concentration of 100 µM and further diluted with ddH₂O to a concentration of 10 µM to be used for real-time qPCR.

Table 2.12: Primers used for gene expression analysis in mouse by qPCR.

Primer	Sequence (5' – 3')	UPL Probe
<i>Acly</i> F	GCCCTGGAAGTGGAGAAGAT	#10
<i>Acly</i> R	CCGTCCACATTCAGGATAAGA	#10
<i>Fmn2</i> F	AACAGCAGAAGCCTTTTGTC	#89
<i>Fmn2</i> R	TTCTGCCAGTGGGAAGACA	#89
<i>GluR1</i> F	GCCCAATGCAGAGCTCAC	#100
<i>GluR1</i> R	GTCACTCCACTCGAGGTAAC	#100
<i>Gsk3a</i> F	GAGCCACAGATTACACCTCGT	#76
<i>Gsk3a</i> R	CTGGCCGAGAAGTAGCTCAG	#76
<i>Hprt1</i> F	TCCTCCTCAGACCGCTTTT	#95
<i>Hprt1</i> R	CCTGGTTCATCATCGCTAATC	#95
<i>Igf2</i> F	CGCTTCAGTTTGTCTGTTCG	#40
<i>Igf2</i> R	GCAGCACTCTTCCACGATG	#40
<i>Igfbp7</i> F	CCCTCCATGAAATACCACTGA	#110
<i>Igfbp7</i> R	GGCTGTCTGAGAGCACCTTT	#110
<i>Marcks11</i> F	GGCAGCCAGAGCTCTAAGG	#19
<i>Marcks11</i> R	TCACGTGGCCATTCTCCT	#19
<i>Myst4</i> F	GCAACAAAGGGCAGCAAG	#19
<i>Myst4</i> R	AGACATCTTTAGGAAACCAAGACC	#19

<i>Ncdn</i> F	GCTCCTTAGCACCTCTCCAG	#75
<i>Ncdn</i> R	GCAGCTGCGAAGAAACCT	#75
<i>Prkca</i> F	ACAGACTTCAACTTCCTCATGGT	#60
<i>Prkca</i> R	CTGTCAGCAAGCATCACCTT	#60
<i>Shank3</i> F	AGGACGTCCGCAATTACAAC	#97
<i>Shank3</i> R	AAGCTCAAAGTTCCCTGCAA	#97
<i>Snap25</i> F	GCTCCTCCACTCTTGCTACC	#88
<i>Snap25</i> R	CAGCAAGTCAGTGGTGCTTC	#88
<i>Hdac1</i> F	TGCTGGACTTACGAAACAGC	#81
<i>Hdac1</i> R	GTCGTTGTAGGGCAGCTCAT	#81
<i>Hdac2</i> F	CTCCACGGGTGGTTCACT	#45
<i>Hdac2</i> R	CCCAATTGACAGCCATATCA	#45
<i>Hdac3</i> F	TTCAACGTGGGTGATGACTG	#32
<i>Hdac3</i> R	TTAGCTGTGTTGCTCCTTGC	#32
<i>Hdac4</i> F	CACACCTCTTGAGGGTACAA	#53
<i>Hdac4</i> R	AGCCCATCAGCTGTTTTGTC	#53
<i>Hdac5</i> F	GAGTCCAGTGCTGGTTACAAAA	#105
<i>Hdac5</i> R	TACACCTGGAGGGGCTGTAA	#105
<i>Hdac6</i> F	GAAGGAGGAGCTGATGTTGG	#64
<i>Hdac6</i> R	TCATGTACTGGGTTGTCTCCAT	#64
<i>Hdac7</i> F	GCCCTTGAGAGAACAGTCCA	#45
<i>Hdac7</i> R	CCAAGGGCTCAAGAGTTCTG	#45
<i>Hdac9</i> F	TTGCACACAGATGGAGTGG	#32
<i>Hdac9</i> R	GGCCCATAGGAACCTCTGAT	#32
<i>Hdac10</i> F	TTCCAGGATGAGGATCTTGC	#60
<i>Hdac10</i> R	ACATCCAATGTTGCTGCTGT	#60
<i>Hdac11</i> F	ATCATGGCAGGGAAGCTG	#77
<i>Hdac11</i> R	CACTGGAGCAGTGGTGA	#77
<i>Sirt1</i> F	TCGTGGAGACATTTTAAATCAGG	#104
<i>Sirt1</i> R	GCTTCATGATGGCAAGTGG	#104
<i>Sirt2</i> F	CACTACTTCATCCGCCTGCT	#66
<i>Sirt2</i> R	CCAGCGTGTCTATGTTCTGC	#66
<i>Sirt3</i> F	TGCTACTCATTCTTGGGACCTC	#7
<i>Sirt3</i> R	GGGCACTGATTCTGTACTGC	#7
<i>Sirt5</i> F	CCAGCTTTAGCAGGAAAAGG	#21
<i>Sirt5</i> R	GACTGGGATTCTGGCGTCT	#21
<i>Sirt6</i> F	ACGCGGATAAGGGCAAGT	#82
<i>Sirt6</i> R	CTCCCACACCTTGCGTTC	#82

<i>Sirt7</i> F	TGCAACTCCTCATGAATGAACT	#80
<i>Sirt7</i> R	CGCCAAGGAGAAGATTGG	#80
<i>Hprt1</i> F	TCCTCCTCAGACCGCTTTT	#95
<i>Hprt1</i> R	CCTGGTTCATCATCGCTAATC	#95

The following primers were used for semi-quantitative PCR to verify *Hdac6* expression in *Hdac6* KO and WT mice (Table 2.13).

Table 2.13: Primers used to analyse *Hdac6* expression by semi-quantitative PCR.

Primer	Sequence (5' – 3')
<i>Hdac6</i> sqPCR F	GCTCAGCACAATCTTATGGATG
<i>Hdac6</i> sqPCR R	GCCAAAACCTATAGTGGACCAG
<i>Gapdh</i> sqPCR F	CCTTGAGATCAACACGTACCAG
<i>Gapdh</i> sqPCR R	CGCCTGTACTACTCCACCAC

2.3.3.7. Chromatin Immunoprecipitation

Chromatin Immunoprecipitation (ChIP) was performed using the DNA-Shearing Kit and One-Day ChIP Kit (Diagenode, Liege, Belgium) according to the manufacturer's instructions. The following modifications were applied to optimize the procedure for hippocampal tissue. Half of the hippocampus from each mouse was homogenized and processed in 500 μ l of buffers A, B and C and 240 μ l of buffer D from the DNA-Shearing Kit. The chromatin was sheared in a Bioruptor (Diagenode, Liege, Belgium) with the settings: High, 30 sec ON, 30 sec OFF, for 25 min. Sheared chromatin was incubated in 4 μ l of antibody in an ultrasonic cleaner (VWR, Leuven, Belgium) for 1 h. The antigen-antibody complex was incubated with pre-blocked beads with an excess of 500 μ l ChIP buffer for 60 min on a rotating disc at 4 °C. The antigen-antibody-beads complex was washed twice in ChIP buffer. The precipitated DNA was analysed in a BioAnalyzer (Agilent, Böblingen, Germany) according to the manufacturer's instructions. Specific genes were analysed by qPCR (Roche Applied Science, Mannheim, Germany).

2.3.4. DNA Electrophoresis

PCR products were analysed using agarose gel electrophoresis. A 1% agarose gel was prepared by adding 1.5 mg agarose powder (Carl Roth, Karlsruhe, Germany) to 150 ml TAE buffer (40 mM Tris, 20 mM acetic acid, 1 mM EDTA, pH 8.5) and boiling in a microwave oven (800 W) till the agarose dissolved completely. The DNA intercalating agent, ethidium bromide, was added to the agarose solution at a final concentration of 0.5 µg/ml. The agarose solution was cooled shortly by shaking and poured into a casting tray (BIO-RAD, Germany) with a sample comb and allowed to solidify at RT. After solidification, the comb was removed and the gel was placed in the electrophoresis chamber and covered with TAE buffer. The PCR products were then pipetted into the wells along with the 5 µl of the GeneRuler™ 100 bp DNA Ladder (Fermentas, St. Leon-Rot, Germany) in one well, the chamber was closed with the lid and the power leads were connected power supply unit. The DNA was resolved by passing current at 120 V for about 45 min. After resolution, the gel was documented using the Gel iX Imager (Intas Science Imaging Instruments GmbH, Göttingen, Germany).

2.3.5. Restriction Digestion

Restriction digestion was performed to isolate the *Hdac6* cDNA fragment (insert) from a plasmid. This process was used to further ligate the DNA fragment obtained with a vector or detect the presence of the desired insert in the plasmid. The *Hdac6*-pGEMT Easy construct (5 µg) was restriction digested using *XbaI* and *AgeI* restriction enzymes at 37 °C for 1 h (Fermentas, St. Leon-Rot, Germany, Table 2.14). The FUp93dGW (1 µg) vector was also digested with *XbaI* and *AgeI* simultaneously.

Table 2.14: Reaction mix for restriction digestion of *Hdac6*-pGEMT Easy and FUp93dGW.

Reagent	Volume
<i>Hdac6</i> -pGEMT Easy or FUp93dGW	15.0 μ l
<i>Xba</i> I restriction enzyme	1.0 μ l
<i>Age</i> I restriction enzyme	4.0 μ l
10x Tango buffer	5.0 μ l
PCR-grade water	25.0 μ l
Total volume	50.0 μl

The digestion products were resolved in a 1% agarose gel by electrophoresis (Section 2.3.4). The bands corresponding to *Hdac6* (3.6 kb) and FUGW vector backbone (11 kb) were excised from the gel. The *Hdac6* cDNA and FUGW vector were purified using the QIAquick Gel Extraction Kit (Qiagen, Hilden, Germany) according to the instructions provided.

2.3.6. DNA Ligation

Following restriction digestion and purification from an agarose gel, the purified insert (*Hdac6*) and vector (FUGW) were ligated at 4 °C overnight using the T4 DNA Ligase (Fermentas, St. Leon-Rot, Germany, Table 2.15).

Table 2.15: Reaction mix for ligation of *Hdac6* and FUGW.

Reagent	Volume
Insert	6 μ l
Vector	1 μ l
10x T4 DNA Ligase buffer	1 μ l
T4 DNA Ligase	1 μ l
Total volume	10 μl

2.3.7. Transformation of *Escherichia coli*

Following overnight ligation, 5 μ l of the ligation mix (Table 2.15) was used to transform chemically *E. coli* cells (Strain: XL-1 Blue). Frozen competent *E. coli* cells were thawed on ice and 2 μ l of the ligation mix were added. The mixture was incubated on ice for 20 min followed by 42 °C for 45 sec and then on ice for 5 min. The cells were then suspended in 900 μ l of lysogeny broth or LB medium (Bertani, 1951) and shaken at 1000 rpm at 37 °C for 90 min in a Thermomixer Comfort (Eppendorf, Hamburg, Germany). After incubation, 100 μ l of the bacterial suspension were plated on LB-agar plates with Ampicillin (100 μ g/ml) using a Drigalski spatula and incubated at 37 °C overnight in an incubator.

LB Medium (1000 ml): 10 g Bacto Tryptone, 5 g yeast extract, 10 g NaCl, pH adjusted to 7.5 with NaOH, dissolved in ddH₂O and sterilized by autoclaving.

LB Agar (1000 ml): 15 g agar added to 800 ml LB medium, dissolved by heating, volume adjusted to 1000 ml using ddH₂O and sterilized by autoclaving. The sterile LB agar was poured into 10 cm dishes.

Individual bacterial colonies were picked and cultured in 5 ml LB medium by shaking at 200 rpm overnight at 37 °C in an orbital shaker. After overnight proliferation, the culture was used to purify the plasmid as described below (Section 2.3.8).

2.3.8. Plasmid Purification

Plasmid purification was performed using buffers P1, P2 and P3 (Qiagen, Hilden, Germany). After overnight incubation, the *E. coli* cells were harvested by centrifugation at 7,000 \times g at RT for 8 min. The bacterial pellet was resuspended in 300 μ l chilled buffer P1 and transferred to a 1.5 ml microcentrifuge tube. To this suspension, 300 μ l of buffer P2 were added, mixed by inversion and incubated at RT for 5 min. To this, 300 μ l of chilled buffer P3 were added and mixed immediately by inverting the tube. The mixture was centrifuged at 16,000 rpm for 15 min at 4 °C in a tabletop centrifuge. The supernatant was transferred to a new tube and incubated at 50 °C for 5 min. A 50 μ l sample was taken in a new tube and DNA was precipitated by adding 35 μ l of

isopropanol and centrifuging at 16,000 rpm for 15 min at 4 °C in a tabletop centrifuge. The supernatant was aspirated and the pellet was incubated in 2.0 µl of 10x Tango buffer, 0.5 µl of *XbaI*, 0.5 µl of *AgeI* and 17 µl of PCR-grade water at 37 °C for 2 h. Loading dye was mixed to the solution and resolved in an agarose gel by electrophoresis to analyse if the clones contained the insert. The original lysates from the positive clones were transferred to PhaseLock Gel Heavy tubes and 800 µl of phenol/chloroform/isoamyl alcohol (25:24:1) solution were added and centrifuged at 16,000 rpm for 1 min at RT in a tabletop centrifuge. The upper phase was transferred to a new 1.5 ml tube and 800 µl of chloroform were added and mixed by vigorous shaking. The mixture was centrifuged at 16,000 rpm for 1 min at RT in a tabletop centrifuge. The upper phase was aspirated and transferred to a new 1.5 ml tube. DNA was precipitated by adding 700 µl of isopropanol and centrifuging at 16,000 rpm for 15 min at 4 °C in a tabletop centrifuge. The supernatant was aspirated and the pellet was resuspended in 30 µl of PCR-grade water. DNA concentration was measure using a NanoDrop spectrophotometer (Peqlab, Erlangen, Germany). The purified plasmid was stored, till further use, at -20 °C.

2.3.9. Protein Extraction

Total proteins were isolated from frozen brain tissue for molecular analysis. Crude protein extracts were prepared in TX buffer. Alternatively, proteins were also isolated using the TRI-Reagent after RNA isolation (Section 2.3.1.2).

2.3.9.1. Crude Extraction of Proteins from Brain Tissue

Total proteins were extracted from frozen brain tissue by adding TX extraction buffer (50 mM Tris-HCl pH 7.5, 150 mM NaCl, 2 mM EDTA, 1% Triton X-100, volumes mentioned in Table 2.16). The Complete Protease Inhibitor Cocktail (Roche Applied Science, Mannheim, Germany, 1 tablet/10 ml buffer) was added to the extraction buffer before use and dissolved by vortexing. The tissue was homogenised using sterile micropestles in 1.5 ml microcentrifuge tubes to yield a homogenous tissue lysate that

was rotated on a rotating disc at 20 rpm for 10 min at 4 °C. The lysate was then spun at 10,000 rpm for 10 min at 4 °C in a Microcentrifuge 5415 R (Eppendorf, Hamburg, Germany). The supernatant containing total proteins was isolated and stored at -20 °C till further use.

Table 2.16: Volumes of TX extraction buffer used for different regions from an adult mouse brain.

Brain Region	Volume of TX Buffer
Septum	100 µl
Hypothalamus	100 µl
Hippocampus	500 µl
Cortex	800 µl
Cerebellum	500 µl

2.3.9.2. Extraction of Proteins Using TRI-Reagent

After RNA isolation, the organic phase was stored at -20 °C for protein isolation (Section 2.3.1.2). To precipitate proteins, 1.5 ml of isopropanol was added to the organic phase. The mixture was incubated at RT for 10 min and spun at 12,000 × g for 10 min at 4 °C. The supernatant was discarded and the pellet was washed 3 times by adding 2 ml of wash solution (0.3 M guanidine hydrochloride in 95% ethanol). During each wash cycle, the pellet was incubated in the wash solution at RT for 20 min and centrifuged at 7,500 × g for 5 min at 4 °C. After the last wash step, the supernatant was discarded and the pellet was air dried at RT and dissolved in a solution of 9 M urea in 0.01 M PBS.

2.3.9.3. Isolation of Synaptosomal and PSD Protein Fractions

To analyse protein levels at the synapse, the synaptosomal and post-synaptic density (PSD) protein fractions were isolated from mouse hippocampus and cortex. The hippocampus from an adult mouse brain was homogenised in 4 ml Buffer 1 in a Dounce homogeniser (7 ml Tissue Grinder, Wheaton, Millville, USA). The homogenate (H) was

transferred to a 15 ml centrifuge tube and spun at $800 \times g$ for 10 min at 4°C . The supernatant (S1) was transferred to an SS34 tube (oak ridge centrifuge tube, 50 ml, Nalgene®, Rochester, NY, USA) and centrifuged at $9,200 \times g$ for 15 min at 4°C . The supernatant (S2) was removed and stored on ice. The pellet was resuspended in 5 ml Buffer 1 and about 500 μl of this suspension (P2) were saved in a 1.5 ml microcentrifuge tube on ice as the crude synaptosomal fraction and 5 ml of Buffer 2 were added to the rest. The mixture was stirred using a magnetic stirrer for 15 min at 4°C on a magnetic plate and then centrifuged at $33,000 \times g$ for 20 min at 4°C . Meanwhile, a sucrose gradient was prepared by pipetting 1.5 ml of 1.5 M sucrose solution into an ultracentrifuge tube and 1.5 ml of 1.0 M sucrose solution on top gently using an insulin syringe. The supernatant from the last centrifugation was discarded and the pellet was resuspended in 0.5 ml of Buffer 2 and gently loaded on the sucrose gradient and centrifuged at $167,000 \times g$ for 14 h at 4°C in an ultracentrifuge (Rotor: TH-660, Thermo Scientific, Langensfeld, Germany). The supernatant was discarded and the pellet was dissolved in 500 μl of Buffer 3 and centrifuged at $200,000 \times g$ for 2 h at 4°C in an ultracentrifuge with a fixed angle rotor (S120AT, Thermo Scientific, Langensfeld, Germany). The supernatant was discarded and the pellet was dissolved in TX extraction buffer with protease inhibitor cocktail (Section 2.3.9.1). To dissolve the pellet completely, the suspension was heated at 55°C and mixed by vortexing until complete dissolution of the pellet to yield the PSD fraction. The contents of different fractions purified by this Synaptosomal and PSD Fractionation method are described in Table 2.17.

Table 2.17: Description of different fractions collected by Synaptosomal and PSD Fractionation.

S. No.	Fraction	Contents
1.	H Fraction	Crude Tissue Homogenate
2.	S2 Fraction	Nuclear Debris
3.	P2 Fraction	Crude Synaptosomes
4.	PSD Fraction	Post-Synaptic Density

The components of the buffers and solutions used in this method are described below.

- **Buffer 1:** 0.32 M sucrose, 4 mM HEPES (pH 7.6 adjusted with NaOH), 1 mM MgCl_2 , 0.5 mM CaCl_2 , 0.5 mM DTT and 1 mM EDTA in ddH_2O .

- **Buffer 2:** 0.32 M sucrose, 12 mM Tris-HCl (pH 8.1) and 1% Triton X-100 in ddH₂O.
- **Buffer 3:** 150 mM KCl and 1% Triton X-100 in ddH₂O.
- **Sucrose Gradient:** 1.5 M sucrose (lower phase) and 1.0 M sucrose (upper phase) solutions prepared in 1 mM NaHCO₃.
- **Protease Inhibitor:** The Complete Protease Inhibitor Cocktail (1 tablet/10 ml, Roche Applied Science, Mannheim, Germany) was added to all buffers and the sucrose gradient before use.

2.3.9.4. Determination of Protein Concentration

Protein concentration was determined based on the Bradford protein assay (Bradford, 1976). Bradford reagent was prepared by diluting the Roti®-Quant reagent (Carl Roth GmbH, Karlsruhe, Germany) 5-fold in 0.01 M PBS pH 7.0. Bovine serum albumin (BSA, Carl Roth, Karlsruhe, Germany) was chosen to prepare standard dilutions to generate a standard curve of optical density versus protein concentration. A 1.28 µg/µl solution of BSA in ddH₂O was used as a stock to be diluted serially to yield 50 µl solutions of following dilutions: 1.0, 2.0, 4.0, 8.0, 16.0, 32.0 and 64.0 µg/µl respectively. A sample of the protein lysate (1 µl) and the BSA solutions (50 µl) were dissolved in Bradford reagent to a total volume of 1 ml in a glass spectrophotometer cuvette (10 mm × 4 mm × 45 mm, Sarstedt, Nümbrecht, Germany), mixed by vortexing shortly and incubated at RT for 5 min. The Bradford reagent (1 ml) was taken in a separate cuvette as a blank reference. Optical density was measured using a BioPhotometer (Eppendorf, Hamburg, Germany) at a wavelength of 595 nm. Based on the optical densities of the BSA solutions, the BioPhotometer generates a standard curve and calculates the concentration of proteins in the test samples.

2.3.10. Protein Electrophoresis

For biochemical analysis, total proteins were resolved by the process of sodium dodecyl sulphate polyacrylamide gel electrophoresis (SDS-PAGE). Specific proteins of interest were analysed using western blot.

2.3.10.1. Preparation of Protein Lysates for SDS-PAGE

Protein lysates were mixed with SDS loading buffer to denature the proteins by disrupting the disulphide bonds present in their tertiary structures. The mixture was incubated at 98 °C for 3 min to hasten further denaturing of proteins and centrifuged shortly. The protein solution was stored at 4 °C till further use.

SDS Loading Buffer: 50 mM Tris-HCl pH 6.8, 100 mM DTT, 4% SDS, 0.1% Bromophenol blue and 10% glycerol in ddH₂O.

2.3.10.2. SDS-PAGE

Proteins were resolved by SDS-PAGE (BIO-RAD Laboratories, Munich, Germany). Two glass plates were used in the gel polymerisation unit, a spacer plate (1.5 mm) on the outer side and a plane glass plate on the inner side. The acrylamide gel consisted of two parts, a 10% resolving gel and a 5% stacking gel. The resolving gel was prepared as described in Table 2.18 and poured between the plates and allowed to polymerise at RT. After solidification of the resolving gel, the stacking gel was prepared as explained in Table 2.18 and poured over the resolving gel. A comb was inserted between the plates to create wells and the stacking gel was allowed to polymerise at RT. After polymerisation, the comb was gently removed and the gel along with the plates was inserted into the electrophoresis chamber. The chamber was filled with SDS electrophoresis buffer. Protein samples were mixed with SDS loading buffer (Section 2.3.10.1) and 20 µg of proteins were pipetted into the wells and 5 µl of the PageRuler™ Prestained Protein Ladder were loaded in one of the wells. The proteins were resolved

according to their molecular weights by passing current at 60 V for 35 min and then at 120 V till the bromophenol blue front reached the bottom of the gel. For optimal resolution of proteins lighter than 30 kDa, a 15% resolving gel was used.

Table 2.18: Components of an SDS-polyacrylamide gel (10 ml).

Components	10% Resolving Gel	15% Resolving Gel	5% Stacking Gel
ddH ₂ O	4.0 ml	2.3 ml	6.8 ml
30% Acrylamide	3.3 ml	5.0 ml	1.7 ml
1.5 M Tris pH 8.8	2.5 ml	2.5 ml	-
1.0 M Tris pH 6.8	-	-	1.25 ml
10% SDS	0.1 ml	0.1 ml	0.1 ml
10% APS	0.1 ml	0.1 ml	0.1 ml
TEMED	0.004 ml	0.004 ml	0.01 ml

SDS Electrophoresis Buffer: 25 mM Tris, 250 mM glycine and 0.1% SDS in ddH₂O.

2.3.11. Coomassie Staining

Following SDS-PAGE, the gel was fixed by incubation in 500 ml of gel fixing solution for 1 h at RT with gentle agitation. The fixing solution is then removed and the gel was incubated overnight in gel washing solution at RT with gentle agitation. The gel was then stained with 400 ml of Coomassie solution for 3 h at RT with gentle agitation. The Coomassie solution was aspirated and stored at RT for further use and the gel was washed in 400 ml of destain solution with gentle agitation and several changes until the protein bands were clearly visible without any background staining. The protein bands were visualised over a white light illuminator.

Gel Fixing Solution: 50% ethanol (v/v) and 10% acetic acid (v/v) in ddH₂O.

Gel Washing Solution: 50% methanol (v/v) and 10% acetic acid (v/v) in ddH₂O.

Coomassie Solution: 0.1% Coomassie Blue R350 (w/v), 20% methanol (v/v) and 10% acetic acid (v/v) in ddH₂O.

Destain Solution: 50% methanol (v/v) and 10% acetic acid in ddH₂O.

2.3.12. Western Blot

The process of western blot was used to detect specific proteins of interest and also quantify their levels. The levels of β -actin were used as loading control.

2.3.12.1. Protein Transfer

Following electrophoresis, proteins were transferred to a nitrocellulose membrane using the Trans-Blot Cell tank transfer system (BIO-RAD Laboratories, Munich, Germany) filled with transfer buffer. Transfer was performed by applying current at constant voltage (60 V) for 14 h at 4 °C.

Transfer Buffer: 192 mM glycine, 25 mM Tris-HCl pH 8.3, 20% methanol.

2.3.12.2. Immunoblot

Following transfer, the membrane was washed shortly in 0.01 M PBS at RT and incubated in 5% milk in 0.01 M PBS at RT for 1 h to block non-specific sites. Primary antibody was dissolved in 0.5% milk in 0.01 M PBS and added to the membrane overnight at 4 °C. The membrane was then washed in 0.01 M PBS with 0.1% Triton X-100 thrice and then incubated in secondary antibody dissolved in 0.5% milk in 0.01 M PBS for 2 h at RT in the dark. The membrane was washed twice in 0.01 M PBS with 0.1% Triton X-100 and once with 0.01 M PBS in the dark. The membrane was scanned using the Odyssey Infrared Imaging System (LI-COR Biotechnology GmbH, Bad Homburg, Germany).

Table 2.19: Antibodies used for Western Blot.

Primary Antibody	Manufacturer	Dilution
Anti-Ac-H3K9	Millipore	1:5000
Anti-Ac-H3K12	Millipore	1:2500
Anti-Ac-H4K5	Millipore	1:2000
Anti-Ac-H4K8	Millipore	1:1000
Anti-Ac-H4K12	Abcam	1:5000
Anti-Ac-H4K16	Millipore	1:2000
Anti-HDAC6	Millipore	1:1000
Anti-Ac- α -Tubulin	Sigma-Aldrich	1:1000
Anti- β -Actin	Santa Cruz	1:1000
Anti-PSD-95	Santa Cruz	1:1000
Anti-Synaptophysin	Sigma-Aldrich	1:1000
Anti-GluR1	Synaptic Systems	1:1000
Anti-GAPDH	Chemicon	1:10000
Anti-NeuN	Chemicon	1:1000
Anti- β -Amyloid (4G8)	Covance	1:10000
Secondary Antibody	Manufacturer	Dilution
Anti-mouse IgG 680CW	LI-COR	1:15000
Anti-mouse IgG 800CW	LI-COR	1:15000
Anti-rabbit IgG 680CW	LI-COR	1:15000
Anti-rabbit IgG 800CW	LI-COR	1:15000

2.4. Immunohistochemistry

2.4.1. Immunohistochemistry on Paraffin Sections

Brain tissue, fixed in 4% PFA, was embedded in paraffin wax and cut using a microtome to yield 5 μ thick sections that were mounted on pre-coated glass slides. Deparaffinisation and hydration were performed by the following incubations: twice for 10 min in xylene, 10 min in 100%, 10 min in 95%, 10 min in 75% and 10 min in 50% ethanol, and twice for 5 min in ddH₂O at RT. Antigen retrieval was achieved by boiling the sections in 10 mM sodium citrate for 10 min in a microwave oven (800 W). The

sections were washed in tap water and twice in 0.01 M PBS. Non-specific sites were blocked by incubation in blocking buffer (5% goat serum + 0.3% Triton X-100 in 0.01 M PBS) for 90 min. Immunolabelling was performed by incubation in primary antibody diluted in blocking buffer at 4 °C overnight on an orbital shaker. Thereafter, the sections were washed 3 times for 10 min each in antibody wash buffer (1% goat serum + 0.2% Triton X-100 in 0.01 M PBS) at RT. Secondary antibody incubation was carried out at RT for 2 h with Alexa488 or Cy3 conjugated goat polyclonal anti-rabbit IgG or anti-mouse IgG antibodies dissolved in blocking buffer (1:500, Jackson Immunoresearch Laboratories). The sections were washed 3 times for 10 min each in 0.01 M PBS, incubated in 4',6-diamidino-2-phenylindole (DAPI, 10 µg/ml) for 20 min and washed twice in 0.01 M PBS at RT. The sections were dehydrated retrogressively in the alcohol and xylene solutions mentioned above. The slides were covered with glass cover slips using Permount anti-fade medium, dried at RT in the dark and stored at 4 °C in the dark.

2.4.2. Immunohistochemistry on Frozen Sections

Brain tissue, fixed in 4% PFA, was cut using a cryostat to yield 30 µ sections that were stored in cryoprotectant solution at -20 °C. For immunostaining, sections were washed in 0.01 M PBS with 0.1% Triton X-100. Blocking of non-specific binding sites, antibody incubation and washing and DAPI incubation steps were carried out as described in section 2.4.1. The sections were then mounted on SuperFrost glass slides and dried at RT in the dark. The slides were then covered with glass cover slips by adding Mowiol anti-fade medium and stored at 4 °C in the dark.

Cryoprotectant Solution (1000 ml): 300 g sucrose, 10 g poly-vinyl-pyrrolidone (PVP-40), 500 ml 0.2 M phosphate buffer (PB) and 300 ml ethylene glycol. PVP-40 was dissolved in PB, sucrose was added and dissolved by stirring followed by ethylene glycol. Finally, the volume was adjusted to 1000 ml with ddH₂O. Cryoprotectant was stored at -20 °C.

2.4.3. Confocal Microscopy

Immunolabelled mouse brain sections were imaged using a Leica AOBS SP2 confocal microscope (Leica Microsystems, Wetzlar, Germany). The 488 nm and 561 nm lasers were used to excite the Alexa488 and the Cy3 conjugated secondary antibodies respectively.

2.4. Cell Culture

2.4.1. Primary Hippocampal Neurons

Primary hippocampal neuronal cultures were prepared from newborn 129/Sv mouse pups (P0). Briefly, pups were sacrificed by decapitation and the hippocampi were isolated after incising the skull and meningeal membranes. Papain digestion and mechanical trituration were performed to yield a homogenous cell suspension. Cells were counted using the Neubauer chamber and subsequently plated on 13 mm glass cover slips, pre-coated with 1% (w/v) poly-D-lysine, in 24-well plates for immunocytochemistry and pre-coated 35 mm glass bottom culture dishes (MatTek Corporation, Ashland, MA, USA) for live imaging at a density of 50,000 cells/dish. Cultures were incubated at 37 °C, 5% CO₂ and 60% relative humidity and treated with floxuridine 4 days after plating to restrict astrocytic growth. The cultures were nourished by half medium changes after 7 days *in vitro* (DIV). Experiments were performed at the age of 15 DIV.

2.4.2. Generation of Lentivirus and Infection of Neurons

A small-scale lentivirus was prepared with *Hdac6*-FUGW construct to infect mouse primary hippocampal cultures. HEK293 cells were grown in a 6-well culture plate and used to generate the virus.

Plasmids used: *Hdac6*-FUGW (2.0 µg), vsvg (0.5 µg) and Δ8.9 (1.5 µg)

Transfection reagent: 376 µl DMEM (without supplements) mixed with 12 µl TransIT-293 reagent and incubated for 5 min at RT.

DNA preparation: *Hdac6*-FUGW plasmid (2.0 µg) mixed with 0.5 µl of vsvg (1.0 µg/µl) and 1.2 µl of Δ8.9 (1.25 µg/µl).

The transfection reagent was added to the prepared DNA, mixed thoroughly and incubated at RT for 30 min. The mixture was added to the HEK293 cells and incubated at 37 °C with 5% CO₂. After 24 h, the HEK293 cells were transferred to 32 °C with 5% CO₂. After 48 h, the cells were scraped in the medium and centrifuged at 2,000 × g for 15 min. The supernatant containing the lentivirus was aspirated and stored as 400 µl aliquots at -80 °C.

The neurons were infected with the lentivirus by adding 50 µl of the supernatant and incubated at 37 °C with 5% CO₂ in a humid incubator for 7 days to achieve optimal expression of the target gene.

2.4.3. β-Amyloid Oligomerisation and Neuronal Treatment

Lyophilised monomeric Aβ₁₋₄₂ was purchased from Innovagen, Lund, Sweden and stored at -20 °C. Oligomerisation of Aβ₁₋₄₂ was performed as published previously (Klein, 2002). To prepare Amyloid-β-derived diffusible ligands (ADDLs), monomeric Aβ₁₋₄₂ was dissolved in 1,1,1,3,3,3-hexafluoro-2-propanol (HFIP) to yield a solution of 1 mM concentration, which was incubated at RT for 60 min in closed tubes to give a clear, colourless solution. Since HFIP is corrosive, all steps were carried out under a fume hood. The solution was placed on ice for 10 min and then aliquoted into non-siliconised 1.5 ml tubes. The HFIP was allowed to evaporate overnight by leaving the tubes open under the fume hood. All traces of HFIP were removed using a speedvac. The peptide films deposited on the tube walls can be stored at -80 °C till further use.

The peptide film was removed from -80 °C and kept on ice. A 5 mM stock solution was prepared by dissolving the peptide film in 100% fresh anhydrous DMSO. This stock was further diluted to a 100 µM solution with Ham's F12 medium (without phenol red) and incubated at 4 °C for 24 h. The solution was centrifuged at 14,000 × g for 10 min at 4 °C. The resulting supernatant was the ADDL preparation.

2.4.4. Live Imaging of Mitochondrial Trafficking

Primary hippocampal cultures grown in 35 mm glass bottom cell culture dishes (MatTek Corporation, Ashland, MA, USA) were treated with 10 mM MitoTracker Red FM dye (Molecular Probes, Eugene, OR, USA) for about 30 min to label all mitochondria. Mitochondrial trafficking was analysed using a Perkin-Elmer confocal spinning disk microscope. Cultures were maintained at 37 °C and 5% CO₂ in a humid incubator mounted on the microscope stage. Live imaging was performed by taking an image every 30 sec for 5 min before and 30, 60 and 90 min and 24 h after ADDL treatment. The videos were analysed using the Image-Pro PLUS software (Media-Cybernetics, Bethesda, MD, USA).

2.4.5. Immunocytochemistry

Primary neuronal cultures grown on sterile glass cover slips in 24-well cell culture plates were washed by chilled 0.01 M PBS and fixed in 4% PFA for 30 min at RT. The cells fixed on the cover slips were immunolabelled in a humid chamber according to the procedure described for frozen mouse brain sections (Section 2.4.2). Primary antibody incubation was carried out at 4 °C overnight in a humid chamber.

2.5. Data Analysis

Data were analysed by unpaired student's T-test and two-way ANOVA (Analysis of Variance) and $p < 0.05$ was considered significant. Values are displayed as mean \pm standard error of mean (SEM). Graphs were generated using GraphPad Prism.

3. Results

This study focuses on the role of histone deacetylases (HDACs) in cognition and Alzheimer's disease (AD). Previous studies have shown that HDACs can be promising drug targets in attenuating cognitive impairment in AD. In this study, treatment with a non-specific HDAC inhibitor, sodium butyrate, could improve cognition in a transgenic AD mouse model, APPPS1-21. This was accomplished by upregulation of genes involved in memory consolidation. However, HDAC inhibition did not affect the amyloid pathology exhibited by these mice. Additionally, the role of a particular class II histone deacetylase, HDAC6, in cognition and AD was investigated in greater detail. It was found that loss of *Hdac6* in APPPS1-21 mice improved learning and memory. These findings have given us a deeper insight into the molecular mechanisms underlying HDAC activity in the mouse brain and propose HDACs, particularly HDAC6, as promising drug targets to improve cognition in Alzheimer's disease.

3.1. HDAC Inhibition in APPPS1-21 mice

APPPS1-21 double transgenic mice (13 – 15 mo) were orally administered sodium butyrate (SB) in peanut butter (400 mg per mouse) to inhibit HDACs. Vehicle treated APPPS1-21 mice were taken as controls. Following 6 weeks of treatment, learning and memory was evaluated in the APPPS1-21 mice as described in section 2.2. The mice were sacrificed for molecular and histological analysis after behavioural testing (Sections 2.1.5 and 2.1.6).

3.1.1. Cognition in APPPS1-21 mice upon SB treatment

The effect of HDAC inhibition on associative memory was analysed using the fear conditioning paradigm. SB treatment resulted in enhanced associative memory in APPPS1-21 mice as shown by significantly higher freezing behaviour in the context ($p = 0.0185$) and tone ($p = 0.0365$) dependent fear conditioning paradigms (Fig. 3.1).

Both the SB and vehicle groups showed normal activity before receiving the shock (Fig. 3.1). Response to the electric shock was not different between the SB and vehicle treated groups (Fig. 3.1).

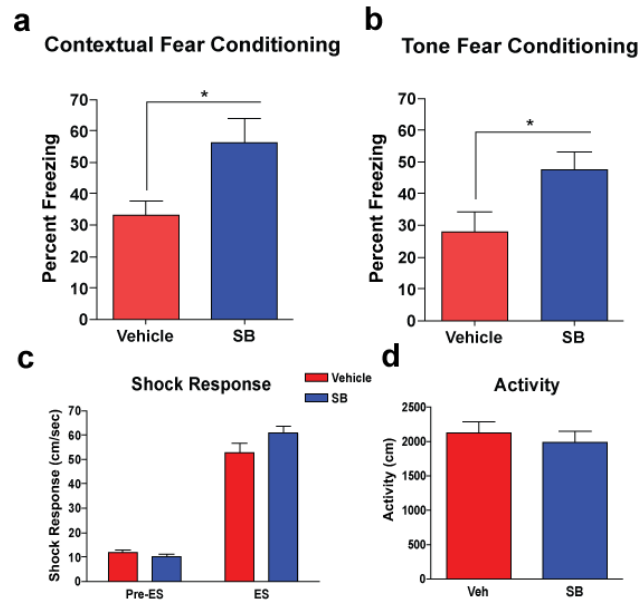


Figure 3.1: Fear Conditioning in APPPS1-21 mice upon SB treatment. (a, b) Freezing levels in SB and vehicle treated APPPS1-21 mice in context (a) and tone (b) dependent fear conditioning. (c, d) Response to the electric shock (c, ES) and basal activity (d) during training ($n = 8$, $p < 0.05$).

Exploratory behaviour and basal anxiety were analysed using the open field and elevated plus-maze tests respectively. No change in exploratory behaviour was observed in the open field test in APPPS1-21 mice upon SB treatment. The total distance travelled in the open field and the time spent in the central and peripheral regions of the field were not significantly different between SB and vehicle treated groups (Fig. 3.2). In the elevated plus-maze task, the SB treated mice spent significantly less time in the closed arms compared to the vehicle treated group (Fig. 3.3). Overall activity assessed by total distance travelled in the plus-maze was not different between the two groups (Fig. 3.3). This indicates that SB treatment leads to decreased basal anxiety levels in APPPS1-21 mice.

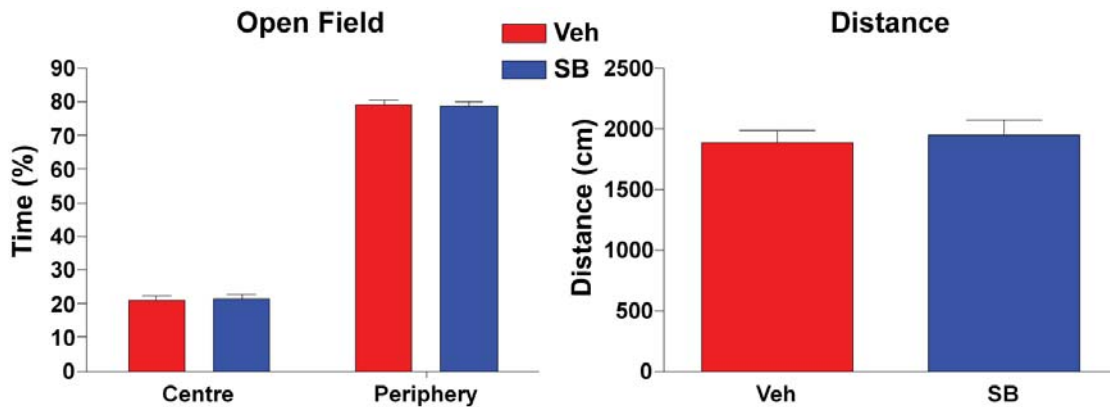


Figure 3.2: Exploratory behaviour in APPPS1-21 mice upon SB treatment shown by percentage time spent by SB and vehicle treated APPPS1-21 mice in the central and peripheral regions of the open field (left) and total distance travelled (right) ($n = 8$).

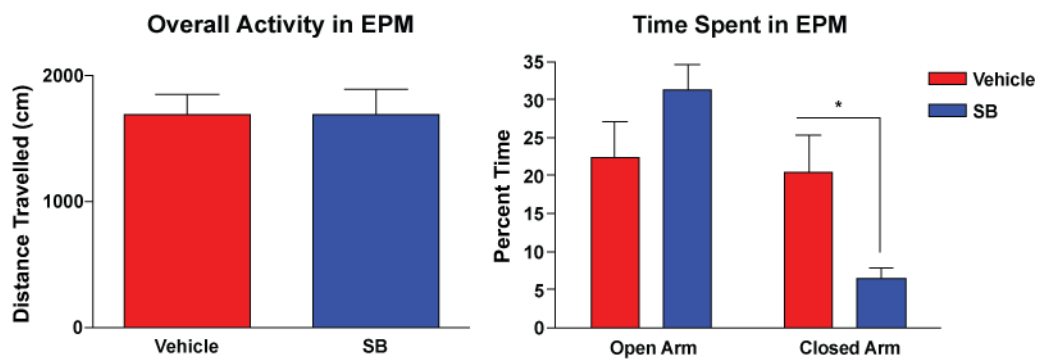


Figure 3.3: Basal anxiety in treated APPPS1-21 mice shown by overall distance travelled (left) in the elevated plus-maze (EPM) and percentage time spent in the open and closed regions of the EPM ($n = 8$, $p < 0.05$).

Spatial memory was analysed using the Morris water maze task (Section 2.2.5). It has been previously reported that APPPS1-21 mice exhibit impaired spatial learning at 8 months of age (Radde, 2006). We did not observe any difference in spatial learning between the SB and vehicle treated APPPS1-21 mice. Both groups did not exhibit any significant acquisition of spatial memory during 8 days of training in the water maze task (Fig. 3.4). In the probe test, both groups failed to exhibit any significant preference to the target region as indicated by comparable times spent in different quadrants of the pool (Fig. 3.4). This indicates that SB treatment does not improve spatial memory deficits in APPPS1-21 at this advanced stage of pathology.

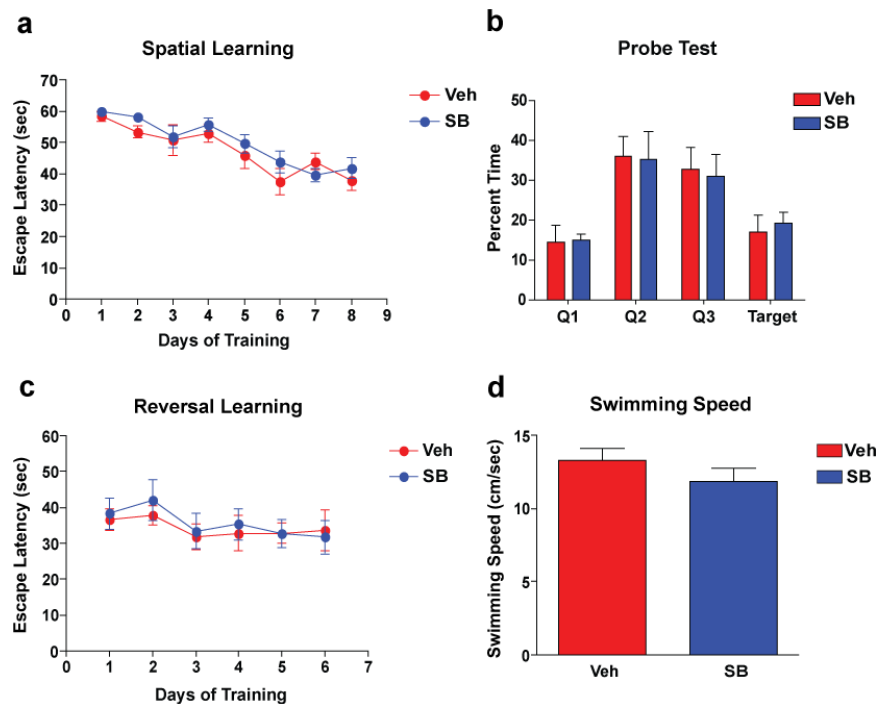


Figure 3.4: Spatial memory in SB and vehicle treated APPPS1-21 mice. (a) Spatial learning shown by escape latency upon training in SB and vehicle treated APPPS1-21 mice. (b) Time spent in different quadrants of the water maze. (c) Escape latency during reversal learning upon training. (d) Average swimming speed in the water maze.

3.1.2. Histone acetylation in APPPS1-21 mice upon SB treatment

To dissect the molecular mechanism underlying the beneficial effect of SB treatment on cognition, changes in histone acetylation in the brain were analysed. Unpublished work in our laboratory has shown that the APPPS1-21 mice exhibit hypoacetylation of histones in the brain compared to wild type controls (Section 1.3.3). Western blot (Section 2.3.12) analysis was performed on protein extracts from APPPS1-21 brains after SB treatment revealed that acetylation was significantly elevated at specific lysine residues on histones H3 and H4 such as H3K14, H4K5, H4K12 and H4K16 in the hippocampus (Fig. 3.5, $p < 0.05$) and H3K9 and H4K12 in the cortex (Fig. 3.5, $p < 0.05$) compared to vehicle treated group. SB treatment could rescue the reduced acetylation observed in this transgenic AD mouse model.

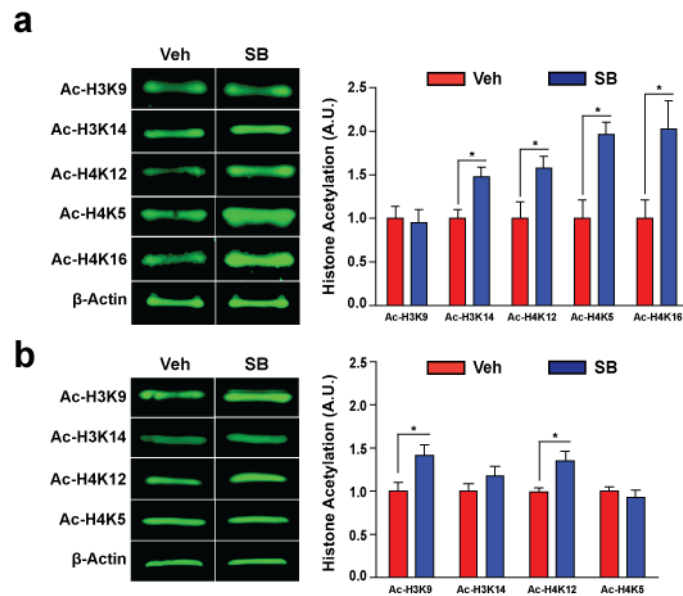


Figure 3.5: Histone acetylation changes in APPPS1-21 mice upon SB treatment. (a, b) Representative western blot images for histone acetylation at specific lysine residues in the hippocampus (a) and cortex (b) of SB and vehicle treated APPPS1-21 mice. Densitometric quantification of western blot is shown on the right in each panel ($n = 4$, $p < 0.05$).

3.1.3. Gene expression changes upon SB treatment

The process of memory consolidation involves changes in gene expression. Previous work from our laboratory has suggested a group of genes that are differentially regulated during consolidation of fear memory (Peleg, 2010). These include *Myst4*, *Fmn2*, *Marcks11*, *Gsk3 α* , *Prkca*, *Acly*, *Shank3*, *Ncdn*, *Igf2* and *Igfbp7*. Additionally, the expression of genes known to be involved in synaptic plasticity such as *Snap25* and *GluR1* was also investigated.

The expression of the genes mentioned above in the hippocampi and cortices of SB treated APPPS1-21 mice was analysed by qPCR (Section 2.3.3.4). The SB treated group exhibited a significant upregulation of *Myst4*, *Fmn2*, *Marcks11*, *Gsk3 α* , *GluR1*, *Snap25* and *Prkca* in the hippocampus and *Marcks11* in the cortex (Fig. 3.6, $p < 0.05$). The expression of *Acly*, *Ncdn*, *Igf2* and *Igfbp7* were not significantly altered upon SB treatment. *Shank3* was marginally upregulated in the cortex ($p = 0.053$). Gene expression was normalized to the expression of the housekeeping gene *Hprt1*.

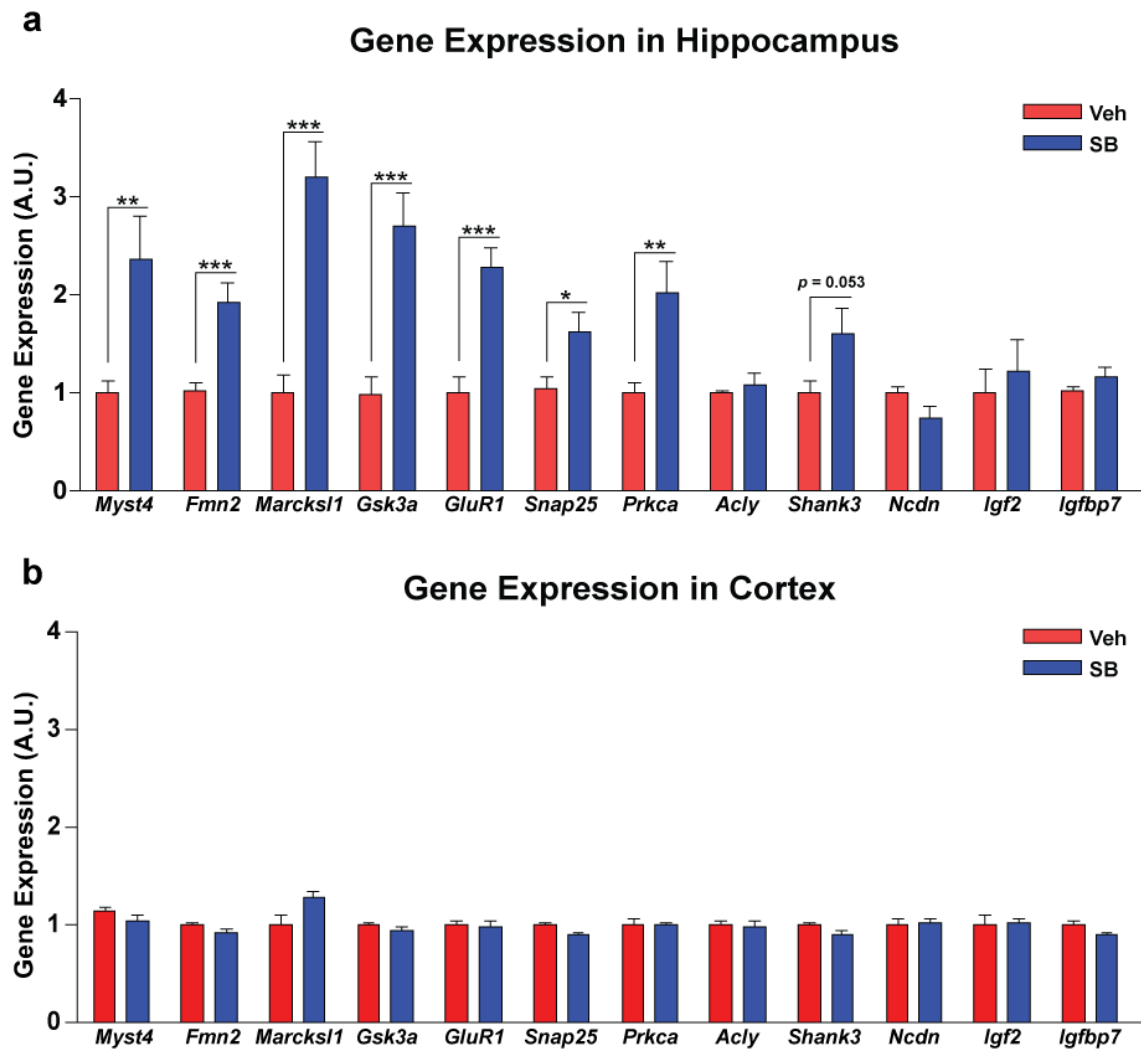


Figure 3.6: Quantitative real-time PCR analysis of gene expression in SB and vehicle treated APPPS1-21. Gene expression levels in the hippocampus (a) and cortex (b) of APPPS1-21 mice normalised to *Hprt1* expression (n = 4, * $p < 0.05$, ** $p < 0.01$, *** $p < 0.001$).

To test if the observed upregulation in gene expression translated into similar changes in corresponding protein levels, western blot analysis was performed. In particular, SNAP-25 was chosen because of its involvement in synaptic transmission and plasticity. The levels of the synaptosomal-associated protein, SNAP-25, were found to be significantly elevated in the hippocampii of SB treated APPPS1-21 mice compared to vehicle treated mice (Fig. 3.7, $p < 0.05$).

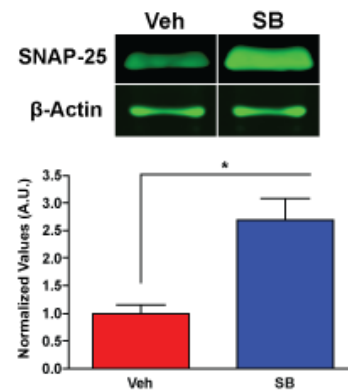


Figure 3.7: Representative western blot images (top) for SNAP-25 in hippocampal protein lysates from SB and vehicle treated APPPS1-21 mice. Bottom panel shows densitometric quantification of western blot is shown. Protein levels were normalised to levels of β -actin.

3.1.5. Amyloid plaque levels upon SB treatment

The APPPS1-21 model displays robust β -amyloid pathology in the form of hippocampal and cortical amyloid plaques (Radde, 2006). To study if SB treatment affected amyloid pathology in the APPPS1-21 mice, we analysed levels of β -amyloid plaques by immunohistochemistry (Section 2.4). Plaque levels were not different between the SB and vehicle treated groups (Fig. 3.8).

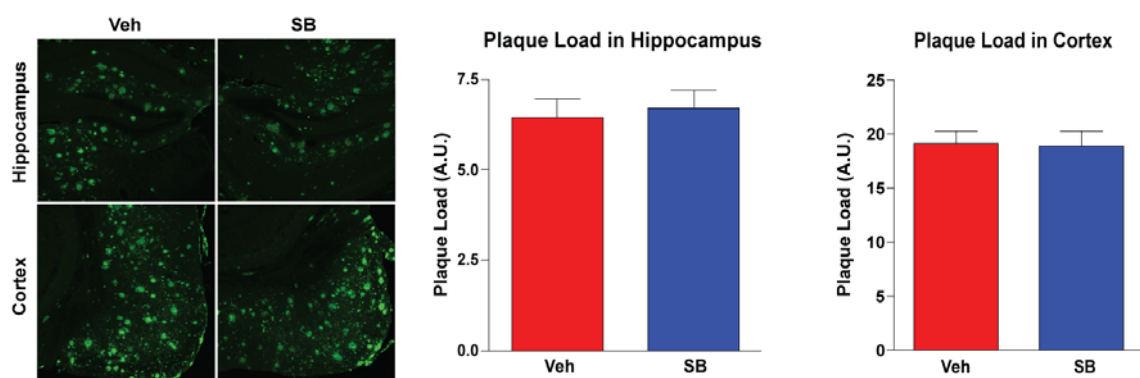


Figure 3.8: Amyloid plaque load in APPPS1-21 mice. Representative confocal microscopy images (left) of immunolabelled β -amyloid plaques in SB and vehicle treated APPPS1-21 mice in hippocampus and cortex. Densitometric quantification of immunostaining in hippocampus (middle) and cortex (right).

3.2. HDAC6 in the mouse brain

HDACs may function as lysine deacetylases on proteins other than histones. Such post-translational modifications of proteins could be crucial to neuronal function without directly affecting gene expression. Therefore, the next objective was to understand the role of such a non-histone deacetylase in cognition and neurodegeneration. HDAC6 is a unique member of the HDAC superfamily by virtue of its two catalytic domains and its action on non-histone proteins like α -tubulin (Section 1.3.5.3). Therefore, the role of HDAC6 in neuronal function during learning and memory was analysed using global *Hdac6* knockout mice. Furthermore, loss of HDAC6 function was used as a possible therapeutic tool against cognitive impairment in a transgenic mouse model of AD. This study was aimed at addressing the question: Is the loss of HDAC6 activity beneficial or detrimental to cognition in mice?

3.2.1. *Hdac6* expression in brain regions

To understand the role of *Hdac6* in the mammalian brain, the expression of *Hdac6* in the pre-frontal cortex, hippocampus, cortex and cerebellum of wild type (3 mo) mice was analysed. The qPCR primers and the UPL probes indicated in Table 2.12 were used. Among the regions analysed, *Hdac6* expression was lowest in the cerebellum (Fig. 3.9b). *Hdac6* expression in the pre-frontal cortex, hippocampus and the rest of cortex were comparable to each other and significantly higher than the cerebellum (Fig. 3.9b). Gene expression was normalized to the expression of the housekeeping gene *Hprt1*.

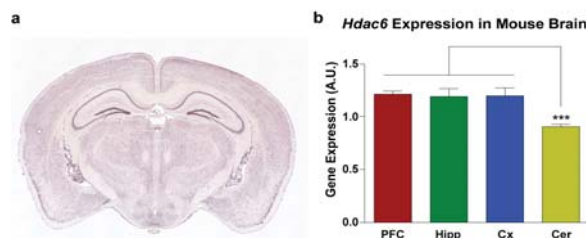


Figure 3.9: (a) In situ hybridisation showing *Hdac6* expression in the mouse brain from the Allen Brain Atlas (<http://www.brain-map.org/>). (b) *Hdac6* expression in different mouse brain regions analysed by qPCR using the Roche UPL ($n = 3$, $p < 0.001$). Gene expression was normalised to *Hprt1* expression. PFC: pre-frontal cortex, Hipp: hippocampus, Cx: rest of cortex, Cer: cerebellum.

3.2.2. HDAC6 protein levels in the brain

HDAC6 protein levels were analysed in protein lysates from the pre-frontal cortex, hippocampus, rest of cortex and cerebellum using western blot. Levels of HDAC6 were similar in the pre-frontal cortex, hippocampus and rest of cortex but significantly lower in the cerebellum (Fig. 3.10). The levels of α -tubulin acetylation were also analysed in the brain by western blot. Concurrent with HDAC6 protein levels, α -tubulin acetylation was similar in the pre-frontal cortex, hippocampus and rest of cortex but significant higher in the cerebellum (Fig. 3.10).

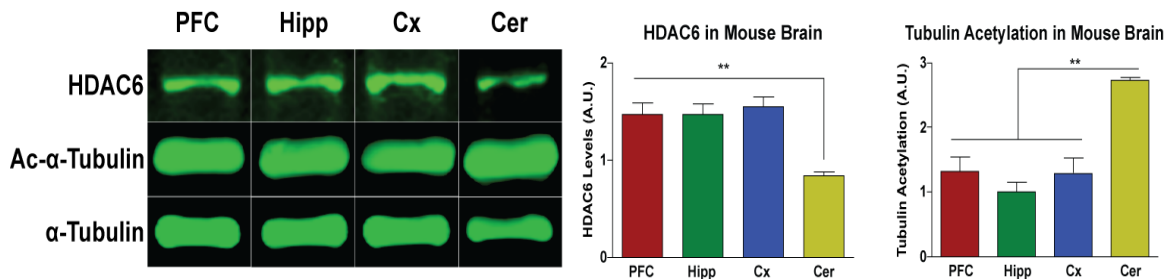


Figure 3.10: Representative western blot images (left) for HDAC6, acetylated α -tubulin and total α -tubulin levels in different mouse brain regions. Densitometric quantification of western blot is shown for HDAC6 (centre) and α -tubulin acetylation (right), normalised to total α -tubulin levels ($n = 3$, $p < 0.01$). PFC: pre-frontal cortex, Hipp: hippocampus, Cx: rest of cortex, Cer: cerebellum.

3.2.3. Subcellular localisation of HDAC6 by Western Blot

Nuclear and cytoplasmic protein fractions were extracted from frozen brain tissue as mentioned in section 2.3.9 and used to perform western blot (Section 2.3.12) to confirm the subcellular localisation of HDAC6 indicated by immunohistochemistry. HDAC6 was detected in cytoplasmic but not nuclear protein fractions from wild type mice (Fig. 3.11). The β -actin protein was selected as a loading control.

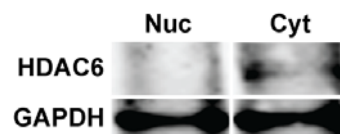


Figure 3.11: Representative western blot images for HDAC6 on cytoplasmic and nuclear protein fractions from mouse brain. GAPDH was taken as a loading control.

3.2.4. Overexpression of *Hdac6* in neuronal culture

Since the anti-HDAC6 antibody was not suitable for immunohistochemistry, the subcellular localisation of HDAC6 was further analysed in primary mouse hippocampal cultures. The *Hdac6* cDNA was cloned in the FUGW lentiviral vector with an eGFP reporter and used to infect primary hippocampal neurons (Section 2.4.2). The neurons were imaged using confocal microscopy, which revealed that HDAC6 localised to the cytoplasm and not the nucleus in primary hippocampal neurons (Fig. 3.12). Additionally, higher levels of HDAC6 were detected in the neuronal soma than the dendrites or axons. To correlate the localisation of HDAC6 with its function, immunostaining for acetylated α -tubulin was performed on primary neurons fixed with paraformaldehyde. Tubulin acetylation was detected in the cytoplasm in neuronal soma and dendrites (Fig. 3.12). However, correlative with the detection of HDAC6, levels of α -tubulin acetylation in the soma were significantly lower than the dendrites (Fig. 3.12).

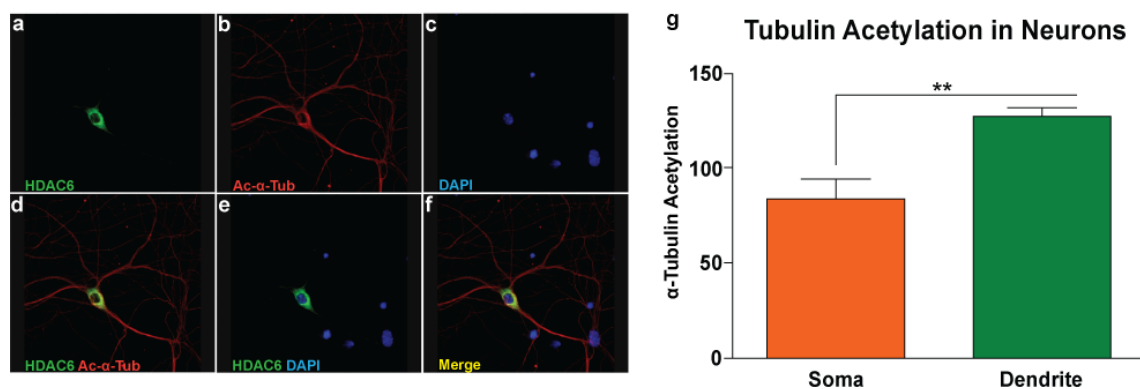


Figure 3.12: Lentiviral overexpression of *Hdac6* in mouse hippocampal neurons. (a-f) Confocal microscopy images showing *Hdac6*-eGFP (a), acetylated α -tubulin (b), DAPI (c), overlay of *Hdac6*-eGFP and acetylated α -tubulin (d), overlay of *Hdac6*-eGFP (e) and DAPI and a merge (f). (g) Quantification of immunoreactivity to acetylated α -tubulin in neuronal soma and dendrites ($n = 5$, $p < 0.01$).

3.3. Basic Characterisation of *Hdac6* knockout mice

To understand the role of HDAC6 in brain functions, *Hdac6* knockout (KO) mice were employed (Section 2.1.1). They were characterised using biochemical, histological and behavioural techniques with wild type (WT) littermates as controls.

3.3.6. *Hdac6* mRNA and protein levels in *Hdac6* KO mice

The loss of *Hdac6* mRNA and protein in the *Hdac6* KO mice was verified using PCR and western blot. RNA isolated from hippocampii and cortices of WT and *Hdac6* KO mice was used to perform semi-quantitative PCR for *Hdac6* with the primers mentioned in section 2.3.3.3. A distinct amplification product resulting from *Hdac6* primers was detected in the WT hippocampus and cortex indicating the presence of *Hdac6* mRNA but not in *Hdac6* KO mice (Fig. 3.13). The expression of the housekeeping gene *Gapdh* expression was detected in all mice in the hippocampus and cortex (Fig. 3.13). This indicates that the *Hdac6* gene is not expressed in *Hdac6* KO brains. HDAC6 protein levels were analysed in *Hdac6* KO mice using western blot. Protein lysates from WT and *Hdac6* KO hippocampii and cortices were resolved by SDS-PAGE (Section 2.3.10) and analysed with the anti-HDAC6 antibody (Table 2.19). Western blot analysis revealed the expected protein band in protein lysates from WT mice but not the *Hdac6* KO mice (Fig. 3.14). Levels of β -actin protein were similar in all lanes indicating that the same amounts of proteins were loaded. This finding verifies the loss of HDAC6 in the brains of *Hdac6* KO mice.

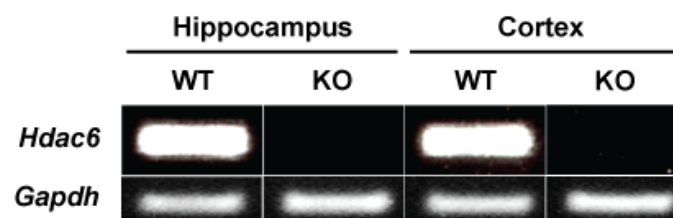


Figure 3.13: Semi-quantitative PCR for *Hdac6* mRNA levels in the hippocampus and cortex of *Hdac6* KO and WT mice. *Gapdh* expression was taken as an internal reference.

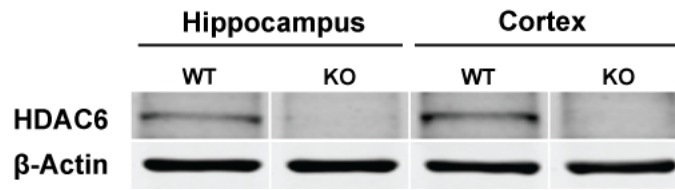


Figure 3.14: Representative western blot images for HDAC6 protein in hippocampal and cortical lysates from *Hdac6* KO and WT mice. β -actin was taken as a loading control.

3.3.1. Phenotype of *Hdac6* KO mice

Hdac6 knockout mice exhibited normal growth and body morphology compared to WT littermates (Fig. 3.15) at the age of 3 months. They were sexually mature and reproduced normally. Home cage behaviour, feeding and grooming were unchanged in the *Hdac6* KO mice. Body weight was also not altered in the *Hdac6* KO mice compared to WT controls at 3 months of age (Fig. 3.16).

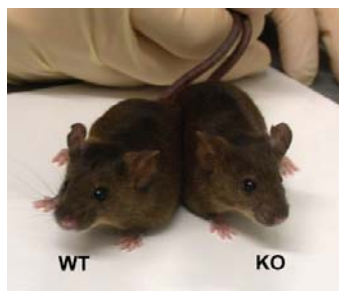


Figure 3.15: Photograph showing normal appearance of *Hdac6* KO mouse compared to WT at 3 months of age.

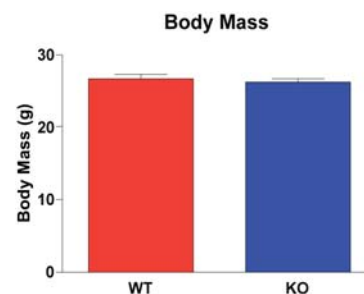


Figure 3.16: No difference in body weight between WT and *Hdac6* KO mice at 3 months of age (n = 3).

3.3.2. Brain morphology in *Hdac6* KO mice

The brains from *Hdac6* KO mice were morphologically indistinguishable from WT brains (Fig. 3.17) at 3 months of age. Brain mass was also not different (Fig. 3.17). Basic histological analysis showed that the *Hdac6* knockout brains exhibited normal cellular structure as shown by NeuN immunolabelling (Fig. 3.18). Additional

immunostaining for dendritic and synaptic markers such as MAP2 and synaptophysin also revealed no significant differences between KO and WT mice (Fig. 3.19).

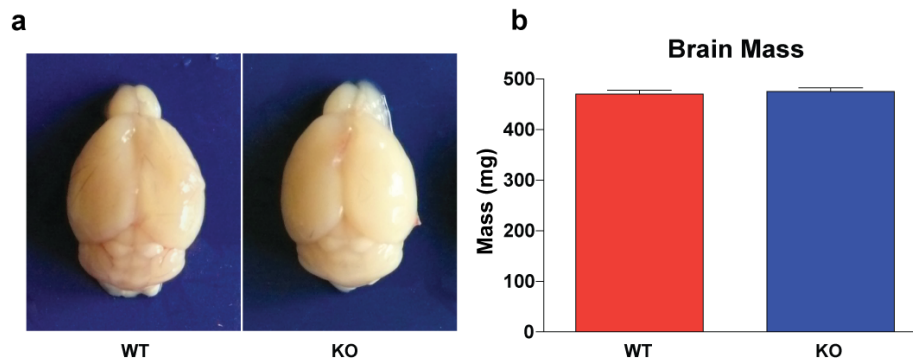


Figure 3.17: Photograph showing brain morphology (a) and bar graph showing brain mass (b) in WT and *Hdac6* KO mice (n = 3).

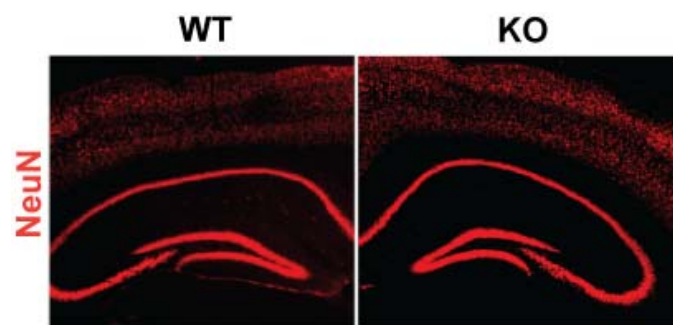


Figure 3.18: Representative confocal microscopy images showing NeuN immunoreactivity in the hippocampus and cortex in an *Hdac6* KO and WT mice.

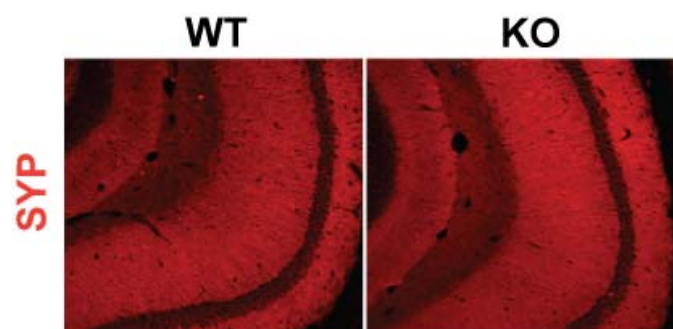


Figure 3.19: Representative confocal microscopy images showing synaptophysin (SYP) immunoreactivity in the CA1 region of the hippocampus in *Hdac6* KO and WT mice.

3.3.3. Analysis of proteins in *Hdac6* KO mice

Total hippocampal and cortical protein lysates from WT and *Hdac6* KO mice were resolved by SDS-PAGE (Section 2.3.10.2). The gel was stained using the Coomassie solution (Section 2.3.11). In this staining procedure, only one additional protein band was detected in protein lysates from *Hdac6* KO close to 55 kDa (Fig. 3.20) in comparison with WT controls. This band (Fig. 3.20, enclosed in red) was identical to acetylated α -tubulin in mass. This was expected, as HDAC6 is a known deacetylase of α -tubulin. To confirm this, acetylated α -tubulin was detected in *Hdac6* KO mice using western blot. The KO mice exhibited a significantly higher level of α -tubulin acetylation in the hippocampus and cortex (Fig. 3.21). The band detected in western blot corresponded exactly with the additional band observed in coomassie staining of *Hdac6* KO brain protein extracts.

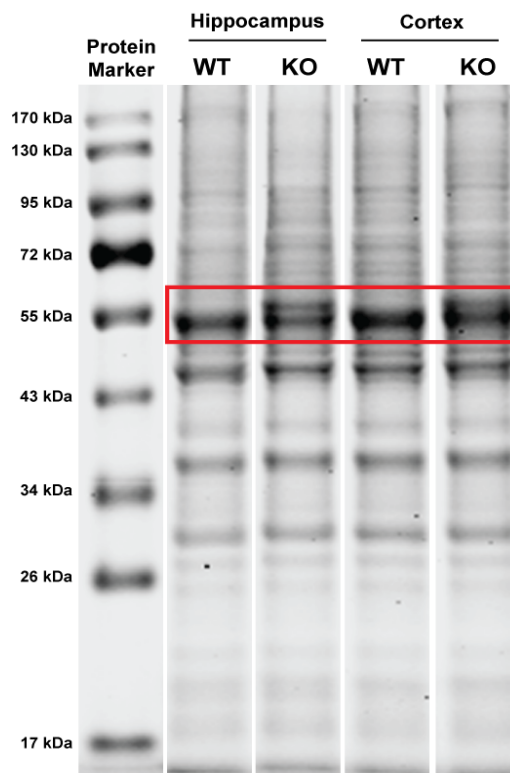


Figure 3.20: Photograph of a coomassie stained SDS polyacrylamide gel showing individual proteins resolved from hippocampal and cortical lysates of WT and *Hdac6* KO mice.

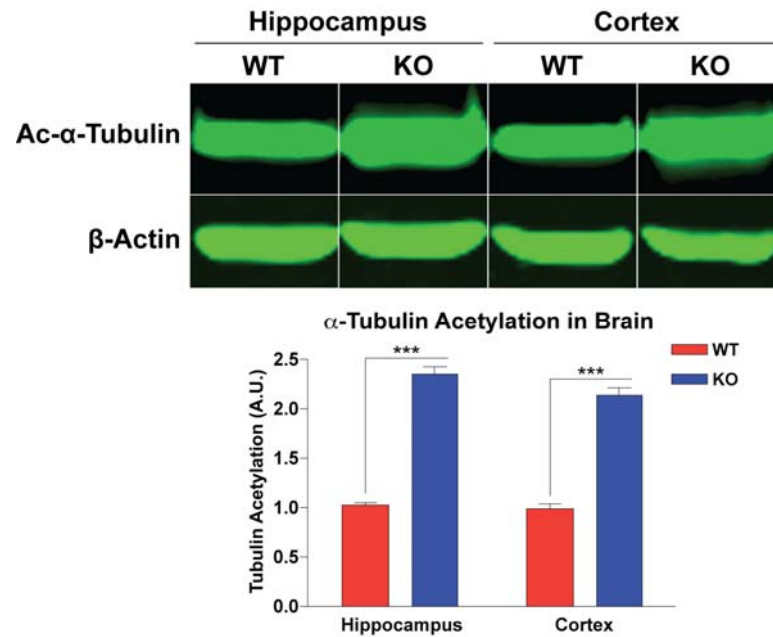


Figure 3.21: Representative western blot images showing α -tubulin acetylation in the hippocampus and cortex of *Hdac6* KO mice compared to WT controls. Tubulin acetylation was normalised to levels of β -actin. Densitometric quantification of western blot is shown in the bottom panel ($n = 3$, $p < 0.001$).

3.3.4. Histone acetylation in *Hdac6* KO mice

To investigate if HDAC6 deacetylates histones in the mouse brain, we analysed levels of histone acetylation in the hippocampus and cortex of *Hdac6* KO and WT mice by western blot and immunohistochemistry. No differences in histone acetylation at H3K9 and H4K8 (Fig. 3.22) were detected using western blot and H3K14 (Fig. 3.23) using immunohistochemistry in the brain. This suggests that loss of *Hdac6* does not affect histone acetylation in the mouse brain.

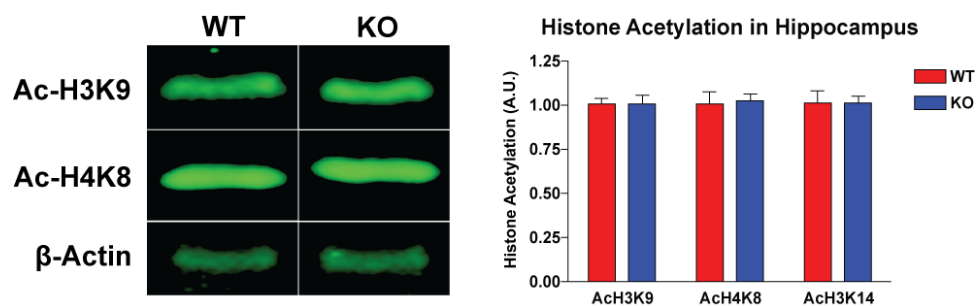


Figure 3.22: Representative western blot images (left) along with densitometric quantification (right) showing histone acetylation at H3K9 and H4K8 in the hippocampus of *Hdac6* KO mice.

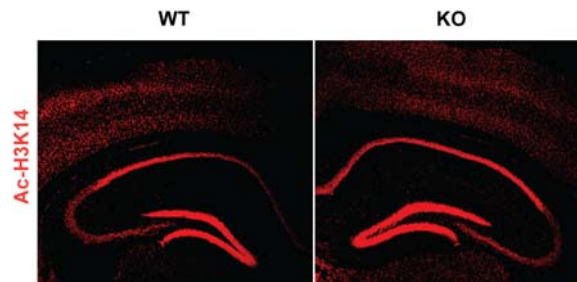


Figure 3.23: Representative confocal images of immunohistochemistry for acetylated H3K14 in hippocampus of *Hdac6* KO and WT mice.

3.3.5. Expression of histone deacetylases in *Hdac6* KO mice

The expression of other members of the mammalian HDAC family was analysed in total RNA isolated from hippocampii of WT and *Hdac6* KO mice by qPCR (Section 2.3.3.4). The expressions of *Hdac4*, *Hdac9*, *Hdac11* and *Sirt3* were altered upon loss of *Hdac6* (Fig. 3.24). The expressions of the other *Hdac* and *Sirt* genes were not different between WT and *Hdac6* KO mice (Fig. 3.24). It was intriguing to investigate the expression of *Sirt2*, another known α -tubulin deacetylase. However, as shown in Fig. 3.24, the expression of *Sirt2* was not different between WT and *Hdac6* KO mice. These results show that loss of *Hdac6* leads to marginal changes in the expression of some few HDAC family members in the mouse hippocampus.

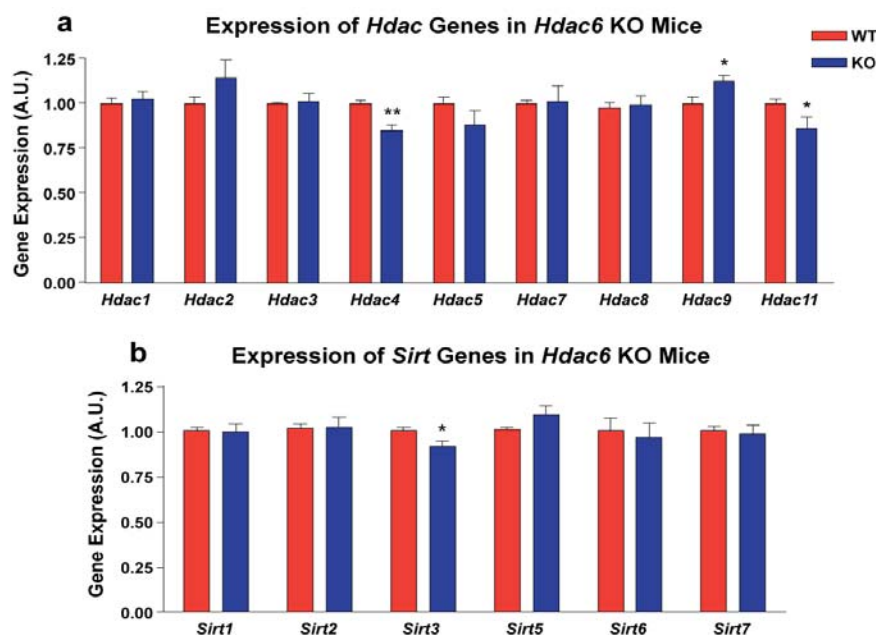


Figure 3.24: Expression of *Hdac* and *Sirt* genes in *Hdac6* KO and WT mice ($n = 3$, $p < 0.05$).

3.3.6. Expression of cognition-induced genes in *Hdac6* KO mice

To evaluate if HDAC6 played a role in the regulation of gene expression, the expression of genes known to be involved in memory consolidation was analysed by qPCR (Section 2.3.3.4). As shown in Fig. 3.25, there was no difference in the expression of *Fmn2*, *Marcks11*, *Snap25*, *Prkca*, *Myst4* or *GluR1* in the hippocampus between WT and *Hdac6* KO mice. This indicates that HDAC6 might not be involved in regulation of gene expression under basal conditions.

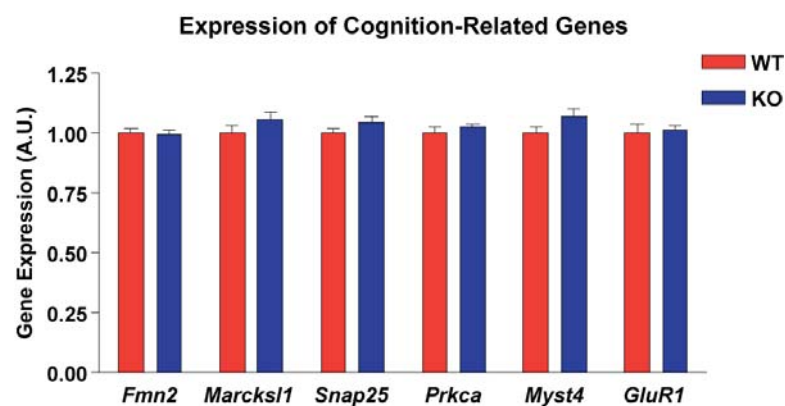


Figure 3.25: Expression genes regulated in memory consolidation in *Hdac6* KO and WT mice by qPCR (n = 3). Gene expression was normalised to *Hprt1* expression.

3.4. Behavioural Characterisation of *Hdac6* KO mice

The role of HDAC6 in cognition was analysed by the behavioural characterisation of *Hdac6* KO mice. Cognitive assessment of *Hdac6* KO mice was performed at 3 months of age to study their behaviour in young adulthood. Age-matched wild type littermates were taken as controls.

3.4.1. Basal anxiety and exploratory behaviour in *Hdac6* KO mice

Basal anxiety was assessed by the elevated plus-maze task (Section 2.2.2). The times spent in the open and closed arms of the maze were not different between *Hdac6* KO

and WT mice (Fig. 3.26). There was no difference in activity shown by the mice indicated by the total distance travelled in the maze (Fig. 3.26). This indicates that basal anxiety is not altered upon the loss of HDAC6 in mice.

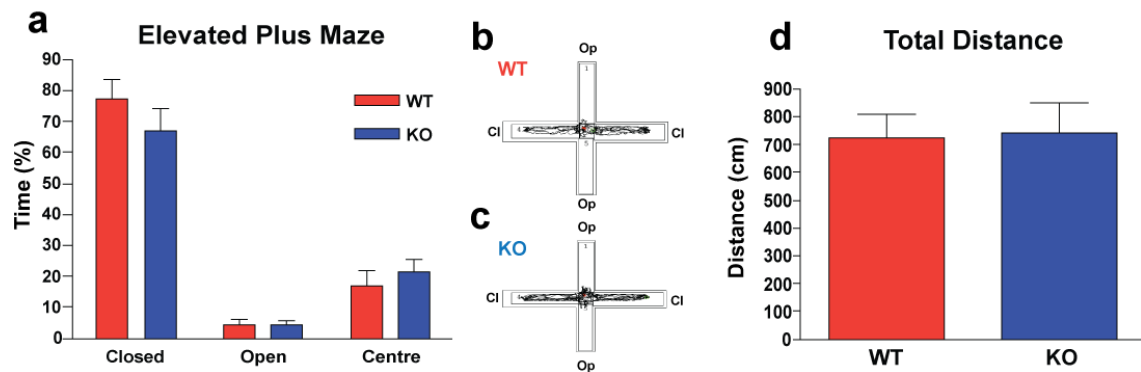


Figure 3.26: Basal anxiety levels in *Hdac6* KO mice (n = 8). (a) Percentage time spent in the closed, open and central regions of the elevated plus-maze (EPM). (b, c) Representative traces of movement of WT and KO mice in the EPM (Op: open arms, Cl: closed arms). (d) Overall activity in the EPM shown by total distance covered by the mice.

Exploratory behaviour was measured by exposing the mice to the open field (Section 2.2.1). Both WT and *Hdac6* KO mice explored the open field in a similar manner. The times spent in different parts of the field (centre and periphery) were similar between *Hdac6* knockout and WT mice (Fig. 3.27). This finding indicates that basal exploratory behaviour is not affected by lack of HDAC6 in mice.

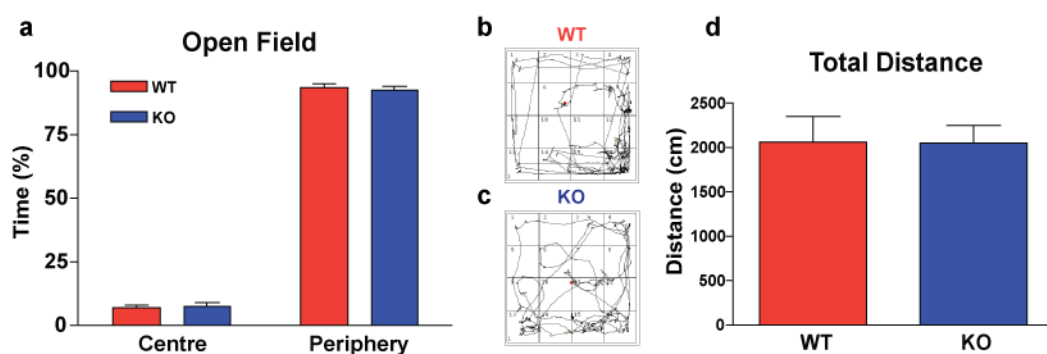


Figure 3.27: Exploratory behaviour in *Hdac6* KO mice (n = 8). (a) Percentage time spent in the central and peripheral regions of the open field. (b, c) Representative traces of movement of WT and KO mice in the open field. (d) Overall activity in the field shown by total distance covered by the mice.

3.4.2. Associative memory in *Hdac6* KO mice

The contextual fear conditioning paradigm (Section 2.2.3) was used to assess associative memory in *Hdac6* KO and WT mice. Basal activity upon exposure to the context and in response to the electric shock was not different between the two groups (shown by speed of movement before and upon delivery of shock, Fig. 3.28). Both groups exhibited robust freezing behaviour when tested 24 h after training. Freezing behaviour was not different between the *Hdac6* KO and WT groups at 3 months of age (Fig. 3.28). This shows that associative memory is unaltered in *Hdac6* KO mice.

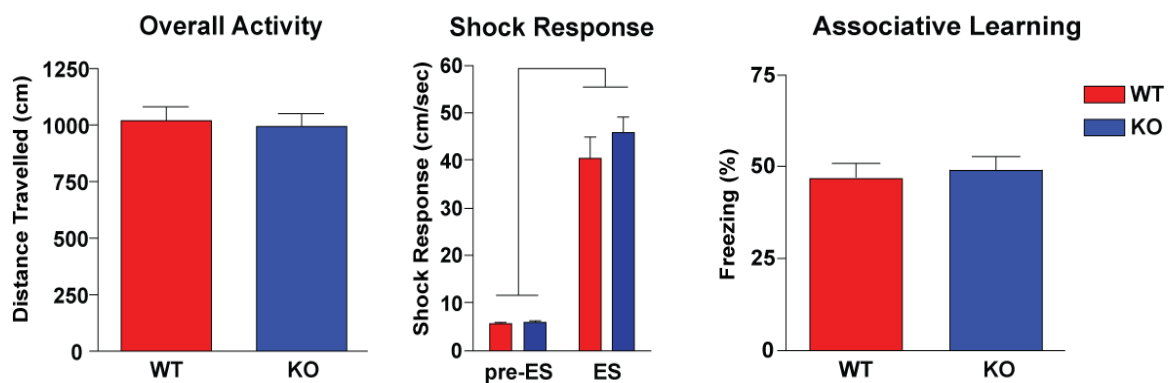


Figure 3.28: Long-term associative memory in *Hdac6* KO mice analysed by contextual fear conditioning. Basal activity shown by *Hdac6* KO mice upon exposure to a novel context (left), response to an electric foot shock (centre) and level of freezing exhibited upon testing (right) ($n = 10$).

3.4.3. Spatial memory in *Hdac6* KO mice

Spatial learning and memory were analysed in the Morris Water Maze task (Section 2.2.5). As shown, both WT and *Hdac6* KO mice showed progressively decreasing escape latencies in response to training and reached the criterion of 10 s after 6 consecutive days of training (Fig. 3.29a). On day 7, the probe test (Section 2.2.5) was performed to assess the spatial memory acquired by the mice during training. The WT group showed a significant preference to the target quadrant indicated by the times spent in different quadrants of the pool (Fig. 3.29b). However, the *Hdac6* KO mice exhibited a significantly higher preference ($p = 0.038$) to the target quadrant than the

WT controls (Fig. 3.29b). Swimming speed was not different between the two groups (Fig. 3.29d) indicating that motor skills were not affected by loss of *Hdac6* in mice.

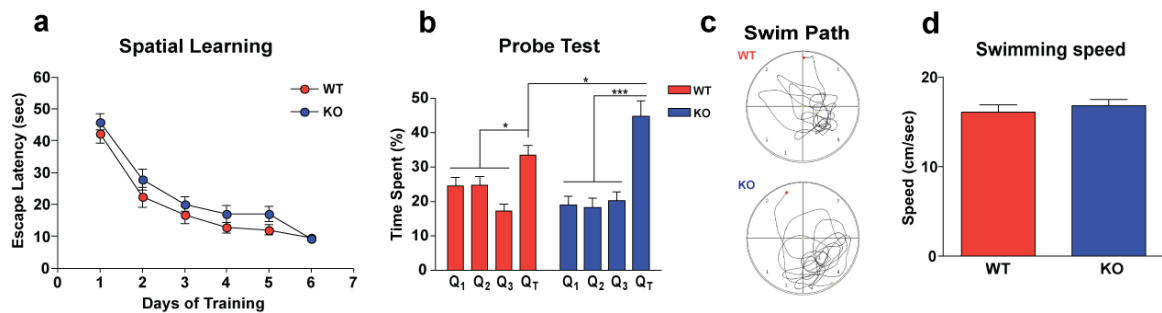


Figure 3.29: Spatial learning in *Hdac6* KO mice analysed in the Morris water maze (n = 10). (a) Escape latency curves in WT and KO mice upon training. (b) Percentage time spent in difference quadrants of the pool in the probe test showing target preference in KO compared to WT ($p < 0.05$). (c) Representative swim traces of WT and KO mice in the water maze. (d) swimming speed in KO compared to WT.

3.4.4. Motor function in *Hdac6* KO mice

Motor function was further tested using the rotarod performance test (Section 2.2.6). Both WT and *Hdac6* KO mice responded well to habituation. Rotarod performance during the test phase was not altered upon loss of *Hdac6* in mice (Fig. 3.30).

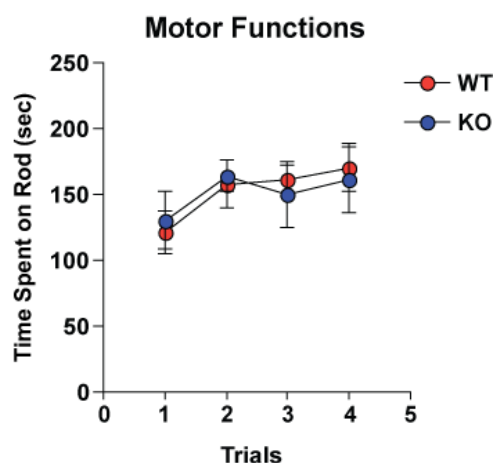


Figure 3.30: Motor functions in *Hdac6* KO mice analysed by the rotarod performance test. Graph showing rotarod performance in KO mice compared to WT.

3.5. Acute inhibition of HDAC6 in mice

To study the effect of pharmacological HDAC6 inhibition on learning and memory, WT mice (2 months) were intrahippocampally administered a specific HDAC6 inhibitor, ST27 (Prof. Manfred Jung, University of Freiburg, Germany), immediately following training on the contextual fear conditioning paradigm (Sections 2.2.3 and 2.2.4). Vehicle treated mice were taken as controls. Associative memory was tested 24 h after training and freezing behaviour was measured. Mice that received ST27 showed a significant increase in freezing compared to vehicle treated controls (Fig. 3.31, $p = 0.035$). Response to the shock was not different between the two groups (Fig. 3.31). After testing, the mice were sacrificed and α -tubulin acetylation was analysed in the hippocampus by western blot. The ST27 treated mice exhibited a higher level of α -tubulin acetylation compared to controls indicating inhibition of HDAC6 activity (Fig. 3.32). This result suggests that acute inhibition of HDAC6 can improve associative memory in mice possibly by the upregulation of α -tubulin acetylation in the hippocampus.

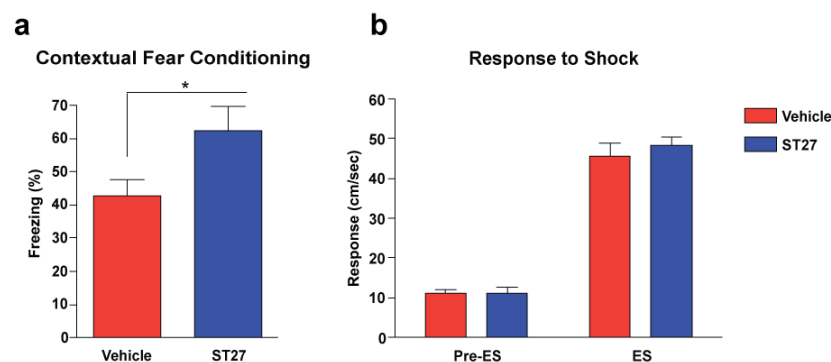


Figure 3.31: Associative memory upon intrahippocampal ST27 treatment. (a) Freezing levels in ST27 treated WT mice compared to vehicle treated controls ($n = 11$, $p < 0.05$). (b) Response to electric shock (ES) shown by mean velocity before and after shock.

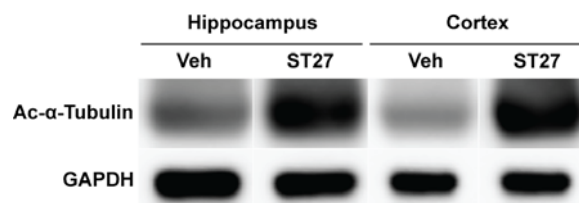


Figure 3.32: Representative western blot images showing elevated α -tubulin acetylation upon ST27 treatment in the hippocampus and cortex indicating the inhibition of HDAC6.

3.6. Loss of *Hdac6* in APPPS1-21 mice

The results described above led to an intriguing question: Is the loss of *Hdac6* beneficial or detrimental in Alzheimer's disease? To address this question, the double transgenic APPPS1-21 mice (Radde, 2006) were bred with *Hdac6* KO mice to generate a mouse model of AD deficient specifically in HDAC6. The role of HDAC6 in AD was investigated by behavioural and molecular characterisation of APPPS1-21-HD6^{-/-} mice. WT and APPPS1-21 littermates were taken as controls.

3.6.1. Basal anxiety and exploration in APPPS1-21-HD6^{-/-} mice

The elevated plus-maze test was performed to assess basal anxiety. The times spent in the open and closed arms of the maze were not different between WT, APPPS1-21 and APPPS1-21-HD6^{-/-} mice (Fig. 3.33). This indicates that basal anxiety in APPPS1-21 mice is similar to WT controls and the loss of *Hdac6* does not affect basal anxiety in APPPS1-21 mice.

When exposed to the open field, the times spent by the mice in the central and peripheral parts of the field were similar in all the three groups (WT, APPPS1-21 and APPPS1-21-HD6^{-/-}) (Fig. 3.33). Therefore, exploratory behaviour was not different in both APPPS1-21 and APPPS1-21-HD6^{-/-} mice compared to WT controls.

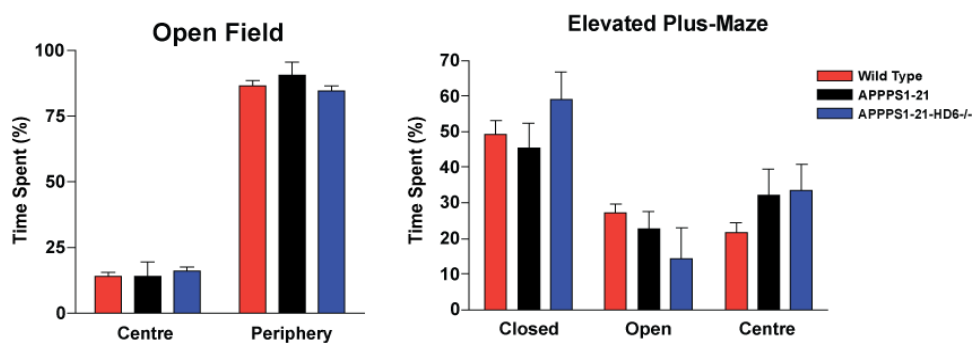


Figure 3.33: Exploratory behaviour and basal anxiety levels in APPPS1-21 mice upon loss of *Hdac6* shown by percentage time spent in the central and peripheral regions in the open field (left) and percentage times spent in the closed, open and central regions in the elevated plus-maze (right) measured between WT, APPPS1-21 and APPPS1-21-HD6^{-/-} mice (n = 10).

3.6.2. Associative memory in APPPS1-21-HD6^{-/-} mice

The APPPS1-21 mice showed significantly impaired associative memory compared to WT controls in the contextual fear conditioning test (Fig. 3.34) indicated by significantly lower freezing measured in APPPS1-21 mice. However, loss of *Hdac6* completely rescued the impairment in associative memory observed in APPPS1-21 mice (Fig. 3.34). There was no difference in freezing behaviour between WT and APPPS1-21-HD6^{-/-} mice. Basal activity in the context and response to the electric shock were similar in all three groups (Fig. 3.34).

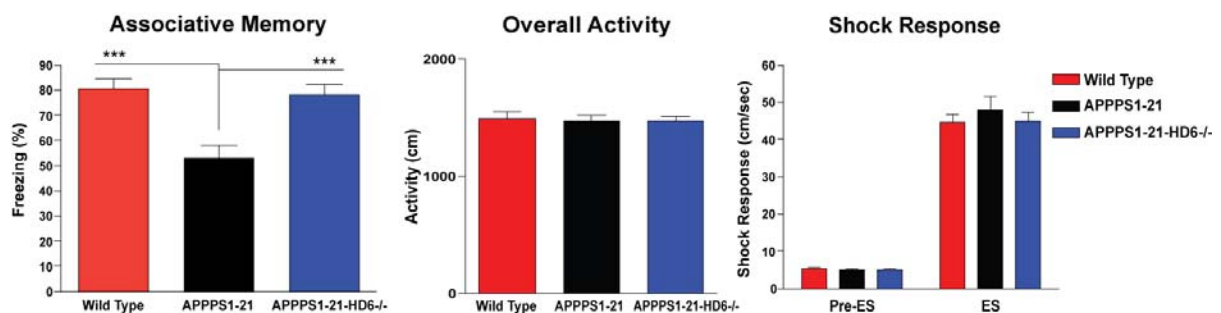


Figure 3.34: Attenuation of associative memory impairment by loss of *Hdac6*. Freezing levels in WT, APPPS1-21 and APPPS1-21-HD6^{-/-} groups. Overall activity shown by total distance covered (centre) and response to shock shown by mean velocity before and after shock administration (right) in the groups (n = 10, $p < 0.001$).

3.6.3. Spatial memory in APPPS1-21-HD6^{-/-} mice

Spatial learning in the Morris water maze was normal in both APPPS1-21 and APPPS1-21-HD6^{-/-} mice compared to WT controls as indicated by the escape latency curves during training (Fig. 3.35a). However, the probe test revealed that the APPPS1-21 mice were significantly impaired in acquiring spatial memory compared to WT mice. Unlike the WT controls, the APPPS1-21 mice showed no significant preference to the target quadrant of the pool (Fig. 3.35b). Interestingly, loss of *Hdac6* rescued the impairment on APPPS1-21 mice as shown by a significant target preference in the APPPS1-21-HD6^{-/-} mice (Fig. 3.35b) as indicated by the times spent in different quadrants of the pool. Number of target visits was not different between the three groups. This indicates

that loss *Hdac6* can possibly help attenuate the impairment in spatial memory observed in AD.

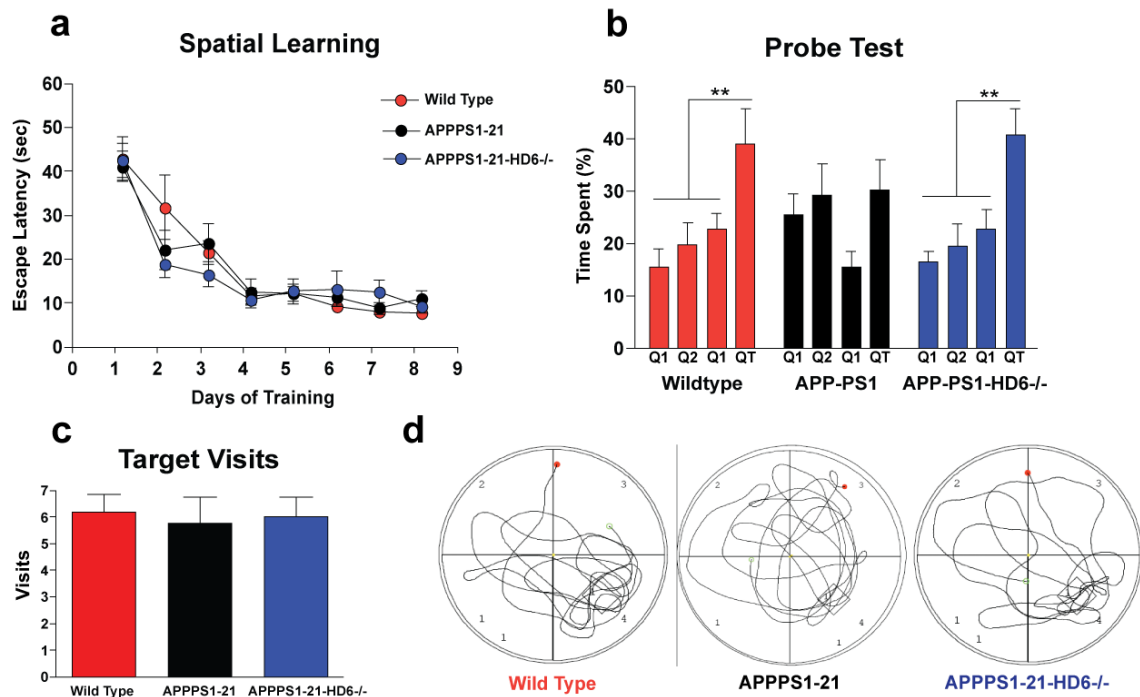


Figure 3.35: Spatial memory in APPPS1-21 mice upon loss of *Hdac6* analysed in the Morris water maze. (a) Escape latency curves exhibited by WT, APPPS1-21 and APPPS1-21-HD6^{-/-} mice during training. (b) Target preference in the probe test shown by the WT, APPPS1-21 and APPPS1-21-HD6^{-/-} groups. (c) Graph showing number of visits to the target region in the probe test. (d) Representative swim traces of the three groups showing significant preference for the target region in WT and APPPS1-21-HD6^{-/-} mice but not in the APPPS1-21 group (n = 10, p < 0.01)

3.6.4. Molecular analysis of loss of *Hdac6* in APPPS1-21 mice

Following behavioural analysis, the hippocampi and cortices were extracted from the WT, APPPS1-21 and APPPS1-21-HD6^{-/-} mice for molecular analysis.

3.6.4.1. Tubulin acetylation in APPPS1-21-HD6^{-/-} mice

Tubulin acetylation was analysed in protein lysates from hippocampi from WT, APPPS1-21 and APPPS1-21-HD6^{-/-} mice by western blot (Section 2.3.12). The

APPPS1-21 mice showed significantly decreased α -tubulin acetylation compared to WT controls (Fig. 3.36). This reduction in α -tubulin acetylation could be rescued by loss of *Hdac6* in APPPS1-21 mice. The APPPS1-21-HD6^{-/-} mice showed significantly higher α -tubulin acetylation compared to the APPPS1-21 mice (Fig. 3.37, 3.38).

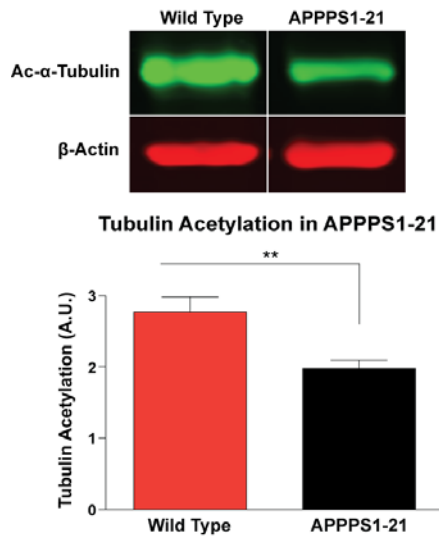


Figure 3.36: Representative western blot images (top) showing reduced hippocampal α -tubulin acetylation in APPPS1-21 mice compared to WT. Densitometric quantification of western blot is shown in the lower panel ($n = 3, p < 0.01$).

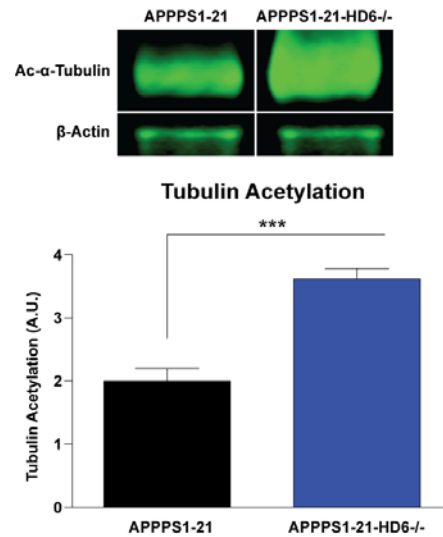


Figure 3.37: Representative western blot images (top) showing enhanced α -tubulin acetylation in APPPS1-21-HD6^{-/-} mice compared to the APPPS1-21 group. Densitometric quantification of western blot is provided in the lower panel ($n = 3, p < 0.01$).

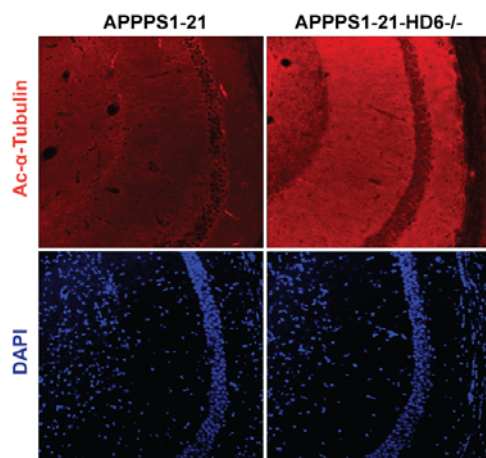


Figure 3.38: Representative images showing higher α -tubulin acetylation in APPPS1-21-HD6^{-/-} mice in the CA1 region by immunohistochemistry.

3.6.4.2. Levels of synaptic markers in APPPS1-21-HD6^{-/-} mice

Immunoblot analysis was performed on total proteins extracted from APPPS1-21 and APPPS1-21-HD6^{-/-} mice with antibodies against proteins involved in synaptic plasticity such as synaptophysin (SYP), post-synaptic density protein PSD-95 and AMPA receptor subunit GluR1. Levels of GluR1 were slightly enhanced upon loss of *Hdac6* in APPPS1-21 mice (Fig. 3.39). There were no differences detected in the levels of any of the other proteins between APPPS1-21 and APPPS1-21-HD6^{-/-} mice (Fig. 3.39).

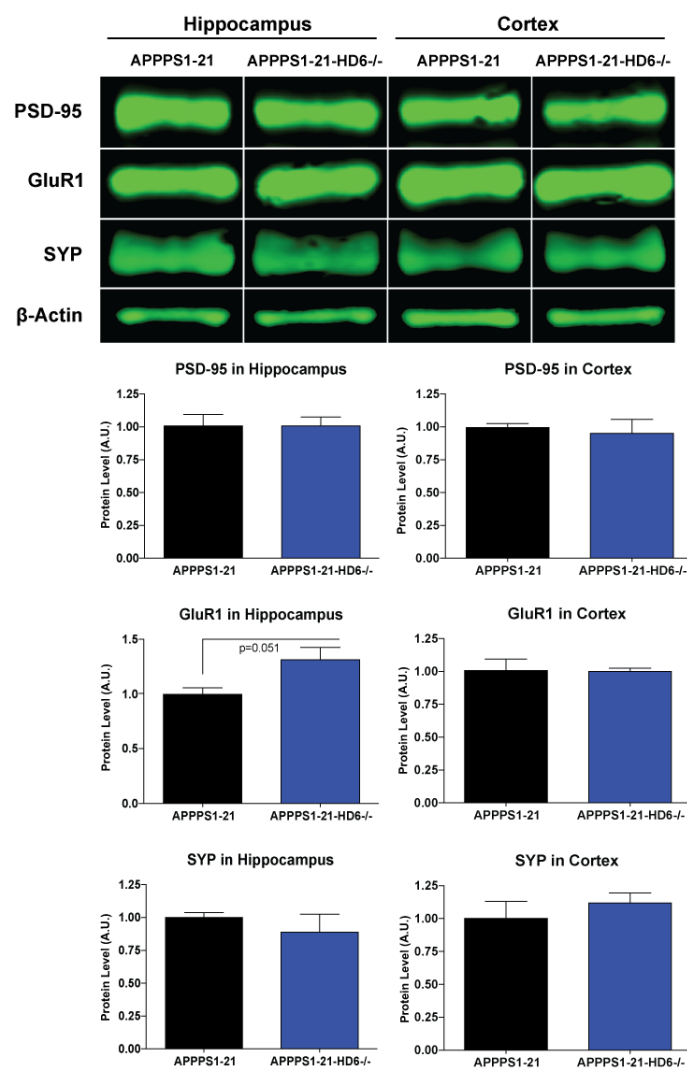


Figure 3.39: Representative western blot images (top) showing levels of the synaptic plasticity related proteins PSD-95, GluR1 and synaptophysin (SYP) in hippocampal and cortical protein extracts of APPPS1-21 and APPPS1-21-HD6^{-/-} mice. Quantification of western blots showing a mild increase in hippocampal GluR1 levels in APPPS1-21-HD6^{-/-} ($p = 0.051$) mice ($n = 3$).

3.6.4.3. Analysis of hippocampal synaptosomal and post-synaptic density fractions from APPPS1-21-HD6^{-/-} mice

Hippocampal synaptosomal and PSD protein fractions were isolated from APPPS1-21 and APPPS1-21-HD6^{-/-} mice (Section 2.3.9.3). Levels of synaptophysin (SYP) and PSD-95 were analysed using western blot (Section 2.3.12). PSD-95 was detected in both the synaptosomal and PSD fractions and enriched in the PSD fraction (Fig. 3.40). SYP was detected only in the synaptosomal fraction indicating the quality of fractionation (Fig. 3.40). The loss of *Hdac6* did not affect the levels of any of the above-mentioned proteins in APPPS1-21 mice (Fig. 3.40). This shows that basic synaptic functions could be unaffected in APPPS1-21-HD6^{-/-} mice compared to APPPS1-21 mice.

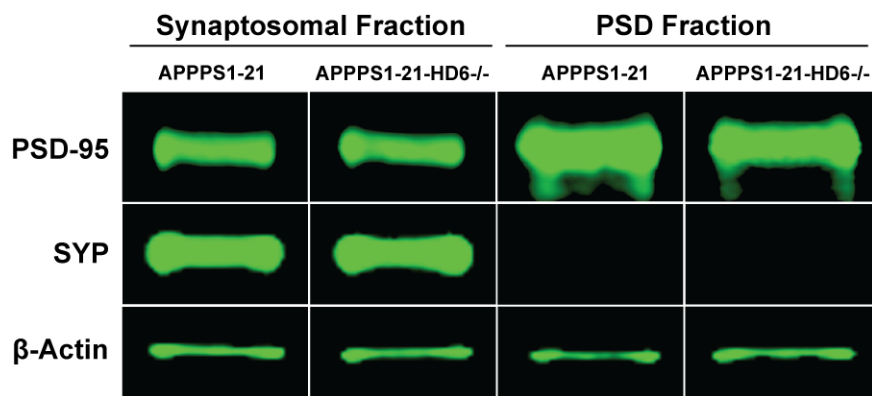


Figure 3.40: Representative images for western blot analysis of synaptosomal and post-synaptic density (PSD) protein fractions from APPPS1-21 and APPPS1-21-HD6^{-/-} mice. PSD-95 was enriched in the PSD fraction in both groups and synaptophysin (SYP) was detected only in the synaptosomal fractions.

3.6.4.4. Levels of β -amyloid plaques upon loss of *Hdac6* in APPPS1-21 mice

To analyse the effect of loss of *Hdac6* on amyloid pathology in the APPPS1-21 mice, levels of β -amyloid plaques were measured by immunolabelling using an A β -specific antibody. Confocal microscopy revealed that levels and distribution of β -amyloid plaques were unaltered in APPPS1-21 upon loss of *Hdac6* (Fig. 3.41). This shows that loss of *Hdac6* might be beneficial without affecting amyloid pathology.

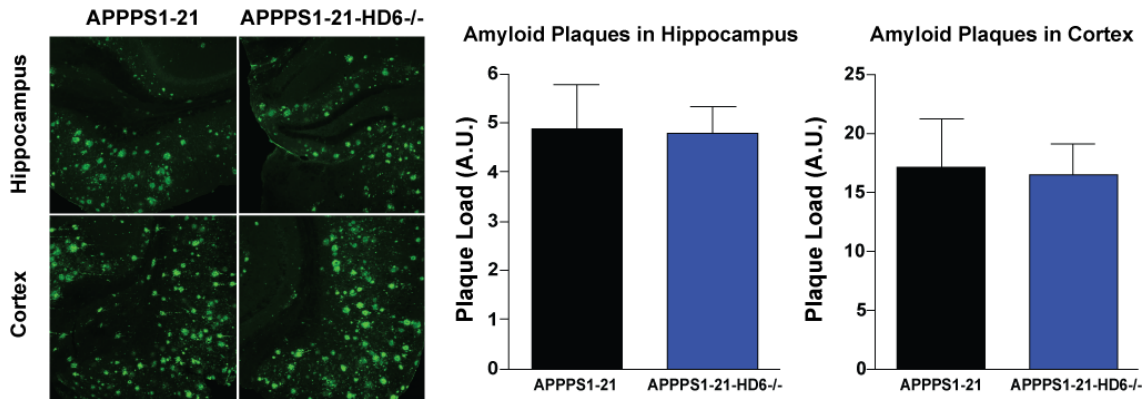


Figure 3.41: Representative confocal microscopy images (left) of immunolabelled amyloid plaques in the hippocampus and cortex of APPPS1-21 and APPPS1-21-HD6^{-/-} mice. Densitometric quantification of staining in hippocampus (middle) and cortex (right).

3.7. Mitochondrial trafficking in neurons

Intracellular trafficking of mitochondria was analysed in primary hippocampal neuron culture. Acute treatment with A β -derived diffusible ligands (ADDL) impaired the movement of mitochondria in WT neurons (Fig. 3.42) as shown by reduced percentage of moving mitochondria. However, the neurons from *Hdac6* KO did not show any ADDL-induced impairment of mitochondrial trafficking (Fig. 3.42). This shows that loss of *Hdac6* might be beneficial for the maintenance of intraneuronal mitochondrial transport in mice.

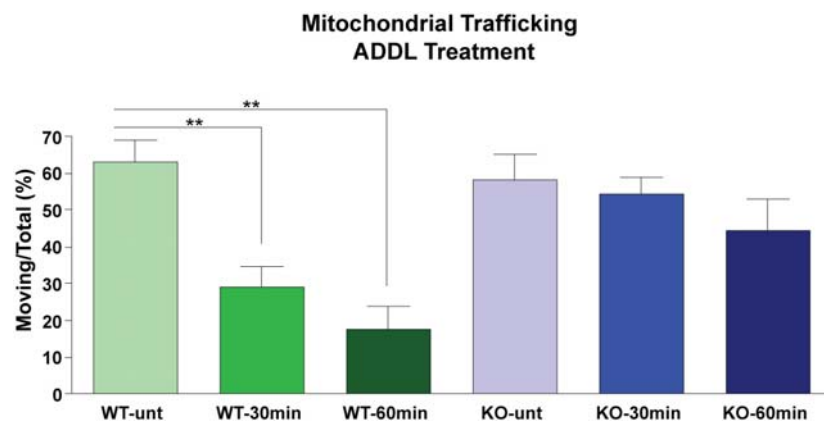


Figure 3.42: Mitochondrial trafficking upon ADDL treatment. Graph showing moving mitochondria as a percentage of total mitochondria in WT and *Hdac6* KO hippocampal cultures before and 30 and 60 min after ADDL treatment (n = 5, p < 0.01).

4. Discussion

Histone deacetylases (HDACs) are being increasingly recognised as promising drug targets for therapy against neurodegeneration. HDAC inhibitors have been used to improve cognition in mouse models of neurodegeneration (Sananbenesi, 2009). The findings described in this study attempt to delve into the molecular mechanisms underlying HDAC inhibition in Alzheimer's disease (AD). The effect of pan-HDAC inhibition on learning and memory was studied using sodium butyrate, a well-known HDAC inhibitor, on a transgenic AD mouse model. More specifically, the role of a class II histone deacetylase, HDAC6, in cognition was analysed in detail using an *Hdac6* knockout mouse model. Additionally, the effect of loss of *Hdac6* in AD was studied by combining the *Hdac6* KO model with a transgenic AD mouse model.

4.1. HDAC inhibition in APPPS1-21 mice

The effect of chronic HDAC inhibition in AD was studied by oral administration of sodium butyrate (SB) in APPPS1-21 double transgenic mice (Radde, 2006) for six weeks followed by behavioural and molecular analysis.

4.1.1. SB treatment improves cognition in APPPS1-21 mice

Oral SB treatment of double transgenic APPPS1-21 mice led to a significant improvement of learning and memory as analysed using the contextual and tone fear conditioning paradigms (Section 3.1.1). This finding accords with the results obtained in similar studies that show improved associative memory in transgenic AD mouse models upon treatment with HDAC inhibitors such as Trichostatin A (TSA), sodium phenylbutyrate and sodium butyrate (Francis, 2009; Kilgore, 2010; Ricobaraza, 2009). Francis and colleagues have shown that treatment with Trichostatin A (TSA), another non-specific HDAC inhibitor, could improve associative memory in contextual fear conditioning in APP/PS1 mice that carry mutated A β PP (K679N:M671L) and PS1

(M146L) genes (Francis, 2009). They observed elevated pan-histone H4 acetylation in the APP/PS1 mice at the age of 3 to 4 months upon TSA treatment. Kilgore and co-workers have reported that treatment with HDAC inhibitors such as sodium valproate, sodium butyrate and suberoylanilide hydroxamic acid (SAHA) improves contextual fear memory in 6-month-old APP^{swe}/PS1^{dE9} mice (Kilgore, 2010). In their study, acute HDACi treatment also resulted in elevated pan-histone H4 acetylation in their AD mouse model. Recent work by Ricobaraza and others suggests that treatment with sodium 4-phenylbutyrate (4-PBA) can be neuroprotective in Tg2576 AD transgenic mice at the age of 16 months (Ricobaraza, 2009). These studies have shown the beneficial effects of HDAC inhibition in transgenic AD mouse models.

However, all the above-mentioned studies have investigated the effects of HDACi treatment at early stages of pathology in their respective transgenic models. In humans, due to delayed diagnosis of the disease, AD pathology is often found to be at an advanced stage before the possibility of therapeutic intervention. Therefore, before HDAC inhibitors are used in clinical trials for the treatment of AD, as attempted in this study, it is crucial to investigate if HDAC inhibition might be beneficial at advanced stages of AD pathology in transgenic animal models.

The results reported in this study show that sodium butyrate treatment could improve associative memory in APPPS1-21 mice even at the age of 14 months when the mice show severe β -amyloid pathology and cognitive impairment. The APPPS1-21 mice exhibit robust AD pathology and cognitive deficits at the age of 8 months (Radde, 2006). Therefore, improvement of cognition at the age of 14 months signifies that orally administered SB can rescue cognitive impairment even at an advanced pathological stage. However, there was no improvement in spatial learning in APPPS1-21 mice upon SB treatment (Section 3.1.1). This indicates that the amelioration of spatial memory deficits might require early intervention. This is a crucial finding as spatial memory has been shown to be impaired in mild cognitive impairment (MCI) already (Laczo, 2010) where as impairment of fear memory occurs later in disease progression (Hamann, 2002; Hoefer, 2008). Therefore, pharmacological intervention at an advanced stage of AD might be more likely to rescue associative memory impairment than spatial memory impairment, which probably requires early diagnosis and treatment in humans.

Exploratory behaviour was not altered in the APPPS1-21 mice upon SB treatment (Section 3.1.1). However, SB treatment reduced basal anxiety in the APPPS1-21 mice (Section 3.1.1). This finding verifies that the elevated freezing observed in fear conditioning was a result of enhanced learning and not increased anxiety. Collectively, the results discussed in this section indicate that HDAC inhibition can improve associative memory in mice even at an advanced stage of AD pathology.

4.1.2. SB treatment upregulates histone acetylation

Since we used a non-specific HDAC inhibitor for treatment, it was crucial to analyse its effect of histone acetylation in detail. As described in section 3.1.2, orally administered SB could elevate acetylation at specific lysine residues on histones in the brain. The sites affected by SB treatment were also found to be hypoacetylated in the APPPS1-21 mouse model (Section 1.3.3). This indicates that SB treatment can rescue specific deficits in histone acetylation associated with AD pathology. This is especially important as the acetylation of different lysines on histones can be involved in the regulation of diverse cellular processes. Recent work from our laboratory has shown that acetylation of H4K12 could be involved in age-related cognitive impairment (Peleg, 2010). Another study has reported the involvement of H3K14 acetylation in hippocampal memory formation (Reul, 2009). Therefore, in addition to the pan-histone acetylation levels analysed in previous studies (Francis, 2009; Kilgore, 2010; Ricobaraza, 2009), the investigation of acetylation at specific lysine residues on histones gives us a more detailed understanding of epigenetic reprogramming in the brain. Additionally, this study also shows that the hippocampus could be more responsive to SB treatment than the cortex as shown by the hyperacetylation of a greater number of lysine residues in the hippocampus. This might indicate a higher level of chromatin plasticity in the hippocampus compared to the cortex. However, a detailed analysis of different sub-cortical regions would yield a deeper insight into cortical histone acetylation.

4.1.3. Enhanced gene expression upon SB treatment

Previous findings from our research group suggest that the process of memory consolidation involves the upregulation of specific genes by epigenetic reprogramming. SB treatment of APPPS1-21 mice resulted in the robust upregulation of *Myst4*, *Fmn2*, *Marcks11*, *Gsk3 α* , *GluR1*, *Snap25* and *Prkca* in the hippocampus and *Marcks11* in the cortex (Section 3.1.3). One of these upregulated genes, *Myst4*, codes for a histone acetyltransferase (HAT) and might play a role in SB-induced upregulation of histone acetylation and regulate gene expression. Another gene, *Snap25*, codes for the synaptosomal-associated protein SNAP-25 that is known to be involved in synaptic plasticity (Matteoli, 2009). SB treatment also resulted in significantly higher protein levels of SNAP-25 in the hippocampus (Fig. 3.7). The AMPA receptor subunit GluR1 has been widely studied and found to be crucial in synaptic plasticity and cognition (Maren, 2005; O'Neill, 2004; Sanderson, 2008). Therefore, the upregulation of these genes might constitute the molecular mechanism underlying the cognitive improvement observed in APPPS1-21 mice upon SB treatment. Additionally, similar to the observations in histone acetylation changes, the gene expression changes were far greater in the hippocampus compared to the cortex. The hippocampus is one of the highly plastic regions in the mammalian brain and also severely affected in AD (Van Hoesen, 1990). Therefore, epigenetic reprogramming of gene expression in the hippocampus might prove to be an effective tool in improving cognitive functions and synaptic plasticity.

4.1.4. SB treatment does not affect β -amyloid plaques

One of the characteristic histopathological features of AD is the presence of extracellular aggregates of A β 42 known as β -amyloid plaques. However, the role of β -amyloid plaques in the pathogenesis of AD is still unclear. Recently, it has been suggested that soluble oligomers of β -amyloid might be involved in neurodegeneration (Haass, 2007). Several attempts to combat AD by immunisation against A β 42 have not been successful in attenuating the cognitive impairment observed in AD patients (Gilman, 2005; Vellas, 2009). In this study, no differences were observed in β -amyloid

plaque load and distribution in APPPS1-21 mice upon SB treatment (Fig. 3.8). This finding concurs with previously published results on the beneficial effects of 4-PBA in Tg2576 AD transgenic mice (Ricobaraza, 2009). This indicates that HDAC inhibition can improve cognition in APPPS1-21 mice without affecting β -amyloid plaques.

4.1.5. Summary

The findings discussed above suggest that HDAC inhibition in APPPS1-21 mice using sodium butyrate can improve cognition. SB treatment leads to upregulation of specific genes involved in memory consolidation and synaptic plasticity possibly by hyperacetylation of specific lysine residues on histones H3 and H4. However, SB treatment did not affect β -amyloid plaque levels in APPPS1-21 mice.

4.2. HDAC6 in the brain

HDAC6 is a unique member of the HDAC superfamily as it acts not on histones but on cytoplasmic substrates like α -tubulin (Zhang, 2003; Zhao, 2010). This makes it an ideal candidate for investigation of non-histone protein acetylation. The covalent post-translational modification of proteins has been shown to be critical for the process of memory formation (Sunyer, 2008). Therefore, the role of HDAC6 in neuronal function during cognition and AD was investigated in global *Hdac6* KO mice and double transgenic APPPS1-21 mice using behavioural and molecular techniques.

4.2.1. HDAC6 in the mouse brain

According to the in situ hybridization images available in the Allen Mouse Brain Atlas (<http://www.brain-map.org/>), *Hdac6* expression could be detected in all regions of the adult mouse brain. Another recent study has shown that *Hdac6* is expressed in all regions of the adult rat brain albeit lower than other class I and class II *Hdac* genes (Broide, 2007). In this study, *Hdac6* expression was analysed in the pre-frontal cortex,

hippocampus, rest of cortex and cerebellum by qPCR (Section 3.2.1). The lowest expression of *Hdac6* was observed in the cerebellum. The expression of *Hdac6* was in the brain regions essential for learning and memory and severely affected in AD such as pre-frontal cortex, hippocampus and the rest of cortex was comparable to each other and significantly higher than the cerebellum.

Next, HDAC6 protein levels were analysed in different brain regions by western blot. Concurrent with *Hdac6* expression, proteins levels were comparable in the pre-frontal cortex, hippocampus and rest of cortex but significantly lower in the cerebellum (Section 3.2.2). HDAC6 is known to deacetylate α -tubulin at lysine 40 in the brain (Hubbert, 2002; Southwood, 2007). As expected, levels of α -tubulin acetylation were similar in the pre-frontal cortex, hippocampus and rest of cortex but significantly higher in the cerebellum. Previous studies have shown that acetylation of α -tubulin at lysine 40 enhances transport of cargo proteins (Reed, 2006) and also facilitates neuronal migration (Creppe, 2009).

4.2.2. Subcellular localisation of HDAC6

Although HDAC6 has been classified as a histone deacetylase (de Ruijter, 2003), its role in the deacetylation of histone proteins has not been established so far. A recent study reported that HDAC6 associates with the promoter and gene body regions of active genes in human CD4⁺ T cells (Wang, 2009b). However, it is not clear if HDAC6 plays a role in the nucleus in the nervous system. Therefore, the subcellular distribution of HDAC6 was analysed using western blot on mouse brain lysates and overexpression of *Hdac6* in primary hippocampal neurons with an eGFP reporter. HDAC6 protein was detected exclusively in the cytoplasm of hippocampal neurons and not in the nucleus (Section 3.2.4). Moreover, the intensity of HDAC6-eGFP negatively correlated with immunoreactivity to acetylated α -tubulin in the neuronal soma (Fig. 3.12g). This finding shows that HDAC6 might not play a direct role in histone acetylation and gene expression in neurons under basal conditions.

4.2.3. Basic characterisation of *Hdac6* knockout mice

The role of HDAC6 in the brain was analysed using a global *Hdac6* knockout (KO) mouse model. In this model, the *Hdac6* gene was disrupted by the insertion of a neomycin resistance gene. The mice were characterised using molecular, histological and behavioural techniques with wild type (WT) littermates as controls.

4.2.3.1. Basic morphology and brain structure in *Hdac6* KO mice

The *Hdac6* KO mice exhibited normal body structure, body weight and home cage behaviour compared to WT controls (Section 3.3.1) in young adulthood. Sexual maturity was also not affected upon loss of *Hdac6* as the KO mice could breed and produce offspring similar to the WT mice. This indicates that loss of *Hdac6* does not exert any severe effect on the growth and development of mice. This could be due to the activation of certain compensatory mechanisms during prenatal and postnatal development. A detailed developmental analysis of *Hdac6* KO mice, especially during the embryonic stage might give us a deeper insight into any such mechanisms. Alternatively, it is also possible that *Hdac6* might not play a role in basic metabolic and physiological pathways in mice. At least, in this study, loss of *Hdac6* did not impair basic biological processes in mice. Basic brain morphology was examined by extracting the brains of *Hdac6* KO and WT mice (Section 3.3.2). There were no differences in the size, mass and shape of brains between WT and KO mice. This indicates that loss of *Hdac6* does not induce any loss or gain of brain tissue in mice. Recently, Zhang and colleagues have reported that HDAC6-deficient mice generated on a C57BL/6 strain background exhibit slightly higher body weight at 3 and 5 months of age and also an increase in tibial bone size and mineral content (Zhang, 2008). These effects might be strain-related, as we do not see any change in body weight in our *Hdac6* KO model. Apart from this, Zhang and colleagues have not reported any major differences in the morphology of HDAC6-deficient mice.

4.2.3.2. Histone acetylation in *Hdac6* KO mice

As described in Section 3.3.4, western blot and immunohistological analyses revealed that histone acetylation was not affected in the hippocampus upon loss of *Hdac6* in mice. This further indicates that HDAC6 might not play a direct role in histone acetylation in the mouse brain. Interestingly, Zhang and colleagues have also reported that histone H4 acetylation in the testis is not altered in the *Hdac6* KO mice used in their study (Zhang, 2008). Collectively, the above-mentioned findings challenge the role of HDAC6 as a histone deacetylase and indicate that this unique HDAC family member might act on non-histone cytoplasmic substrates.

4.2.3.3. Tubulin acetylation in *Hdac6* KO mice

HDAC6 is a unique member of the HDAC family as it acts on cytoplasmic substrates such as α -tubulin (Hubbert, 2002). Therefore, an increase in α -tubulin acetylation was expected upon loss of *Hdac6* in mice. Resolution of hippocampal and cortical proteins from WT and *Hdac6* KO mice by SDS-PAGE followed by Coomassie staining revealed an additional protein band of molecular weight 55 kDa in the *Hdac6* KO mice (Section 3.3.3). The α -tubulin protein has a molecular weight of 55 kDa in mice. Therefore this additional band detected in KO mice probably represents hyperacetylated α -tubulin due to HDAC6 deficiency. This was confirmed by further western blot and immunohistochemical analyses showing that α -tubulin acetylation was significantly enhanced in *Hdac6* KO mice in the hippocampus and cortex. This is in contrast with results obtained in another study on HDAC6-deficient mice where the authors observed no difference in tubulin acetylation in the brain (Zhang, 2008). The antibody used by Zhang and colleagues to detect acetylated α -tubulin is different from the one used in this study (Table 2.19). The disparity in results between the two studies could be a result of a difference in the specificity of the antibodies used. Moreover, the authors analysed α -tubulin acetylation in total brain lysates (Zhang, 2008). A more detailed analysis in specific brain regions like hippocampus and cortex presented here revealed hyperacetylation of α -tubulin in the *Hdac6* KO mice. Hyperacetylation of α -tubulin has

been to shown to enhance microtubular transport of essential cargo proteins (Deribe, 2009; Dompierre, 2007; Gao, 2010) and also mitochondria (Chen, 2010). Therefore, elevated α -tubulin acetylation observed in brain regions involved in cognition such as hippocampus and cortex in our *Hdac6* KO mice might be beneficial for cognition.

4.2.3.4. Expression of Hdac genes in Hdac6 KO mice

The deficiency of HDAC6 in the *Hdac6* KO mice was analysed by biochemistry. Semi-quantitative PCR and western blot analyses verified the lack of *Hdac6* mRNA and protein respectively in the hippocampus and cortex of *Hdac6* KO mice (Section 3.3.5). The expression of other *Hdac* genes was analysed in the hippocampus of *Hdac6* KO mice using qPCR to investigate any compensatory effect on *Hdac* expression. The expression of *Hdac4*, *Hdac11* and *Sirt3* was slightly decreased and *Hdac9* slightly increased in the *Hdac6* KO mice. The expression of all other *Hdac* genes was unaltered upon loss of *Hdac6*. Importantly, the expression of *Sirt2*, another known deacetylase of α -tubulin in glial cells (Southwood, 2007), was not changed in *Hdac6* KO mice. Therefore, in the *Hdac6* KO mouse model used in this study, there was no drastic upregulation or downregulation of other *Hdac* genes detected.

4.2.3.5. Role of HDAC6 in gene expression

The expression of genes that are upregulated in memory consolidation was analysed in the hippocampus of *Hdac6* KO mice using qPCR (Section 3.3.6). Loss of *Hdac6* did not affect the expression of *Fmn2*, *Marcks11*, *Snap25*, *Prkca*, *Myst4* or *GluR1*. This result further argues against the direct involvement of HDAC6 in the regulation of gene expression in the mouse brain. In contrast to its role in regulating gene expression in CD4⁺ T cells (Wang, 2009b), HDAC6 in neurons could possibly play a role in microtubular stability and transport through the deacetylation of α -tubulin (Hubbert, 2002; Zhang, 2003; Zhao, 2010).

4.2.4. Behavioural analysis of *Hdac6* KO mice

The role of HDACs in learning and memory is still not entirely clear. Recent studies have shown that loss of *Hdac2* led to the enhancement of associative memory in mice (Guan, 2009) but loss of *Sirt1* caused impairment of short-term and long-term fear memory (Michan, 2010). These studies indicate that different members of the HDAC family might play distinct roles in cognition. Therefore, the role of HDAC6 in learning and memory was analysed in *Hdac6* KO mice using a battery of behavioural tests. Basal anxiety and exploratory behaviour was unchanged in the *Hdac6* KO mice (Section 3.6). Long-term associative memory was also unaltered upon loss of *Hdac6* in mice (Section 3.4). However, the *Hdac6* KO mice showed an increased preference for the target region in the water maze probe test (Section 3.4). These results indicate that loss of *Hdac6* is not detrimental to cognition but in fact, might contribute to improvement of spatial memory. This finding is crucial as spatial memory deficits have been commonly observed in cognitive disorders such as Mild Cognitive Impairment (MCI) and AD (Iachini, 2009). The *Hdac6* KO mice showed no deficits in motor functions as shown by normal swimming speed in the water maze (Section 3.4) and normal performance in the rotarod test (Section 3.4).

4.2.5. Pharmacological inhibition of HDAC6 in mice

HDAC inhibitors such as sodium butyrate, valproate and SAHA have proven to be potential enhancers of learning and memory in mice and have been proposed as promising therapeutic agents against neurodegeneration (Butler, 2006; Fischer, 2007; Hahnen, 2008; Peleg, 2010). In addition to such non-specific HDAC inhibitors, it is important to investigate the inhibition of specific HDACs in learning and memory. For this purpose, cognition was analysed in mice treated with a specific HDAC6 inhibitor, ST27, using contextual fear conditioning. Unlike the observation in *Hdac6* KO mice, the acute inhibition of HDAC6 improved long-term associative memory in mice (Section 3.5). It is possible that the genetic loss of *Hdac6* in mice might have triggered compensatory mechanisms during growth and development, which resulted in normal fear memory in the *Hdac6* KO mice. However, acute inhibition of HDAC6 could

possibly exert immediate effects on cognition resulting in improved consolidation of fear memory.

4.2.6. Summary

Hdac6 mRNA and protein were detected in the mouse brain. HDAC6 seemed to be localised to the cytoplasm in neurons suggesting that it might not be involved in histone acetylation. The role of HDAC6 in the brain was analysed using an *Hdac6* KO mouse model. Compared to WT controls, the *Hdac6* KO mice exhibited elevated α -tubulin acetylation in the brain and enhanced spatial memory in the water maze task. Loss of *Hdac6* did not affect histone acetylation or expression of genes involved in memory consolidation in the hippocampus. Acute pharmacological inhibition of HDAC6 in the brain improved associative memory in mice. These results indicate that, unlike other HDACs, HDAC6 might not be involved in epigenetic regulation of gene expression in the brain. Moreover, loss of *Hdac6* could be beneficial to learning and memory in mice. This indicates that HDAC6 could be a promising therapeutic target for learning and memory disorders.

4.3. Loss of *Hdac6* attenuates AD pathology

The results obtained so far indicate that loss of HDAC6 activity is not detrimental for cognition in mice. At the molecular level, the principal change observed upon loss of *Hdac6* was elevation of α -tubulin acetylation. The next goal was to study the lack of HDAC6 in a model for AD. Therefore, the *Hdac6* KO mice were bred with the double transgenic APPPS1-21 Alzheimer's mouse model (Radde, 2006). The mice were characterised using behavioural and molecular biological techniques.

4.3.1. Loss of *Hdac6* improves cognition in APPPS1-21 mice

The APPPS1-21 transgenic mice exhibit cognitive deficit at the early age of 8 months (Radde, 2006). In this study, the APPPS1-21 mice also exhibited impaired associative memory in fear conditioning and impaired spatial memory in the water maze probe test (Section 3.6.3) at 8 months of age. However, loss of *Hdac6* in APPPS1-21 mice led to a significant improvement in both contextual fear memory and spatial memory (Section 3.6.2) without affecting basal anxiety levels or exploratory behaviour in the open field (Section 3.6.1). This shows that the specific loss of HDAC6 activity can rescue cognitive impairment in this AD mouse model. In addition, this supports the findings reported by others showing that loss of HDAC activity could attenuate the cognitive impairment in neurodegeneration (Fischer, 2007; Kilgore, 2010; Ricobaraza, 2009). Currently, our therapeutic arsenal against cognitive impairment in AD is greatly limited. The strategies targeting β -amyloid pathology such as immunisation against A β have not been successful in abating the cognitive symptoms that severely deteriorate the quality of life in AD patients (Lemere, 2010). Therefore, this finding presents HDAC6 as a possible target for cognitive therapy in AD.

4.3.2. Molecular analysis of *Hdac6* loss in AD pathology

The molecular mechanism behind the improvement of cognitive functions in APPPS1-21 mice upon loss of *Hdac6* was investigated using histological and biochemical techniques. Loss of *Hdac6* did not affect the amount of β -amyloid plaques in the APPPS1-21 mice (Section 3.6.4.4). A previous study has also shown that HDAC inhibitors could improve cognition in an AD mouse model without affecting A β plaque levels (Ricobaraza, 2009). These findings argue against the notion that β -amyloid plaques are responsible for the aetiology of AD. Moreover, immunotherapy against A β has not yet been successful in attenuating cognitive impairment in advanced AD (Lemere, 2010).

The cognitive improvement observed in APPPS1-21 mice upon loss of *Hdac6* could possibly be a result of enhancement of synaptic plasticity in the hippocampus. Levels of

proteins involved in synaptic plasticity such as SYP, PSD-95 and GluR1 were analysed in APPPS1-21-HD6^{-/-} mice in total protein extracts from the hippocampus (Sections 3.6.4.2). Loss of *Hdac6* did not alter the levels of these proteins in APPPS1-21 mice. This indicates that HDAC6 probably does not affect the levels of plasticity-related proteins. As shown earlier, loss of *Hdac6* did also not affect the expression of genes involved in memory consolidation in mice (Section 3.3.6).

The decrease in α -tubulin acetylation observed in APPPS1-21 mice could be rescued by loss of *Hdac6* (Section 3.6.4.1). Tubulin acetylation has been shown to be critical for kinesin-1 binding to microtubules and intraneuronal transport of cargo proteins such as JIP1 (Reed, 2006). Hyperacetylation of α -tubulin by HDAC6 inhibition has been shown to be neuroprotective in Huntington's disease (HD) by enhanced transport of BDNF (Dompierre, 2007). Therefore, to investigate if trafficking of plasticity-related proteins was enhanced in APPPS1-21 mice upon loss of *Hdac6*, the levels of SYP, PSD-95 and GluR1 were analysed in synaptosomal and PSD protein fractions. Loss of *Hdac6* did not affect the levels of these markers of synaptic plasticity either in the synaptosomal or the PSD protein fractions from APPPS1-21 mice. Although, further electrophysiological studies are necessary to make a definitive conclusion, these findings indicate that loss of *Hdac6* improves cognition in APPPS1-21 mice possibly via a mechanism other than the direct enhancement of synaptic plasticity.

A previous study has shown that the intraneuronal distribution of mitochondria is disrupted in AD (Wang, 2009a). The same study also suggests that impaired anterograde trafficking of mitochondria in neurons leads to reduced density of mitochondria in the dendrites and a corresponding increase in mitochondrial density in the soma (Wang, 2009a). Additionally, acute treatment of primary rat hippocampal neurons with synthetic A β 1-42 oligomers has been shown to impair mitochondrial trafficking (Rui, 2006). Interestingly, another recent report has shown that inhibition of HDAC6 could improve mitochondrial trafficking in neurons (Chen, 2010). Importantly, trafficking of mitochondrial from soma to synapses has been shown to be crucial for synaptic function (Chang, 2006). Based on these reports, mitochondrial trafficking was analysed in primary mouse hippocampal neurons from WT and *Hdac6* KO mice upon treatment with ADDL (Section 2.4). Mitochondrial trafficking was significantly

impaired in WT neurons upon ADDL treatment (Section 3.7). However, similar to previous findings (Chen, 2010), neurons from *Hdac6* KO mice seemed to be resistant to ADDL-induced impairment of mitochondrial trafficking. Elevation of α -tubulin acetylation upon loss of *Hdac6* could be an underlying mechanism behind this effect. As described in Section 3.7, loss of *Hdac6* leads to a significant increase in α -tubulin acetylation in both WT and APPPS1-21 mice. En masse, these data suggest that loss of *Hdac6* might be protective against impairment of mitochondrial trafficking in AD through the elevation of α -tubulin acetylation.

4.3.3. Summary

These data suggest that loss of *Hdac6* could be protective against cognitive impairment in a transgenic AD mouse model without affecting β -amyloid pathology. Elevation of α -tubulin acetylation resulting in improved mitochondrial trafficking could be a possible mechanism underlying this protective effect of *Hdac6* loss. These findings propose HDAC6 as a potential drug target for therapy against cognitive impairment in Alzheimer's disease.

4.4. Future Outlook

The research presented here shows that loss of HDAC activity might be beneficial for learning and memory in Alzheimer's disease. Cognitive impairment in a transgenic AD mouse model, APPPS1-21, could be rescued by oral treatment with sodium butyrate, a non-specific HDAC inhibitor, by the upregulation of histone acetylation and gene expression in the hippocampus. A definitive link between enhanced histone acetylation and upregulation of gene expression can be established by performing further experiments such as ChIP targeting the specific sites on histones that were found to be hyperacetylated followed by qPCR analysis. This will give us a deeper insight into the specific genomic regions upregulated by enhanced histone acetylation. HDAC inhibition at an earlier pathological stage could help improve other forms of memory such as spatial memory in the APPPS1-21 mice.

The role of HDAC6, a class II member of the HDAC family and a deacetylase of α -tubulin, was investigated in greater detail using an *Hdac6* KO mouse model. Profiling of protein acetylation in WT and *Hdac6* KO mouse brains could help identify other possible targets of HDAC6 in the brain. Loss of *Hdac6* was found to enhance cognition in mice and rescue cognitive impairment in APPPS1-21 mice by elevation of α -tubulin acetylation and facilitation of mitochondrial trafficking. Therefore, HDAC6 can be a promising target for therapy in AD. Treatment of APPPS1-21 mice with specific HDAC6 inhibitors such as ST27 followed by behavioural analysis could yield a deeper insight into pharmacological inhibition of HDAC6 in AD. By virtue of its action on the chaperone Hsp90, HDAC6 might play a role in protein folding and aggregation in the brain. The role of HDAC6 in protein aggregation can be investigated by further biochemical analysis of *Hdac6* KO mice independently and in combination with models of other neurodegenerative disorders such as Huntington's and Parkinson's diseases. Furthermore, generation and survival of newborn neurons should be investigated in the *Hdac6* KO mice. By virtue of its action on microtubules, HDAC6 could possibly play a role in the differentiation and maturation of neural precursor cells.

Acknowledgement

My doctoral work was conceived and conducted under Dr. André Fischer's unstinted supervision at the European Neuroscience Institute Göttingen. Working with Andre has been a great learning experience and has contributed a great deal to my scientific growth and maturity. I express my sincere gratitude to him for this opportunity and his mentorship. I have been a member of the Fischer lab from its inception and have enjoyed seeing it expand and diversify its research focus. All the lab members have been extremely helpful and understanding throughout my stay. Their support has been crucial to my accomplishment. In particular, I wish to thank Tanja for all her cooperation right from day one. Jessica has always been eager to join forces even after leaving our lab and continues to be a great friend. I hope our friendship grows stronger with time. I thank Torsten for his assistance with cloning strategies and proofreading, Roberto for all the amazing discussions we've had apart from his help in nearly every technique I've performed in the lab, Thanasis for his help with primer designing, Farah for her organisational skills, Sanaz for her critical discussions and Shahaf for infusing a bit of his nonchalant attitude towards life in me, especially during hard times. I appreciate Hope and Roman for their assistance in the lab and for the many scientific and philosophical questions we've pondered over together. I wish Cemil all the best in his scientific endeavours. I have had the pleasure of supervising Jonas as he accomplished his bachelor's dissertation in our lab. I have learnt a lot from our technician Susanne, who forms the technical backbone of our group. With a career span longer than my age, she has taught me many valuable lessons about life and also indulged my taste buds with cookies and cakes. The ENI-Göttingen has provided me with a congenial atmosphere to carry out my research along with constant technical and bureaucratic support from its staff. I thank Heiko for all his help with microscopy, Christiane and Sissi for administrative help, Frank and his team for building up some of our behavioural equipment and a lot of technical repair work and Matthias and Ali for their *in silico* assistance. The animal caretakers have been of valuable help during my entire work and I thank them for their efforts. I am grateful to Dr. Oliver Schlüter for

his cooperation and intellectual contributions and his technicians Martina and Sandra for providing neuronal cultures and technical support. Dr. Till Marquardt and Liang have been generous in letting me use their microscope, which was also very helpful. I would also like to thank Dr. Jianrong Lu for providing the *Hdac6* knockout mice.

My family has been my pillar of strength during this phase of my life. Most importantly, none of this would have been possible without the tender love and care my darling wife Ania has given me. Sharing my life with her is the best gift I could have asked for. Her keen eye for detail has been very helpful in organising my thesis. I am forever indebted to my parents, for their blessings, their lifelong effort in bringing me up and their continued emotional support. My little brother Ranga is also one of my best friends in life. I wish I could take a trip back in time and grow up with him all over again. Having entered the mad world of scientific research himself, he is extremely encouraging towards my progress as well.

I will be forever grateful to the Hans and Ilse Breuer Foundation for having supported me with a PhD scholarship for three years. The Eibsee meetings have been very useful in expanding my understanding of Alzheimer's disease and interacting with the research community. Last but not the least, I would like to thank my PhD advisors, Prof. Ralf Heinrich and Prof. Michael Hörner, for their guidance and support.

References

- Alonso, A., Zaidi, T., Novak, M., Grundke-Iqbal, I., & Iqbal, K. (2001). Hyperphosphorylation induces self-assembly of tau into tangles of paired helical filaments/straight filaments. *Proc Natl Acad Sci U S A*, *98*, 6923-6928.
- Alzheimer, A., Stelzmann, R. A., Schnitzlein, H. N., & Murtagh, F. R. (1995). An English translation of Alzheimer's 1907 paper, "Uber eine eigenartige Erkankung der Hirnrinde". *Clin Anat*, *8*, 429-431.
- Areosa Sastre, A., McShane, R., & Sherriff, F. (2004). Memantine for dementia. *Cochrane Database Syst Rev*, CD003154.
- Arriagada, P. V., Growdon, J. H., Hedley-Whyte, E. T., & Hyman, B. T. (1992). Neurofibrillary tangles but not senile plaques parallel duration and severity of Alzheimer's disease. *Neurology*, *42*, 631-639.
- Augustinack, J. C., Schneider, A., Mandelkow, E. M., & Hyman, B. T. (2002). Specific tau phosphorylation sites correlate with severity of neuronal cytopathology in Alzheimer's disease. *Acta Neuropathol*, *103*, 26-35.
- Avvakumov, N., & Cote, J. (2007). Functions of histone acetyltransferases and their link to disease. *Subcell Biochem*, *41*, 295-317.
- Bear, M. F., Connors, B. W., & Paradiso, M. A. (2006). Neuroscience: Exploring the Brain. *Lippincott Williams and Wilkins*.
- Bekinschtein, P., Cammarota, M., Katche, C., Slipczuk, L., Rossato, J. I., Goldin, A., Izquierdo, I., & Medina, J. H. (2008). BDNF is essential to promote persistence of long-term memory storage. *Proc Natl Acad Sci U S A*, *105*, 2711-2716.
- Benson, L. J., Phillips, J. A., Gu, Y., Parthun, M. R., Hoffman, C. S., & Annunziato, A. T. (2007). Properties of the type B histone acetyltransferase Hat1: H4 tail interaction, site preference, and involvement in DNA repair. *J Biol Chem*, *282*, 836-842.
- Bentahir, M., Nyabi, O., Verhamme, J., Tolia, A., Horre, K., Wiltfang, J., Esselmann, H., & De Strooper, B. (2006). Presenilin clinical mutations can affect gamma-secretase activity by different mechanisms. *J Neurochem*, *96*, 732-742.
- Berchtold, N. C., & Cotman, C. W. (1998). Evolution in the conceptualization of dementia and Alzheimer's disease: Greco-Roman period to the 1960s. *Neurobiol Aging*, *19*, 173-189.
- Bertani, G. (1951). Studies on lysogenesis. I. The mode of phage liberation by lysogenic *Escherichia coli*. *J Bacteriol*, *62*, 293-300.
- Bhaskara, S., Chyla, B. J., Amann, J. M., Knutson, S. K., Cortez, D., Sun, Z. W., & Hiebert, S. W. (2008). Deletion of histone deacetylase 3 reveals critical roles in S phase progression and DNA damage control. *Mol Cell*, *30*, 61-72.
- Birks, J. (2006a). Cholinesterase inhibitors for Alzheimer's disease. *Cochrane Database Syst Rev*, CD005593.

- Birks, J., Grimley Evans, J., Iakovidou, V., Tsolaki, M., & Holt, F. E. (2009). Rivastigmine for Alzheimer's disease. *Cochrane Database Syst Rev*, CD001191.
- Birks, J., & Harvey, R. J. (2006b). Donepezil for dementia due to Alzheimer's disease. *Cochrane Database Syst Rev*, CD001190.
- Bishop, N. A., Lu, T., & Yankner, B. A. (2010). Neural mechanisms of ageing and cognitive decline. *Nature*, *464*, 529-535.
- Blanchard, R. J., & Blanchard, D. C. (1969). Crouching as an index of fear. *J Comp Physiol Psychol*, *67*, 370-375.
- Bottino, C. M., Carvalho, I. A., Alvarez, A. M., Avila, R., Zukauskas, P. R., Bustamante, S. E., Andrade, F. C., Hototian, S. R., Saffi, F., & Camargo, C. H. (2005). Cognitive rehabilitation combined with drug treatment in Alzheimer's disease patients: a pilot study. *Clin Rehabil*, *19*, 861-869.
- Braak, H., & Braak, E. (1991). Neuropathological staging of Alzheimer-related changes. *Acta Neuropathol*, *82*, 239-259.
- Bradford, M. M. (1976). A rapid and sensitive method for the quantitation of microgram quantities of protein utilizing the principle of protein-dye binding. *Anal Biochem*, *72*, 248-254.
- Broide, R. S., Redwine, J. M., Aftahi, N., Young, W., Bloom, F. E., & Winrow, C. J. (2007). Distribution of histone deacetylases 1-11 in the rat brain. *J Mol Neurosci*, *31*, 47-58.
- Brookmeyer, R., Gray, S., & Kawas, C. (1998). Projections of Alzheimer's disease in the United States and the public health impact of delaying disease onset. *Am J Public Health*, *88*, 1337-1342.
- Butler, R., & Bates, G. P. (2006). Histone deacetylase inhibitors as therapeutics for polyglutamine disorders. *Nat Rev Neurosci*, *7*, 784-796.
- Butterfield, D. A., Koppal, T., Subramaniam, R., & Yatin, S. (1999). Vitamin E as an antioxidant/free radical scavenger against amyloid beta-peptide-induced oxidative stress in neocortical synaptosomal membranes and hippocampal neurons in culture: insights into Alzheimer's disease. *Rev Neurosci*, *10*, 141-149.
- Buxbaum, J. D., Liu, K. N., Luo, Y., Slack, J. L., Stocking, K. L., Peschon, J. J., Johnson, R. S., Castner, B. J., Cerretti, D. P., & Black, R. A. (1998). Evidence that tumor necrosis factor alpha converting enzyme is involved in regulated alpha-secretase cleavage of the Alzheimer amyloid protein precursor. *J Biol Chem*, *273*, 27765-27767.
- Castellucci, V. F., Blumenfeld, H., Goelet, P., & Kandel, E. R. (1989). Inhibitor of protein synthesis blocks long-term behavioral sensitization in the isolated gill-withdrawal reflex of *Aplysia*. *J Neurobiol*, *20*, 1-9.
- Chain, D. G., Schwartz, J. H., & Hegde, A. N. (1999). Ubiquitin-mediated proteolysis in learning and memory. *Mol Neurobiol*, *20*, 125-142.
- Chang, D. T., Honick, A. S., & Reynolds, I. J. (2006). Mitochondrial trafficking to synapses in cultured primary cortical neurons. *J Neurosci*, *26*, 7035-7045.
- Chang, S., McKinsey, T. A., Zhang, C. L., Richardson, J. A., Hill, J. A., & Olson, E. N. (2004). Histone deacetylases 5 and 9 govern responsiveness of the heart to a subset of stress signals and play redundant roles in heart development. *Mol Cell Biol*, *24*, 8467-8476.

- Chawla, S., Vanhoutte, P., Arnold, F. J., Huang, C. L., & Bading, H. (2003). Neuronal activity-dependent nucleocytoplasmic shuttling of HDAC4 and HDAC5. *J Neurochem*, *85*, 151-159.
- Chen, S., Owens, G. C., Makarenkova, H., & Edelman, D. B. (2010). HDAC6 regulates mitochondrial transport in hippocampal neurons. *PLoS One*, *5*, e10848.
- Choudhary, C., Kumar, C., Gnad, F., Nielsen, M. L., Rehman, M., Walther, T. C., Olsen, J. V., & Mann, M. (2009). Lysine acetylation targets protein complexes and co-regulates major cellular functions. *Science*, *325*, 834-840.
- Cooke, S. F., & Bliss, T. V. (2006). Plasticity in the human central nervous system. *Brain*, *129*, 1659-1673.
- Corkin, S. (2002). What's new with the amnesic patient H.M.? *Nat Rev Neurosci*, *3*, 153-160.
- Costa-Mattioli, M., & Sonenberg, N. (2008). Translational control of gene expression: a molecular switch for memory storage. *Prog Brain Res*, *169*, 81-95.
- Cowan, N. (2001). The magical number 4 in short-term memory: a reconsideration of mental storage capacity. *Behav Brain Sci*, *24*, 87-114; discussion 114-185.
- Creppe, C., Malinouskaya, L., Volvert, M. L., Gillard, M., Close, P., Malaise, O., Laguesse, S., Cornez, I., Rahmouni, S., Ormenese, S., Belachew, S., Malgrange, B., Chapelle, J. P., Siebenlist, U., Moonen, G., Chariot, A., & Nguyen, L. (2009). Elongator controls the migration and differentiation of cortical neurons through acetylation of alpha-tubulin. *Cell*, *136*, 551-564.
- Crusio, W. E., & Schwegler, H. (2005). Learning spatial orientation tasks in the radial-maze and structural variation in the hippocampus in inbred mice. *Behav Brain Funct*, *1*, 3.
- Cupers, P., Orlans, I., Craessaerts, K., Annaert, W., & De Strooper, B. (2001). The amyloid precursor protein (APP)-cytoplasmic fragment generated by gamma-secretase is rapidly degraded but distributes partially in a nuclear fraction of neurones in culture. *J Neurochem*, *78*, 1168-1178.
- Dash, P. K., Orsi, S. A., Zhang, M., Grill, R. J., Pati, S., Zhao, J., & Moore, A. N. (2010). Valproate administered after traumatic brain injury provides neuroprotection and improves cognitive function in rats. *PLoS One*, *5*, e11383.
- de Ruijter, A. J., van Gennip, A. H., Caron, H. N., Kemp, S., & van Kuilenburg, A. B. (2003). Histone deacetylases (HDACs): characterization of the classical HDAC family. *Biochem J*, *370*, 737-749.
- Deribe, Y. L., Wild, P., Chandrashaker, A., Curak, J., Schmidt, M. H., Kalaidzidis, Y., Milutinovic, N., Kratchmarova, I., Buerkle, L., Fetchko, M. J., Schmidt, P., Kittanakom, S., Brown, K. R., Jurisica, I., Blagoev, B., Zerial, M., Stagljar, I., & Dikic, I. (2009). Regulation of epidermal growth factor receptor trafficking by lysine deacetylase HDAC6. *Sci Signal*, *2*, ra84.
- Dompierre, J. P., Godin, J. D., Charrin, B. C., Cordelieres, F. P., King, S. J., Humbert, S., & Saudou, F. (2007). Histone deacetylase 6 inhibition compensates for the transport deficit in Huntington's disease by increasing tubulin acetylation. *J Neurosci*, *27*, 3571-3583.
- Eichenbaum, H. (2001). The hippocampus and declarative memory: cognitive mechanisms and neural codes. *Behav Brain Res*, *127*, 199-207.
- Ellenbogen, J. M., Payne, J. D., & Stickgold, R. (2006). The role of sleep in declarative memory consolidation: passive, permissive, active or none? *Curr Opin Neurobiol*, *16*, 716-722.

- Engelender, S. (2008). Ubiquitination of alpha-synuclein and autophagy in Parkinson's disease. *Autophagy*, 4, 372-374.
- Federman, N., Fustinana, M. S., & Romano, A. (2009). Histone acetylation is recruited in consolidation as a molecular feature of stronger memories. *Learn Mem*, 16, 600-606.
- Fischer, A., Sananbenesi, F., Wang, X., Dobbin, M., & Tsai, L. H. (2007). Recovery of learning and memory is associated with chromatin remodelling. *Nature*, 447, 178-182.
- Francis, Y. I., Fa, M., Ashraf, H., Zhang, H., Staniszewski, A., Latchman, D. S., & Arancio, O. (2009). Dysregulation of histone acetylation in the APP/PS1 mouse model of Alzheimer's disease. *J Alzheimers Dis*, 18, 131-139.
- Gao, Y. S., Hubbert, C. C., & Yao, T. P. (2010). The microtubule-associated histone deacetylase 6 (HDAC6) regulates epidermal growth factor receptor (EGFR) endocytic trafficking and degradation. *J Biol Chem*, 285, 11219-11226.
- Geula, C., & Mesulam, M. M. (1995). Cholinesterases and the pathology of Alzheimer disease. *Alzheimer Dis Assoc Disord*, 9 Suppl 2, 23-28.
- Gilman, S., Koller, M., Black, R. S., Jenkins, L., Griffith, S. G., Fox, N. C., Eisner, L., Kirby, L., Rovira, M. B., Forette, F., & Orgogozo, J. M. (2005). Clinical effects of Abeta immunization (AN1792) in patients with AD in an interrupted trial. *Neurology*, 64, 1553-1562.
- Glozak, M. A., Sengupta, N., Zhang, X., & Seto, E. (2005). Acetylation and deacetylation of non-histone proteins. *Gene*, 363, 15-23.
- Goate, A. M. (1998). Monogenetic determinants of Alzheimer's disease: APP mutations. *Cell Mol Life Sci*, 54, 897-901.
- Goedert, M. (1993). Tau protein and the neurofibrillary pathology of Alzheimer's disease. *Trends Neurosci*, 16, 460-465.
- Grant, P. A., Eberharter, A., John, S., Cook, R. G., Turner, B. M., & Workman, J. L. (1999). Expanded lysine acetylation specificity of Gcn5 in native complexes. *J Biol Chem*, 274, 5895-5900.
- Gravina, S. A., Ho, L., Eckman, C. B., Long, K. E., Otvos, L., Jr., Younkin, L. H., Suzuki, N., & Younkin, S. G. (1995). Amyloid beta protein (A beta) in Alzheimer's disease brain. Biochemical and immunocytochemical analysis with antibodies specific for forms ending at A beta 40 or A beta 42(43). *J Biol Chem*, 270, 7013-7016.
- Grundman, M., Petersen, R. C., Ferris, S. H., Thomas, R. G., Aisen, P. S., Bennett, D. A., Foster, N. L., Jack, C. R., Jr., Galasko, D. R., Doody, R., Kaye, J., Sano, M., Mohs, R., Gauthier, S., Kim, H. T., Jin, S., Schultz, A. N., Schafer, K., Mulnard, R., van Dyck, C. H., Mintzer, J., Zamrini, E. Y., Cahn-Weiner, D., & Thal, L. J. (2004). Mild cognitive impairment can be distinguished from Alzheimer disease and normal aging for clinical trials. *Arch Neurol*, 61, 59-66.
- Guan, J. S., Haggarty, S. J., Giacometti, E., Dannenberg, J. H., Joseph, N., Gao, J., Nieland, T. J., Zhou, Y., Wang, X., Mazitschek, R., Bradner, J. E., DePinho, R. A., Jaenisch, R., & Tsai, L. H. (2009). HDAC2 negatively regulates memory formation and synaptic plasticity. *Nature*, 459, 55-60.

- Guan, Z., Giustetto, M., Lomvardas, S., Kim, J. H., Miniaci, M. C., Schwartz, J. H., Thanos, D., & Kandel, E. R. (2002). Integration of long-term-memory-related synaptic plasticity involves bidirectional regulation of gene expression and chromatin structure. *Cell*, *111*, 483-493.
- Gupta, S., Kim, S. Y., Artis, S., Molfese, D. L., Schumacher, A., Sweatt, J. D., Paylor, R. E., & Lubin, F. D. (2010). Histone methylation regulates memory formation. *J Neurosci*, *30*, 3589-3599.
- Guzowski, J. F. (2002). Insights into immediate-early gene function in hippocampal memory consolidation using antisense oligonucleotide and fluorescent imaging approaches. *Hippocampus*, *12*, 86-104.
- Haass, C., & Selkoe, D. J. (2007). Soluble protein oligomers in neurodegeneration: lessons from the Alzheimer's amyloid beta-peptide. *Nat Rev Mol Cell Biol*, *8*, 101-112.
- Haberland, M., Montgomery, R. L., & Olson, E. N. (2009). The many roles of histone deacetylases in development and physiology: implications for disease and therapy. *Nat Rev Genet*, *10*, 32-42.
- Haggarty, S. J., Koeller, K. M., Wong, J. C., Grozinger, C. M., & Schreiber, S. L. (2003). Domain-selective small-molecule inhibitor of histone deacetylase 6 (HDAC6)-mediated tubulin deacetylation. *Proc Natl Acad Sci U S A*, *100*, 4389-4394.
- Hahnen, E., Hauke, J., Trankle, C., Eyupoglu, I. Y., Wirth, B., & Blumcke, I. (2008). Histone deacetylase inhibitors: possible implications for neurodegenerative disorders. *Expert Opin Investig Drugs*, *17*, 169-184.
- Hamann, S., Monarch, E. S., & Goldstein, F. C. (2002). Impaired fear conditioning in Alzheimer's disease. *Neuropsychologia*, *40*, 1187-1195.
- Hashimoto, M., Rockenstein, E., Crews, L., & Masliah, E. (2003). Role of protein aggregation in mitochondrial dysfunction and neurodegeneration in Alzheimer's and Parkinson's diseases. *Neuromolecular Med*, *4*, 21-36.
- Hebb, D. O. (1949). The organization of behavior.
- Hoefer, M., Allison, S. C., Schauer, G. F., Neuhaus, J. M., Hall, J., Dang, J. N., Weiner, M. W., Miller, B. L., & Rosen, H. J. (2008). Fear conditioning in frontotemporal lobar degeneration and Alzheimer's disease. *Brain*, *131*, 1646-1657.
- Holliday, R. (1994). Epigenetics: an overview. *Dev Genet*, *15*, 453-457.
- Hsiao, K., Chapman, P., Nilsen, S., Eckman, C., Harigaya, Y., Younkin, S., Yang, F., & Cole, G. (1996). Correlative memory deficits, A β elevation, and amyloid plaques in transgenic mice. *Science*, *274*, 99-102.
- Hubbert, C., Guardiola, A., Shao, R., Kawaguchi, Y., Ito, A., Nixon, A., Yoshida, M., Wang, X. F., & Yao, T. P. (2002). HDAC6 is a microtubule-associated deacetylase. *Nature*, *417*, 455-458.
- Iachini, I., Iavarone, A., Senese, V. P., Ruotolo, F., & Ruggiero, G. (2009). Visuospatial memory in healthy elderly, AD and MCI: a review. *Curr Aging Sci*, *2*, 43-59.
- Ittner, L. M., Ke, Y. D., Delerue, F., Bi, M., Gladbach, A., van Eersel, J., Wolfing, H., Chieng, B. C., Christie, M. J., Napier, I. A., Eckert, A., Staufenbiel, M., Hardeman, E., & Gotz, J. (2010). Dendritic function of tau mediates amyloid-beta toxicity in Alzheimer's disease mouse models. *Cell*, *142*, 387-397.

- Jankovic, J. (2008). Parkinson's disease: clinical features and diagnosis. *J Neurol Neurosurg Psychiatry*, *79*, 368-376.
- Kandel, E. R. (2001). The molecular biology of memory storage: a dialog between genes and synapses. *Biosci Rep*, *21*, 565-611.
- Karow, D. S., McEvoy, L. K., Fennema-Notestine, C., Hagler, D. J., Jr., Jennings, R. G., Brewer, J. B., Hoh, C. K., & Dale, A. M. (2010). Relative capability of MR imaging and FDG PET to depict changes associated with prodromal and early Alzheimer disease. *Radiology*, *256*, 932-942.
- Karuppagounder, S. S., Pinto, J. T., Xu, H., Chen, H. L., Beal, M. F., & Gibson, G. E. (2009). Dietary supplementation with resveratrol reduces plaque pathology in a transgenic model of Alzheimer's disease. *Neurochem Int*, *54*, 111-118.
- Katche, C., Bekinschtein, P., Slipczuk, L., Goldin, A., Izquierdo, I. A., Cammarota, M., & Medina, J. H. (2009). Delayed wave of c-Fos expression in the dorsal hippocampus involved specifically in persistence of long-term memory storage. *Proc Natl Acad Sci U S A*, *107*, 349-354.
- Khochbin, S., Verdel, A., Lemercier, C., & Seigneurin-Berny, D. (2001). Functional significance of histone deacetylase diversity. *Curr Opin Genet Dev*, *11*, 162-166.
- Kilgore, M., Miller, C. A., Fass, D. M., Hennig, K. M., Haggarty, S. J., Sweatt, J. D., & Rumbaugh, G. (2010). Inhibitors of class 1 histone deacetylases reverse contextual memory deficits in a mouse model of Alzheimer's disease. *Neuropsychopharmacology*, *35*, 870-880.
- Kim, J. J., & Fanselow, M. S. (1992). Modality-specific retrograde amnesia of fear. *Science*, *256*, 675-677.
- Kimberly, W. T., Zheng, J. B., Guenette, S. Y., & Selkoe, D. J. (2001). The intracellular domain of the beta-amyloid precursor protein is stabilized by Fe65 and translocates to the nucleus in a notch-like manner. *J Biol Chem*, *276*, 40288-40292.
- Kimura, T., Ono, T., Takamatsu, J., Yamamoto, H., Ikegami, K., Kondo, A., Hasegawa, M., Ihara, Y., Miyamoto, E., & Miyakawa, T. (1996). Sequential changes of tau-site-specific phosphorylation during development of paired helical filaments. *Dementia*, *7*, 177-181.
- Klein, W. L. (2002). Abeta toxicity in Alzheimer's disease: globular oligomers (ADDLs) as new vaccine and drug targets. *Neurochem Int*, *41*, 345-352.
- Klose, R. J., & Bird, A. P. (2006). Genomic DNA methylation: the mark and its mediators. *Trends Biochem Sci*, *31*, 89-97.
- Kojro, E., Gimpl, G., Lammich, S., Marz, W., & Fahrenholz, F. (2001). Low cholesterol stimulates the nonamyloidogenic pathway by its effect on the alpha -secretase ADAM 10. *Proc Natl Acad Sci U S A*, *98*, 5815-5820.
- Kopelman, M. D., Thomson, A. D., Guerrini, I., & Marshall, E. J. (2009). The Korsakoff syndrome: clinical aspects, psychology and treatment. *Alcohol Alcohol*, *44*, 148-154.
- Korzus, E., Rosenfeld, M. G., & Mayford, M. (2004). CBP histone acetyltransferase activity is a critical component of memory consolidation. *Neuron*, *42*, 961-972.
- Kotzbauer, P. T., Trojanowsk, J. Q., & Lee, V. M. (2001). Lewy body pathology in Alzheimer's disease. *J Mol Neurosci*, *17*, 225-232.

- Kreitzer, A. C. (2009). Physiology and pharmacology of striatal neurons. *Annu Rev Neurosci*, *32*, 127-147.
- Kumar, A., Naidu, P. S., Seghal, N., & Padi, S. S. (2007). Neuroprotective effects of resveratrol against intracerebroventricular colchicine-induced cognitive impairment and oxidative stress in rats. *Pharmacology*, *79*, 17-26.
- Kumar, P., Padi, S. S., Naidu, P. S., & Kumar, A. (2006). Effect of resveratrol on 3-nitropropionic acid-induced biochemical and behavioural changes: possible neuroprotective mechanisms. *Behav Pharmacol*, *17*, 485-492.
- Kuo, M. H., vom Baur, E., Struhl, K., & Allis, C. D. (2000). Gcn4 activator targets Gcn5 histone acetyltransferase to specific promoters independently of transcription. *Mol Cell*, *6*, 1309-1320.
- Kurdistani, S. K., Tavazoie, S., & Grunstein, M. (2004). Mapping global histone acetylation patterns to gene expression. *Cell*, *117*, 721-733.
- Laczo, J., Andel, R., Vyhnalek, M., Vlcek, K., Magerova, H., Varjassyova, A., Tolar, M., & Hort, J. (2010). Human analogue of the morris water maze for testing subjects at risk of Alzheimer's disease. *Neurodegener Dis*, *7*, 148-152.
- Lagger, G., O'Carroll, D., Rembold, M., Khier, H., Tischler, J., Weitzer, G., Schuettengruber, B., Hauser, C., Brunmeir, R., Jenuwein, T., & Seiser, C. (2002). Essential function of histone deacetylase 1 in proliferation control and CDK inhibitor repression. *EMBO J*, *21*, 2672-2681.
- LeDoux, J. E. (1994). Emotion, memory and the brain. *Sci Am*, *270*, 50-57.
- Lee, Y. S., & Silva, A. J. (2009). The molecular and cellular biology of enhanced cognition. *Nat Rev Neurosci*, *10*, 126-140.
- Lemere, C. A., & Masliah, E. (2010). Can Alzheimer disease be prevented by amyloid-beta immunotherapy? *Nat Rev Neurol*, *6*, 108-119.
- Levenson, J. M., O'Riordan, K. J., Brown, K. D., Trinh, M. A., Molfese, D. L., & Sweatt, J. D. (2004). Regulation of histone acetylation during memory formation in the hippocampus. *J Biol Chem*, *279*, 40545-40559.
- Levine, B., Turner, G. R., Tisserand, D., Hevenor, S. J., Graham, S. J., & McIntosh, A. R. (2004). The functional neuroanatomy of episodic and semantic autobiographical remembering: a prospective functional MRI study. *J Cogn Neurosci*, *16*, 1633-1646.
- Li, B., Carey, M., & Workman, J. L. (2007). The role of chromatin during transcription. *Cell*, *128*, 707-719.
- Liang, K. C., Hon, W., Tyan, Y. M., & Liao, W. L. (1994). Involvement of hippocampal NMDA and AMPA receptors in acquisition, formation and retrieval of spatial memory in the Morris water maze. *Chin J Physiol*, *37*, 201-212.
- Lisman, J., Schulman, H., & Cline, H. (2002). The molecular basis of CaMKII function in synaptic and behavioural memory. *Nat Rev Neurosci*, *3*, 175-190.
- Liu, H., Hu, Q., D'Ercole, A. J., & Ye, P. (2009). Histone deacetylase 11 regulates oligodendrocyte-specific gene expression and cell development in OL-1 oligodendroglia cells. *Glia*, *57*, 1-12.
- Lømo, T. (1966). Frequency potentiation of excitatory synaptic activity in the dentate area of the hippocampal formation. *Acta Physiologica Scandinavica*, *68* (Suppl 277).

- Lubin, F. D., Roth, T. L., & Sweatt, J. D. (2008). Epigenetic regulation of BDNF gene transcription in the consolidation of fear memory. *J Neurosci*, *28*, 10576-10586.
- Marambaud, P., Zhao, H., & Davies, P. (2005). Resveratrol promotes clearance of Alzheimer's disease amyloid-beta peptides. *J Biol Chem*, *280*, 37377-37382.
- Maren, S. (2005). Synaptic mechanisms of associative memory in the amygdala. *Neuron*, *47*, 783-786.
- Matteoli, M., Pozzi, D., Grumelli, C., Condliffe, S. B., Frassoni, C., Harkany, T., & Verderio, C. (2009). The synaptic split of SNAP-25: different roles in glutamatergic and GABAergic neurons? *Neuroscience*, *158*, 223-230.
- Mejat, A., Ramond, F., Bassel-Duby, R., Khochbin, S., Olson, E. N., & Schaeffer, L. (2005). Histone deacetylase 9 couples neuronal activity to muscle chromatin acetylation and gene expression. *Nat Neurosci*, *8*, 313-321.
- Michan, S., Li, Y., Chou, M. M., Parrella, E., Ge, H., Long, J. M., Allard, J. S., Lewis, K., Miller, M., Xu, W., Mervis, R. F., Chen, J., Guerin, K. I., Smith, L. E., McBurney, M. W., Sinclair, D. A., Baudry, M., de Cabo, R., & Longo, V. D. (2010). SIRT1 is essential for normal cognitive function and synaptic plasticity. *J Neurosci*, *30*, 9695-9707.
- Milders, M., Fuchs, S., & Crawford, J. R. (2003). Neuropsychological impairments and changes in emotional and social behaviour following severe traumatic brain injury. *J Clin Exp Neuropsychol*, *25*, 157-172.
- Miller, C. A., & Sweatt, J. D. (2007). Covalent modification of DNA regulates memory formation. *Neuron*, *53*, 857-869.
- Moehlmann, T., Winkler, E., Xia, X., Edbauer, D., Murrell, J., Capell, A., Kaether, C., Zheng, H., Ghetti, B., Haass, C., & Steiner, H. (2002). Presenilin-1 mutations of leucine 166 equally affect the generation of the Notch and APP intracellular domains independent of their effect on Abeta 42 production. *Proc Natl Acad Sci U S A*, *99*, 8025-8030.
- Montgomery, R. L., Davis, C. A., Potthoff, M. J., Haberland, M., Fielitz, J., Qi, X., Hill, J. A., Richardson, J. A., & Olson, E. N. (2007). Histone deacetylases 1 and 2 redundantly regulate cardiac morphogenesis, growth, and contractility. *Genes Dev*, *21*, 1790-1802.
- Morris, R. G. M. (1981). Spatial localization does not require the presence of local cues. *Learning and Motivation*, *12*, 239-260.
- Narlikar, G. J., Fan, H. Y., & Kingston, R. E. (2002). Cooperation between complexes that regulate chromatin structure and transcription. *Cell*, *108*, 475-487.
- Neal, M., & Briggs, M. (2003). Validation therapy for dementia. *Cochrane Database Syst Rev*, CD001394.
- Nelson, P. G. (2005). Activity-dependent synapse modulation and the pathogenesis of Alzheimer disease. *Curr Alzheimer Res*, *2*, 497-506.
- O'Neill, M. J., Bleakman, D., Zimmerman, D. M., & Nisenbaum, E. S. (2004). AMPA receptor potentiators for the treatment of CNS disorders. *Curr Drug Targets CNS Neurol Disord*, *3*, 181-194.
- Pandey, U. B., Nie, Z., Batlevi, Y., McCray, B. A., Ritson, G. P., Nedelsky, N. B., Schwartz, S. L., DiProspero, N. A., Knight, M. A., Schuldiner, O., Padmanabhan, R., Hild, M., Berry, D. L.,

- Garza, D., Hubbert, C. C., Yao, T. P., Baehrecke, E. H., & Taylor, J. P. (2007). HDAC6 rescues neurodegeneration and provides an essential link between autophagy and the UPS. *Nature*, *447*, 859-863.
- Parthun, M. R. (2007). Hat1: the emerging cellular roles of a type B histone acetyltransferase. *Oncogene*, *26*, 5319-5328.
- Peleg, S., Sananbenesi, F., Zovoilis, A., Burkhardt, S., Bahari-Javan, S., Agis-Balboa, R. C., Cota, P., Wittnam, J. L., Gogol-Doering, A., Opitz, L., Salinas-Riester, G., Dettenhofer, M., Kang, H., Farinelli, L., Chen, W., & Fischer, A. (2010). Altered histone acetylation is associated with age-dependent memory impairment in mice. *Science*, *328*, 753-756.
- Petersen, R. C., Smith, G. E., Waring, S. C., Ivnik, R. J., Tangalos, E. G., & Kokmen, E. (1999). Mild cognitive impairment: clinical characterization and outcome. *Arch Neurol*, *56*, 303-308.
- Radde, R., Bolmont, T., Kaeser, S. A., Coomaraswamy, J., Lindau, D., Stoltze, L., Calhoun, M. E., Jaggi, F., Wolburg, H., Gengler, S., Haass, C., Ghetti, B., Czech, C., Holscher, C., Mathews, P. M., & Jucker, M. (2006). Abeta42-driven cerebral amyloidosis in transgenic mice reveals early and robust pathology. *EMBO Rep*, *7*, 940-946.
- Reed, N. A., Cai, D., Blasius, T. L., Jih, G. T., Meyhofer, E., Gaertig, J., & Verhey, K. J. (2006). Microtubule acetylation promotes kinesin-1 binding and transport. *Curr Biol*, *16*, 2166-2172.
- Reid, J. L., Iyer, V. R., Brown, P. O., & Struhl, K. (2000). Coordinate regulation of yeast ribosomal protein genes is associated with targeted recruitment of Esa1 histone acetylase. *Mol Cell*, *6*, 1297-1307.
- Rescorla, R. A., & Wagner, A. R. (1972). A theory of Pavlovian conditioning. Variations in effectiveness of reinforcement and non-reinforcement. *Classical Conditioning II New York: Appleton-Century-Crofts*.
- Reul, J. M., Hesketh, S. A., Collins, A., & Mecinas, M. G. (2009). Epigenetic mechanisms in the dentate gyrus act as a molecular switch in hippocampus-associated memory formation. *Epigenetics*, *4*, 434-439.
- Ricobaraza, A., Cuadrado-Tejedor, M., Perez-Mediavilla, A., Frechilla, D., Del Rio, J., & Garcia-Osta, A. (2009). Phenylbutyrate ameliorates cognitive deficit and reduces tau pathology in an Alzheimer's disease mouse model. *Neuropsychopharmacology*, *34*, 1721-1732.
- Rivieccio, M. A., Brochier, C., Willis, D. E., Walker, B. A., D'Annibale, M. A., McLaughlin, K., Siddiq, A., Kozikowski, A. P., Jaffrey, S. R., Twiss, J. L., Ratan, R. R., & Langley, B. (2009). HDAC6 is a target for protection and regeneration following injury in the nervous system. *Proc Natl Acad Sci U S A*, *106*, 19599-19604.
- Roberson, E. D., Scarce-Levie, K., Palop, J. J., Yan, F., Cheng, I. H., Wu, T., Gerstein, H., Yu, G. Q., & Mucke, L. (2007). Reducing endogenous tau ameliorates amyloid beta-induced deficits in an Alzheimer's disease mouse model. *Science*, *316*, 750-754.
- Rossi-Arnaud, C., Fagioli, S., & Ammassari-Teule, M. (1991). Spatial learning in two inbred strains of mice: genotype-dependent effect of amygdaloid and hippocampal lesions. *Behav Brain Res*, *45*, 9-16.

- Roth, S. Y., Denu, J. M., & Allis, C. D. (2001). Histone acetyltransferases. *Annu Rev Biochem*, *70*, 81-120.
- Rui, Y., Tiwari, P., Xie, Z., & Zheng, J. Q. (2006). Acute impairment of mitochondrial trafficking by beta-amyloid peptides in hippocampal neurons. *J Neurosci*, *26*, 10480-10487.
- Sananbenesi, F., & Fischer, A. (2009). The epigenetic bottleneck of neurodegenerative and psychiatric diseases. *Biol Chem*, *390*, 1145-1153.
- Sanderson, D. J., Good, M. A., Seeburg, P. H., Sprengel, R., Rawlins, J. N., & Bannerman, D. M. (2008). The role of the GluR-A (GluR1) AMPA receptor subunit in learning and memory. *Prog Brain Res*, *169*, 159-178.
- Sastre, M., Steiner, H., Fuchs, K., Capell, A., Multhaup, G., Condron, M. M., Teplow, D. B., & Haass, C. (2001). Presenilin-dependent gamma-secretase processing of beta-amyloid precursor protein at a site corresponding to the S3 cleavage of Notch. *EMBO Rep*, *2*, 835-841.
- Saywell, N., & Taylor, D. (2008). The role of the cerebellum in procedural learning--are there implications for physiotherapists' clinical practice? *Physiother Theory Pract*, *24*, 321-328.
- Schwegler, H., & Crusio, W. E. (1995). Correlations between radial-maze learning and structural variations of septum and hippocampus in rodents. *Behav Brain Res*, *67*, 29-41.
- Schwer, B., & Verdin, E. (2008). Conserved metabolic regulatory functions of sirtuins. *Cell Metab*, *7*, 104-112.
- Scoville, W. B., & Milner, B. (1957). Loss of recent memory after bilateral hippocampal lesions. *J Neurol Neurosurg Psychiatry*, *20*, 11-21.
- Seigneurin-Berny, D., Verdel, A., Curtet, S., Lemerrier, C., Garin, J., Rousseaux, S., & Khochbin, S. (2001). Identification of components of the murine histone deacetylase 6 complex: link between acetylation and ubiquitination signaling pathways. *Mol Cell Biol*, *21*, 8035-8044.
- Selkoe, D. J. (2001). Alzheimer's disease: genes, proteins, and therapy. *Physiol Rev*, *81*, 741-766.
- Selkoe, D. J. (2002). Deciphering the genesis and fate of amyloid beta-protein yields novel therapies for Alzheimer disease. *J Clin Invest*, *110*, 1375-1381.
- Shahbazian, M. D., & Grunstein, M. (2007). Functions of site-specific histone acetylation and deacetylation. *Annu Rev Biochem*, *76*, 75-100.
- Shankar, G. M., Li, S., Mehta, T. H., Garcia-Munoz, A., Shepardson, N. E., Smith, I., Brett, F. M., Farrell, M. A., Rowan, M. J., Lemere, C. A., Regan, C. M., Walsh, D. M., Sabatini, B. L., & Selkoe, D. J. (2008). Amyloid-beta protein dimers isolated directly from Alzheimer's brains impair synaptic plasticity and memory. *Nat Med*, *14*, 837-842.
- Sharma, M., & Gupta, Y. K. (2002). Chronic treatment with trans resveratrol prevents intracerebroventricular streptozotocin induced cognitive impairment and oxidative stress in rats. *Life Sci*, *71*, 2489-2498.
- Southwood, C. M., Peppi, M., Dryden, S., Tainsky, M. A., & Gow, A. (2007). Microtubule deacetylases, SirT2 and HDAC6, in the nervous system. *Neurochem Res*, *32*, 187-195.
- Stahl, S. M. (2000). The new cholinesterase inhibitors for Alzheimer's disease, Part 2: illustrating their mechanisms of action. *J Clin Psychiatry*, *61*, 813-814.

- Strahl, B. D., & Allis, C. D. (2000). The language of covalent histone modifications. *Nature*, *403*, 41-45.
- Sturchler-Pierrat, C., Abramowski, D., Duke, M., Wiederhold, K. H., Mistl, C., Rothacher, S., Ledermann, B., Burki, K., Frey, P., Paganetti, P. A., Waridel, C., Calhoun, M. E., Jucker, M., Probst, A., Staufenbiel, M., & Sommer, B. (1997). Two amyloid precursor protein transgenic mouse models with Alzheimer disease-like pathology. *Proc Natl Acad Sci U S A*, *94*, 13287-13292.
- Sunyer, B., Diao, W., & Lubec, G. (2008). The role of post-translational modifications for learning and memory formation. *Electrophoresis*, *29*, 2593-2602.
- Swank, M. W., & Sweatt, J. D. (2001). Increased histone acetyltransferase and lysine acetyltransferase activity and biphasic activation of the ERK/RSK cascade in insular cortex during novel taste learning. *J Neurosci*, *21*, 3383-3391.
- Tarnow, E. (2009). Short term memory may be the depletion of the readily releasable pool of presynaptic neurotransmitter vesicles of a metastable long term memory trace pattern. *Cogn Neurodyn*, *3*, 263-269.
- Taunton, J., Hassig, C. A., & Schreiber, S. L. (1996). A mammalian histone deacetylase related to the yeast transcriptional regulator Rpd3p. *Science*, *272*, 408-411.
- Tiraboschi, P., Hansen, L. A., Thal, L. J., & Corey-Bloom, J. (2004). The importance of neuritic plaques and tangles to the development and evolution of AD. *Neurology*, *62*, 1984-1989.
- Tulving, E., & Donaldson, W. (1972). Episodic and semantic memory. In *Organization of Memory*.
- Ullman, M. T. (2004). Contributions of memory circuits to language: the declarative/procedural model. *Cognition*, *92*, 231-270.
- Valenzuela-Fernandez, A., Cabrero, J. R., Serrador, J. M., & Sanchez-Madrid, F. (2008). HDAC6: a key regulator of cytoskeleton, cell migration and cell-cell interactions. *Trends Cell Biol*, *18*, 291-297.
- Van Hoesen, G. W., & Hyman, B. T. (1990). Hippocampal formation: anatomy and the patterns of pathology in Alzheimer's disease. *Prog Brain Res*, *83*, 445-457.
- Vaquero, A., Loyola, A., & Reinberg, D. (2003). The constantly changing face of chromatin. *Sci Aging Knowledge Environ*, *2003*, RE4.
- Vassar, R., & Citron, M. (2000). Abeta-generating enzymes: recent advances in beta- and gamma-secretase research. *Neuron*, *27*, 419-422.
- Vellas, B., Black, R., Thal, L. J., Fox, N. C., Daniels, M., McLennan, G., Tompkins, C., Leibman, C., Pomfret, M., & Grundman, M. (2009). Long-term follow-up of patients immunized with AN1792: reduced functional decline in antibody responders. *Curr Alzheimer Res*, *6*, 144-151.
- Verdel, A., Curtet, S., Brocard, M. P., Rousseaux, S., Lemerrier, C., Yoshida, M., & Khochbin, S. (2000). Active maintenance of mHDA2/mHDAC6 histone-deacetylase in the cytoplasm. *Curr Biol*, *10*, 747-749.
- Vogelauer, M., Wu, J., Suka, N., & Grunstein, M. (2000). Global histone acetylation and deacetylation in yeast. *Nature*, *408*, 495-498.

- Vossel, K. A., Zhang, K., Brodbeck, J., Daub, A. C., Sharma, P., Finkbeiner, S., Cui, B., & Mucke, L. (2010). Tau Reduction Prevents A β -Induced Defects in Axonal Transport. *Science*.
- Waddington, C. H. (1953). Epigenetics and Evolution. *Symp. Soc. Exp. Biol.*, 7, 186-199.
- Walker, F. O. (2007). Huntington's disease. *Lancet*, 369, 218-228.
- Walsh, D. M., Klyubin, I., Fadeeva, J. V., Cullen, W. K., Anwyl, R., Wolfe, M. S., Rowan, M. J., & Selkoe, D. J. (2002). Naturally secreted oligomers of amyloid beta protein potently inhibit hippocampal long-term potentiation in vivo. *Nature*, 416, 535-539.
- Wang, X., Perry, G., Smith, M. A., & Zhu, X. (2010). Amyloid-beta-derived diffusible ligands cause impaired axonal transport of mitochondria in neurons. *Neurodegener Dis*, 7, 56-59.
- Wang, X., Su, B., Lee, H. G., Li, X., Perry, G., Smith, M. A., & Zhu, X. (2009a). Impaired balance of mitochondrial fission and fusion in Alzheimer's disease. *J Neurosci*, 29, 9090-9103.
- Wang, Z., Zang, C., Cui, K., Schones, D. E., Barski, A., Peng, W., & Zhao, K. (2009b). Genome-wide mapping of HATs and HDACs reveals distinct functions in active and inactive genes. *Cell*, 138, 1019-1031.
- Wenk, G. L. (2003). Neuropathologic changes in Alzheimer's disease. *J Clin Psychiatry*, 64 Suppl 9, 7-10.
- Woods, B., Spector, A., Jones, C., Orrell, M., & Davies, S. (2005). Reminiscence therapy for dementia. *Cochrane Database Syst Rev*, CD001120.
- Yang, X. J., & Seto, E. (2003). Collaborative spirit of histone deacetylases in regulating chromatin structure and gene expression. *Curr Opin Genet Dev*, 13, 143-153.
- Yang, X. J., & Seto, E. (2008). The Rpd3/Hda1 family of lysine deacetylases: from bacteria and yeast to mice and men. *Nat Rev Mol Cell Biol*, 9, 206-218.
- Zandi, P. P., Anthony, J. C., Khachaturian, A. S., Stone, S. V., Gustafson, D., Tschanz, J. T., Norton, M. C., Welsh-Bohmer, K. A., & Breitner, J. C. (2004). Reduced risk of Alzheimer disease in users of antioxidant vitamin supplements: the Cache County Study. *Arch Neurol*, 61, 82-88.
- Zellner, M. R., & Rinaldi, R. (2009). How conditioned stimuli acquire the ability to activate VTA dopamine cells: a proposed neurobiological component of reward-related learning. *Neurosci Biobehav Rev*, 34, 769-780.
- Zhang, Y., Gilquin, B., Khochbin, S., & Matthias, P. (2006). Two catalytic domains are required for protein deacetylation. *J Biol Chem*, 281, 2401-2404.
- Zhang, Y., Kwon, S., Yamaguchi, T., Cubizolles, F., Rousseaux, S., Kneissel, M., Cao, C., Li, N., Cheng, H. L., Chua, K., Lombard, D., Mizeracki, A., Matthias, G., Alt, F. W., Khochbin, S., & Matthias, P. (2008). Mice lacking histone deacetylase 6 have hyperacetylated tubulin but are viable and develop normally. *Mol Cell Biol*, 28, 1688-1701.
- Zhang, Y., Li, N., Caron, C., Matthias, G., Hess, D., Khochbin, S., & Matthias, P. (2003). HDAC-6 interacts with and deacetylates tubulin and microtubules in vivo. *EMBO J*, 22, 1168-1179.
- Zhao, Z., Xu, H., & Gong, W. (2010). Histone deacetylase 6 (HDAC6) is an independent deacetylase for alpha-tubulin. *Protein Pept Lett*, 17, 555-558.

Curriculum Vitae

Nambirajan Govindarajan

1982

born in Kolkata, India

EDUCATION

Apr. 2007 – date

PhD study, Dr. Andre Fischer, European Neuroscience Institute Göttingen, Germany

Sept. 2003 – Mar. 2005

Masters in Molecular Biology, University of Göttingen, Germany

Aug. 2000 – May 2003

Bachelors in Human Biology, All India Institute of Medical Sciences, New Delhi, India

SCHOLARSHIPS

Jan. 2008 – Dec. 2010

PhD Scholarship from Hans and Ilse Breuer Foundation, Frankfurt, Germany

Sept. 2003 – Mar. 2005

International Max Planck Research Scholarship, University of Göttingen, Germany

May 2002 – June 2002

Summer Training Fellowship, All India Institute of Medical Sciences, New Delhi, India

RESEARCH

Apr. 2007 – date

Doctoral project: The modulation of histone deacetylases attenuates the pathogenesis of Alzheimer's disease

PUBLICATIONS

- Govindarajan N., Lu J., Burkhardt S., Sananbenesi F., Fischer A., Targeting histone deacetylase 6 rescues cognitive decline in a mouse model for Alzheimer's disease (in preparation).
- Govindarajan N., Agis-Balboa R., Walter J., Burkhardt S., Sananbenesi F., Fischer A., HDAC inhibitor treatment improves cognitive function in a mouse model for advanced Alzheimer's disease (in preparation).